TECHNISCHE UNIVERSITÄT MÜNCHEN

Lehrstuhl Entwicklungsgenetik

Examining new interactors of Notch/RBPJκ signalling in adult neural stem cells

Dissertation von
Tobias Johannes Schwarz

Helmholtz Zentrum München
Institut für Entwicklungsgenetik

TECHNISCHE UNIVERSITÄT MÜNCHEN

Lehrstuhl Entwicklungsgenetik

Examining new interactors of Notch/RBPJκ signalling
in adult neural stem cells

Tobias Johannes Schwarz

Vollständiger Abdruck der von der Fakultät Wissenschaftszentrum Weihenstephan für Ernährung, Landnutzung und Umwelt der Technischen Universität München zur Erlangung des akademischen Grades eines

Doktors der Naturwissenschaften

genehmigten Dissertation.

Vorsitzende: Univ.-Prof. A. Schnieke, Ph.D.

Prüfer der Dissertation: 1. Univ.-Prof. Dr. W. Wurst

                        2. Univ.-Prof. Dr. C. Lie,

                            (Friedrich-Alexander Universität Erlangen-Nürnberg)

Die Dissertation wurde am 20. 03. 2012 bei der Technischen Universität München eingereicht und durch die Fakultät Wissenschaftszentrum Weihenstephan für Ernährung, Landnutzung und Umwelt am 25. 07. 2012 angenommen.

Table of contents

1 Zusammenfassung

Die lebenslange Generierung neuer Nervenzellen aus Stammzellen in der subgranulären Schicht des Gyrus Dentatus und in der subventrikulären Schicht der lateralen Ventrikel wird als wichtiger Beitrag zu Lern- und Gedächtnisprozessen gesehen. Eine Voraussetzung für die kontinuierliche Generierung neuer Nervenzellen ist die Erhaltung der neuralen Stammzellpopulation. Zahlreiche molekulare Regulatoren und Signale zur Erhaltung neuraler Stammzellen wurden bereits identifiziert. Wie jedoch diese Signalwege miteinander interagieren um eine verfrühte Differenzierung und damit eine Erschöpfung der neuralen Stammzellpopulation zu verhindern ist gegenwärtig noch unbekannt. Studien belegen, dass der Notch Signalweg und dessen transkriptioneller Effektor RBPJκ bei der Erhaltung der neuralen Stammzellen eine wichtige Rolle spielt.

Ziel der vorliegende Studie war es neue Interaktoren von RBPJκ und des Notch Signalweges zu bestimmen, die zur Erhaltung neuraler Stammzellen beitragen. Ein auf einem Kandidaten basierender Ansatz offenbarte FOXO Transkriptionsfaktoren als Interaktoren des Notch Signalweges. Weiterführende Studien konnten belegen, dass FOXO1 und FOXO3 in hippokampalen Stammzellen aktiv sind und dass beide *in vitro* die Expression des Notch Ziel-Genes *Sox2* positiv regulieren. Interessanterweise führte der konditionale Knockout von Foxo1/3/4 zu einem progressiven Verlust der Stammzellaktivität.

Als weiterer Ansatz zur Entschlüsselung neuer RBPJκ-Interaktoren in adulten neuralen Stammzellen *in vitro* wurden Massenspektroskopische Analysen durchgeführt. Die Untersuchungen ergaben zahlreiche Proteine, welche in Transkription, RNA Prozessierung als auch in neurodegenerativen Erkrankungen involviert sind. Studien von Expressionsmustern und möglichen Interaktionen resultierten in zwei bisher unbekannten RBPJκ Interaktoren: TDP-43 und NFIA. TDP-43 interagierte mit RBPJκ Proteinkomplexen und modulierte die Notch vermittelte Expression von *Hes1*. Im Gegensatz zum Notch Signalweg hatte TDP-43 keinen Einfluss auf den Wnt Signalweg. Des Weiteren führte die Überexpression von TDP-43 ebenfalls zu einer Erhöhung von endogenem HES1 Proteinlevel, wohingegen eine ALS- und FTLD-U assoziierte TDP-43 (A315T) Mutante einen verringerten Effekt auf die Expression des *Hes1* Gens hatte. Der zweite neue gefundene RBPJκ Interaktor NFIA hatte eine inhibitorische Auswirkung auf die durch den Notch

Signalweg induzierte Expression von Hes1. Expressionsanalysen *in vivo* wiesen eine, auf beide neurogenen Nischen begrenzte, starke Expression von NFIA auf. Interessanterweise führte der konditionale Knockout von RBPJκ in hippokampalen Stammzellen zu einer erhöhten Expression von NFIA. Zusammengefasst deuten die vorliegenden Resultate dieser Arbeit sehr stark darauf hin, dass FOXO1 und 3, TDP-43 sowie NFIA wichtige Interaktoren des Notch Signalweges bei der Regulierung und Erhaltung neuraler Stammzellen sind.

2 Summary

The life-long generation of new neurons from stem cells in the SGZ of the dentate gyrus and the SVZ of the lateral ventricles is considered an important contributor to learning and memory. A prerequisite for the continuous generation of new neurons is the maintenance of the neural stem cell pool. A number of essential molecular regulators and signals for neural stem cell maintenance have been identified, but how these signalling pathways interact to prevent precocious differentiation and exhaustion of the stem cell pool is currently unknown. Previous studies have implicated the Notch signalling pathway and its transcriptionally downstream effector RBPJκ in neural stem cell maintenance.

The present study aimed to discover new interactors of RBPJκ and Notch signalling in the regulation of neural stem cell maintenance. A candidate approach revealed FOXO transcription factors as interactors of the Notch signalling pathway. Subsequent analysis demonstrated that FOXO1 and FOXO3 are active in hippocampal stem cells and that both up-regulated the Notch gene target *Sox2 in vitro*. Intriguingly, conditional knockout of FOXO1, 3 and 4 led to a slowly progressive loss of neural stem cell activity. An unbiased mass spectrometry approach to decipher the interactome of RBPJκ in adult neural stem cells *in vitro*, indicated several proteins involved in transcription, RNA processing as well as in neurodegenerative diseases. Analysis of expression patterns and of putative interactions resulted in two hitherto unknown interactors of RBPJκ: TDP-43 and NFIA. TDP-43 was found to interact with RBPJκ protein complexes and to modulate Notch signalling on *Hes1*-gene expression. In contrast, TDP-43 did not modulate Wnt target gene expression. Furthermore, overexpression of TDP-43 resulted in an up-regulation of endogenous Hes1 protein levels. Interestingly, an ALS- and FTDL-U associated TDP-43 (A315T) mutant showed decreased potency for activation of *Hes1* expression. The second novel RBPJκ interactor, NFIA, displayed inhibitory effects on Notch-signalling induced *Hes1* expression. Expression analyses *in vivo* revealed strong expression of NFIA in both neurogenic niches. Interestingly, conditional knockout of RBPJκ in hippocampal stem cells led to an increased expression of NFIA. Taken together, results from this work strongly imply FOXO, NFIA and TDP-43 as important interactors of Notch signalling in the regulation of adult neural stem cell maintenance.

3 Introduction

3.1 Adult neurogenesis and neural stem cells

The term adult neurogenesis describes the generation of new functional neurons in the adult mammalian brain. Adult neurogenesis involves a complex sequence of developmental steps, including proliferation, neuronal fate determination, cell cycle exit, migration, and maturation, and finally the functional integration of the new neurons into preexisting neural circuits. Current data suggest that the primary precursors to new adult-generated neurons are specialized astrocytes that may have stem cell character, i.e. the capacity for lifelong self-renewal and the potential to undergo multi-lineage differentiation (Seri et al., 2001; Filippov et al., 2003; Ahn and Joyner, 2005; Kronenberg et al., 2006; Imayoshi et al., 2008).

Neurogenesis occurs under physiological conditions in two distinct locations of the adult mammalian brain: the subventricular zone (SVZ) of the lateral ventricles and the subgranular zone (SGZ) of the dentate gyrus (DG) in the hippocampus (Zhao et al., 2008).

The most primitive precursors (also termed Type 1 cells) in the SGZ of the DG are commonly identified by the expression of several antigens such as the intermediate filaments glial fibrillary acidic protein (GFAP) and Nestin, the transcription factor SRY (sex determining region Y)-box2 (Sox2) and the fatty acid binding protein 7 (FABP7, also known as brain lipid binding protein, BLBP), by their electrophysiological properties and by their morphology resembling radial glia cells (see fig. 1B) (Steiner et al., 2006). By virtue of the similarity to radial glia (RG) cells, which are multipotent stem cells present during the embryonic brain development, adult hippocampal neural stem cells are also termed RG-like stem cells (Kriegstein and Alvarez-Buylla, 2009). Studies in mice reported that only 1-5 % of Type 1 cells were proliferating as determined by incorporation of the thymidine analogue BrdU (Filippov et al., 2003; Kronenberg et al., 2003; Suh et al., 2007; Lugert et al., 2010), indicating that Type 1 cells divide only occasionally. These Type 1 cells, which are thus largely quiescent, are activated by extrinsic signals, divide and give rise to fast proliferating, so-called transient amplifying Type 2 cells. After a limited number of cell divisions Type 2 cells commit to the neuronal fate (Type 3 cells), become postmitotic, and finally integrate as fully functional mature dentate granule neurons into the preexisting circuits of the hippocampus.

The second neurogenic area in the adult mammalian brain is the SVZ of the lateral ventricles (LV). The SVZ is located close to the ependymal layer of the LVs and consists mainly of three types of precursor cells: stem cells (Type B cells), transient amplifying progenitors (Type C) and neuroblasts (Type A cells). Neuroblasts in the SVZ migrate along the walls of the LVs, coalesce into the rostral migratory stream (RMS) and then migrate tangentially towards the olfactory bulb, where they mature and integrate as fully functionally granular- and periglomerular interneurons (Alvarez-Buylla and Garcia-Verdugo, 2002).
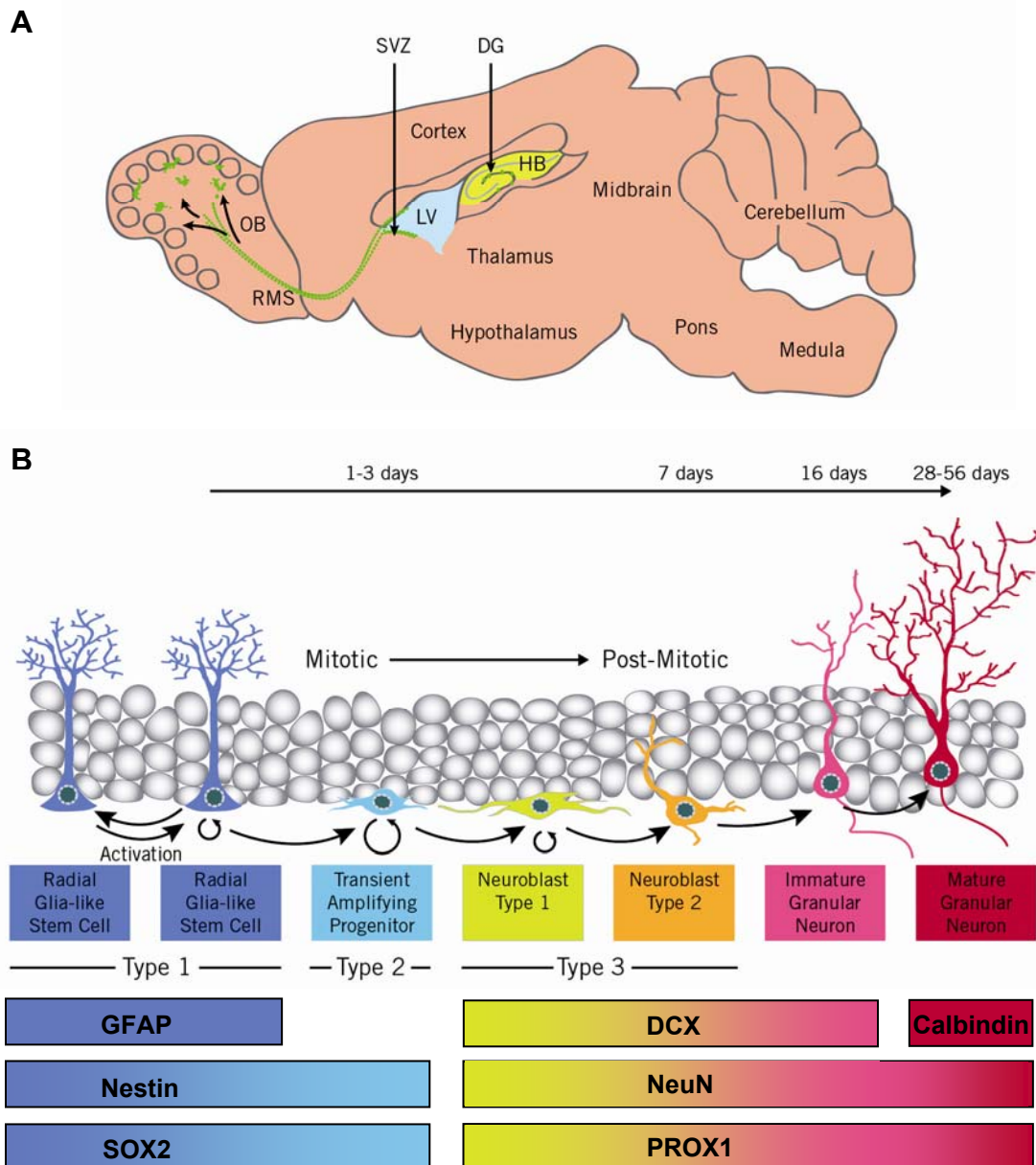
Fig.1 Adult neurogenesis in subventricular zone and dentate gyrus
A) Sagittal section (overview) of adult mouse brain highlighting the two neurogenic niches, where under physiological conditions adult neurogenesis occurs: the subventricular zone (SVZ, arrow) of the lateral ventricles (LV) and the subgranular zone (SGZ) of the dentate gyrus (DG, arrow) in the hippocampus (HP). Stem cells in the SVZ give rise to neuroblasts, which migrate along the rostral migratory stream (RMS, green) towards the olfactory bulb (OB) where they get integrated as fully functionally granular and periglomerular interneurons. **B**) Schematic illustration of developmental stages of adult hippocampal neurogenesis. Radial glia-like stem cells (Type 1 cells) get activated and generate highly proliferative transient amplifying cells (Type 2). These fast dividing cells give rise to neuroblasts (Type 3), which migrate into the granular layer, become post-mitotic and get integrated as fully functionally granular neurons into the hippocampal neuronal circuitry. The developmental stages during adult neurogenesis in DG and SVZ can be distinguished by expression of characteristic markers.

New born neurons in the hippocampus possess distinct neurophysiological properties, i.e. lower threshold of long-term potentiation (LTP), reduced GABAergic (γ-aminobutyric acid) inhibition and the attribute to exhibit a low input specificity that distinguish them from mature granular neurons (Schmidt-Hieber et al., 2004; Esposito et al., 2005; Ge et al., 2006; Marin-Burgin et al., 2012). Current models of adult neurogenesis propose that these immature neurons may be crucial for function and plasticity of the neural network (Aimone et al., 2011; Piatti et al., 2011; Sahay et al., 2011).

Indeed, several studies using loss-of-function strategies described that impaired hippocampal neurogenesis correlates with decreased performance in contextual and spatial memory, which are known to depend on the hippocampus (Sahay et al., 2011; Shors et al., 2001; Saxe et al., 2006; Dupret et al., 2008; Imayoshi et al., 2008b; Zhang et al., 2008; Clelland et al., 2009; Deng et al., 2009; Garthe et al., 2009; Kitamura et al., 2009). Moreover, inhibition of hippocampal neurogenesis also led to increased anxiety-like behavior (Snyder et al., 2011; Bergami et al., 2008; Bergami et al., 2009; Revest et al., 2009). In this regard, Sahay and colleagues (2011) demonstrated, that mice with enhanced hippocampal neurogenesis exhibit decreased anxiety-like behaviour and perform better in contextual fear discrimination learning tasks (Sahay et al., 2011).

Further support for the importance of adult neurogenesis to cognitive function is suggested by findings that decline of cognitive performance during aging correlates with decreasing rate of adult hippocampal neurogenesis (Drapeau et al., 2003; van Praag et al., 2005). Whether decreasing neurogenesis is due to impaired stem cell maintenance or due to an increase in the number of quiescent stem cells is not fully understood and current data are contradictory (Lugert et al., 2010; Manganas et al., 2007; Walker et al., 2008; Aizawa et al., 2009).

3.2 Signal integration by adult neural stem cells

Adult neural stem cells are maintained in a special microenvironment called "neurogenic niche". The concept of a neurogenic niche is based on transplantation experiments showing that signals provided by the adult dentate gyrus or by the subventricular zone microenvironment control neuronal differentiation of the precursor cells (Suhonen et al., 1996; Shihabuddin et al., 2000; Lie et al., 2002). Several studies showed that stem cells interact with the local environment and that

stem cell identity, maintenance as well as proliferation and fate commitment is controlled by various extrinsic and intrinsic signals (Lugert et al., 2010; Kempermann et al., 1997; Parent et al., 1997; van Praag et al., 1999).

A number of studies indicated multiple extrinsic factors such as growth factors, neurotransmitters, hormones, morphogens and cytokines as well as site-specific regulators (Zhao et al., 2008). For example, the transforming growth factor (TGF)-superfamily has been shown to inhibit stem cell proliferation (Wachs et al., 2006). Similarly, decreased proliferation during ageing was correlated with increased activity of the TGFß-effector Smad2 in Type-1 cells in the hippocampus (Kandasamy et al., 2010). In contrast, the canonical Wnt-signalling pathway activated by Wnt3 strongly stimulates both proliferation and fate commitment of hippocampal progenitors (Lie et al., 2005). Insulin-like growth factor 1 (IGF1) signalling and the downstream phosphatidylinositol 3-kinase (PI3K)-signaling cascade have been reported as positive regulators of adult hippocampal neural stem cell proliferation (Bonaguidi et al., 2011; Bruel-Jungerman et al., 2009). Finally, canonical Notch signalling has been recently reported to be essential to hippocampal neural stem cell maintenance (Ables et al., 2010; Ehm et al., 2010; Lugert et al., 2010).

One of the best-studied intracellular factors and target of different signalling pathways is the transcription factor SOX2. SOX2 is highly expressed in the progenitor pool of both adult neurogenic niches and is down-regulated upon early neuronal fate commitment (Steiner et al., 2006). Work by Favaro and colleagues (2009) showed that conditional knockout of *Sox2* strongly reduced the number of RG-like stem cells and proliferation in the dentate gyrus (Favaro et al., 2009). Interestingly, gene targets of SOX2 such as the nuclear tailless receptor (TLX) and the morphogen Sonic hedgehog (SHH) are essential regulators of adult neural stem cell proliferation as well (Niu et al. 2011; Lai et al., 2003; Machold et al., 2003; Shi et al., 2004; Ahn and Joyner, 2005).

How neural stem cells can respond to such a plethora of multiple signals in a coordinate fashion is not fully understood. One possible explanation of how all these different signals might get integrated into a regulatory network to specifically control stem cell identity comes from embryonic stem cell research. Seminal work by Boyer and colleagues (2005) described a core set of transcription factors that cooperatively regulate the expression of genes, which are essential for embryonic stem cell identity and function (Boyer et al., 2005). Further studies also determined that these core

factors not only converge on same gene targets but also physically interact (van den Berg et al., 2010). Strikingly, this core transcriptional network contains several downstream effectors of signalling pathways, suggesting a molecular model how stem cells might integrate the variety of extrinsic signals into a network maintaining stem cell identity (Chen et al., 2008).

3.3 Notch signalling pathway

The Notch pathway is a highly evolutionary conserved signalling pathway essential for both embryonic development and tissue homeostasis in the adult. Dysregulation of Notch signalling has been implicated in several types of cancer and human disorders (Koch and Radtke, 2011). Notch receptors are large single-pass type-1 trans-membrane proteins, which are maintained in a resting, proteolytically resistant conformation on the cell surface. Ligand binding, which requires cell-cell contact, initiates a proteolytic cascade that releases the Notch intracellular domain (NICD) of the receptor from the membrane (Kovall and Blacklow, 2011). The NICD translocates into the nucleus and activates transcription by binding to the transcription factor RBPJκ (recombination signal binding protein for immunoglobulin kappa J region). This core signalling is called the canonical Notch signalling pathway (Borgrefe and Oswald, 2009).

.
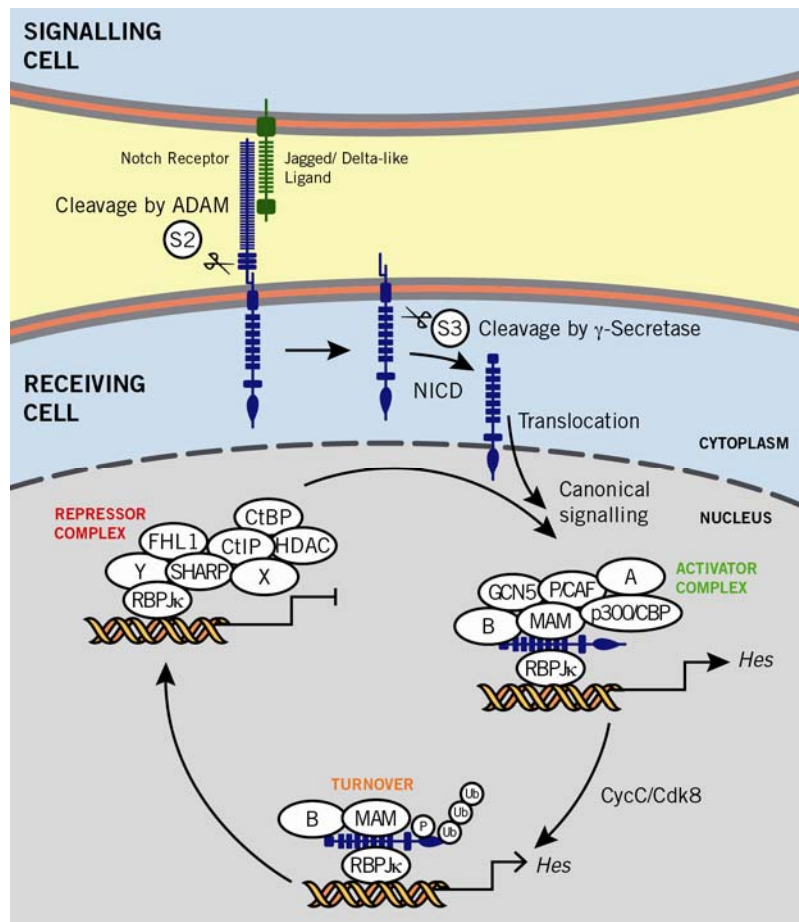
Fig.2 Notch signalling pathway
A) Notch receptors are large single-pass type-1 transmembrane proteins. Ligand binding initiates a proteolytic cascade that releases the Notch intracellular domain (NICD) of the receptor from the membrane. NICD translocates into the nucleus, binds to the transcription factor RBPJκ and activates transcription of Notch target genes such as Hairy and Enhancer of Split (*Hes*) genes. **B**) RBPJκ transcriptional function is determined by the interaction with different protein-cofactors. *Repressor complex*: In the absence of Notch signalling, RBPJκ recruits and interacts with different transcriptional co-repressors to inhibit Notch target gene transcription. *Activator complex*: Upon Notch activation NICD binding to RBPJκ displaces the repressor complex and induces recruitment of co-activators such as Mastermind (MAM) and chromatin modifiers. The assembly of the activator complex leads to transcriptional activation of *Hes*-genes. HES proteins are transcriptional repressors of proneural genes such as *Mash1* or *Neurogenin* and in this line have been associated to neural stem cell maintenance. *Turnover*: Recruitment of MAML1, however, also initiates the turnover of the transcriptional activator complex and proteasomal degradation of NICD. A, B, X, and Z illustrate putative novel interactors (illustration modified from Borgrefe and Oswald, 2009).

Mammals possess four Notch receptors (Notch 1-4), that have both redundant and unique functions, and five canonical transmembrane ligands (Jagged1, Jagged2, Delta-like1, Delta-like3, and Delta-like4) (Borggrefe and Oswald, 2009). The extracellular domain of Notch receptor consists of 29-36 epidermal growth factor

13

(EGF)-like tandem repeats followed by a heterodimerization domain (HD) harboring the unique negative regulatory region (NRR). The HD domain is cleaved during maturation of the Notch precursor protein by furin-like convertases at site 1 (S1) and constitutes the activation switch of the receptor. The cleavage converts the receptor into a heterodimer (extracellular domain, transmembrane and intracellular domain) which is held together in the HD domain by non-covalent interactions. Several reports indicated that EGF repeat 11-12 of Notch is necessary for ligand binding both of Delta-like and Jagged exposed on the cell surface of another cell (Fehon et al., 1990; Rebay et al., 1991). While expression of Notch and ligand in the same cell inhibits Notch signalling (de Celis and Bray, 1997; Klein et al., 1997; Micchelli et al., 1997), binding to ligand *in trans* leads to cleavage by a disintegrin and metalloproteinase (ADAM) at site 2 (S2) in the negative regulatory region. The NRR is essential for preventing cleavage by ADAM in absence of ligands and thus important for activation of Notch signalling (Sanchez-Irizarry et al., 2004). Cleavage by ADAM creates a membrane-tethered intermediate which is then progressively cleaved by the multicomponent enzyme y-secretase from sites 3 and 4 (S3/S4), releasing the intracellular domain. The NICD itself is composed of a RBPJκ association module (RAM) domain, seven ankyrin-repeats (ANK) and a transactivation domain which harbors the nuclear localization signal, a glutamine-rich domain termed OPA (Wharton et al., 1985) together with a proline/glutamic acid/serine/threonine (Pest) motif. The released NICD translocates to the nucleus and interacts through the RAM domain with the Notch nuclear effector RBPJκ [also known as CSL, CBF1 (human), Su(H) (Drosophila), Lag-1 (C.elegans)]. All RBPJκ proteins have a highly conserved core domain of approximately 420 aa, which contains three structural regions: N-terminal domain (NTD), ß-trefoil domain (BTD) and the C-terminal domain (CTD). The NTD and CTD show structural similarity to the Rel homology region, which is present in e.g. the transcription factors nuclear factor kappa-light-chain-enhancer of activated B cells (NF-kB) and nuclear factor of activated T-cells (NFAT) (Kovall and Hendrickson, 2004). In contrast to other Rel-proteins, however, the BTD domain of RBPJκ is located between the NTD and CTD and binds as a monomer to DNA by inserting the NTD into the major groove of the DNA specifically to the core -GGGA- of the consensus sequence 5´-C/TGTGGGAA-3´ (Tun et al., 1994). In the absence of Notch-receptor activation, RBPJκ is functioning as a transcriptional repressor (Hsieh and Hayward, 1995) by directly interacting with co-repressor proteins such as histone

deacetylases (HDAC), silencing mediator of retinoid- and thyroid hormone receptors (SMRT), CBF-1 interacting repressor (CIR), C-terminal binding protein (CtBP) and CtBP-interacting protein (CtIP) (Kovall and Blacklow, 2011; Kao et al., 1998; Hsieh et al., 1999; Oswald et al., 2005). Activation of Notch pathway and binding of NICD to RBPJκ removes the co-repressors and converts RBPJκ into a transcriptional activator (Hsieh and Hayward, 1995; Waltzer et al., 1995). Binding of the ANK domain of NICD to RBPJκ triggers the recruitment of a transcriptional co-activator of the Mastermind family (MAM) (Petcherski and Kimble, 2000; Wu et al., 2000). Formation of the RBPJκ-NICD-MAM ternary complex results in further recruitment of co-activators such as CREB binding protein (CBP), p300 and histone acetyl-transferases (HAT) like GCN5 and PCAF and finally in activation of Notch target genes (Tamura et al., 1995; Kurooka and Honjo, 2000; Kitagawa et al., 2001; Wallberg et al., 2002; Kovall, 2008). The assembly of the RBPJκ-NICD-MAM ternary complex also initiates the turnover of the transcriptional activator complex by recruitment of CycC:CDK8 protein kinase. CycC:CDK8 enhances hyper-phosphorylation of the TAD and PEST domains which leads to Fbw7/Sel10 E3 ubiquitin ligase mediated proteasomal degradation of NICD and termination of transcription (Fryer et al., 2004). Complex modelling and the fact that RBPJκ is predominantly found in nuclei, has led to the assumption that RBPJκ constitutively binds to DNA. Recent findings, however, reported that RBPJκ is also present in the cytosol and that activation of Notch signalling transiently increased RBPJκ on Notch target promoter sites (Krejci and Bray, 2007).

Notch and its ligands are involved in the so called lateral inhibition by activating different gene programs in neighbouring cells leading to distinct cell fates. It has been shown that lateral inhibition is a conserved principle which controls the interplay between stem cells and their progeny to ensure stem cell maintenance as well as the appropriate generation of new cells (Katsube and Sakamoto, 2005). A role for Notch signalling in the regulation of neural stem cells was first implicated by the analysis of Notch1 and RBPJκ mutant mice (de la Pompa et al., 1997). Homozygous Notch 1 KO mice (Swiatek et al., 1994; Conlon et al., 1995) and RBPJκ KO mice (Oka et al., 1995) showed massive developmental abnormalities such as defective somitogenesis and died around embryonic day 11 and 9, respectively. Both phenotypes showed enhanced neuronal differentiation and up-regulation of pro-

neuronal genes such as the <u>b</u>asic <u>h</u>elix-<u>l</u>oop-<u>h</u>elix (bHLH) transcription factors *Mash1* (also known as *Ascl1*), *Neurogenin* as well as *NeuroD*. Recently, studies in Notch1 and in RBPJκ conditional KO mice demonstrated an essential role of Notch signalling in adult stem cell maintenance as well (Ables et al., 2010; Ehm et al., 2010; Imayoshi et al., 2010; Breunig et al., 2007). Loss of RBPJκ in aNSCs resulted in depletion of the stem cell compartment and a transient increase in neurogenesis (Ehm et al., 2010; Imayoshi et al., 2010; Breunig et al., 2007). Ehm and colleagues (2010) found that conditional RBPJκ ablation leads to a transient increase in neurogenesis and finally to the loss of aNSCs. Furthermore, RBPJκ-deficient aNSCs displayed massive self-renewal defects *in vitro*. These results indicate the importance of canonical Notch signalling in adult neural stem cell maintenance and self-renewal capacity.

Interestingly, Ehm and colleagues also found that RBPJκ is directly up-regulating *Sox2*. The transcription factor SOX2 is most closely associated with neural stem cell regulation throughout development (Pevny and Nicolis, 2010) and was shown to be essential for adult hippocampal stem cell maintenance (Favaro et al., 2009). Interestingly, overexpression of SOX2 in RBPJκ deficient neurospheres could rescue aNSC self-renewal *in vitro,* indicating an interaction between Notch signalling and SOX2. The importance of Notch signalling for aNSC maintenance is further supported by findings that loss of Notch1 receptor in hippocampal aNSCs also results in loss of the radial glia-like stem cell population (Ables et al. 2010) and increased neuronal differentiation (Breunig et al., 2007).

Other gene targets of canonical Notch signalling are the <u>H</u>airy and <u>e</u>nhancer of <u>s</u>plit (*Hes*) transcriptional repressors that belong to the bHLH transcription factor family. During embryogenesis *Hes*-genes function as important factors for the development of many organs by maintaining stem- and progenitor cells in an undifferentiated state (Kageyama et al., 2007). HES proteins bind to DNA both as homodimers as well as heterodimers together with other bHLH factors such as HEY1 (<u>He</u>s-related with <u>Y</u>RPW motif1) or HEY2 (Iso et al., 2001; Iso et al., 2002). The mammalian bHLH *Hes*-gene transcription factor family is comprised of seven genes (*Hes1-7*). *Hes1*, *Hes3* and *Hes5* are highly expressed in embryonic neural stem cells but only *Hes1* and *Hes5* are Notch targets. *Hes1* expression can also be regulated through Notch-independent pathways (Hatakeyama et al., 2004). Ablation of *Hes1* or *Hes5* resulted in premature neuronal differentiation and decrease of radial glia cells in developing mice (Ishibashi et al., 1995; Hatakeyama et al., 2004). The decrease of the stem cell

compartment and increase in neurogenesis was even stronger in *Hes1:Hes5* double mutants suggesting a redundant function of both genes during CNS development (Ohtsuka et al., 1998; Ohtsuka et al., 2001). In addition, these studies showed that *Hes1:Hes5* double mutant stem- and progenitor cells in culture also exhibit impaired neurospheres formation. The role of HES1 and HES5 in adult brain is not known so far. Interestingly, using transgenic *Hes5:GFP* reporter mice, it has been shown that *GFP* under the control of the *Hes5* promoter is expressed in Type-1 stem- and progenitor cells in the adult dentate gyrus (Lugert et al., 2010). Moreover, Ehm and colleagues (2010) showed that *Hes1* is also expressed in aNSCs and that *Hes1* is directly regulated by Notch signalling.

HES proteins were described as transcriptional repressors that can inhibit their gene targets either by an active or passive mechanism (Sasai et al., 1992; Ishibashi et al., 1995; Imayoshi et al., 2008a). In the context of stem cells and neurogenesis it is noteworthy that HES proteins suppress pro-neural bHLH transcription factors such as the activators *Mash1*, *E47* (also known as *Cyp4g1*), *Neurogenin 2 (Ngn2)* and *Ngn3*. Passive repression is accomplished by protein interaction of HES proteins with MASH1 or E47. MASH1 normally forms heterodimers with E47 to activate neuronal differentiation genes in progenitor cells. HES1, however, can bind to MASH1 or E47 as well, leading to the formation of non-functional-non-DNA-bound heterodimers (Johnson et al., 1992). On the other hand HES proteins also repress gene target transcription by binding directly to target promoters (active mechanism). In this case, HES can interact with the co-repressor Transducin-like E(spl) genes/Groucho-related gene (TLE/GRG), that recruits histone deacetylases to DNA and thereby inhibits gene transcription (Paroush et al., 1994; Dawson et al., 1995; Grbavec and Stifani, 1996; Chen et al., 1997).

3.4 Forkhead box transcription factors O

Forkhead box (FOX) proteins are an evolutionary conserved family of transcription factors regulating several genes essential for development as well as for the adult organism throughout the animal kingdom (Benayoun et al., 2011; Hannenhalli and Kaestner, 2009). The family is characterized by a 110aa monomeric DNA binding domain, whose three α-helices, three β-sheets and two wing regions form a butterfly-like winged structure (Obsil and Obsilova, 2008). The term Forkhead was named after the *Fork head* mutant in *Drosophila melanogaster* (Weigel et al., 1989).

Currently, over 2000 members are known and subdivided into 19 subfamilies from FOXA to FOXS (Benayoun et al., 2011). The function of these subfamilies is quite diverse, for example: FOXA are pioneer transcription factors and regulate proper gut development, FOXE3 is essential for eye development while FOXP2 is of importance in language acquisition (Ogg et al., 1997; Enard et al., 2002; Cirillo and Zaret, 2007; Medina-Martinez and Jamrich, 2007; Fisher and Scharff, 2009).

The FOXO class of transcription factors has an important role during development and maintenance of various tissues and organs during embryogenesis as well as in the adult organism. Mammalian FOXO proteins are orthologs of DAuer Formation-16 (DAF-16), an essential mediator of insulin signalling in longevity in *Caenorhabditis elegans* (Ogg et al., 1997; Paradis and Ruvkun, 1998; Tissenbaum and Ruvkun, 1998).

In mammals four members have been characterized: FOXO1 (also known as FKHR), FOXO3 (also known as FKHRL1), FOXO4 (also known as AFX or MLLT7) and FOXO6. FOXO1, 3 and 4 show mostly overlapping expression in different organs like in ovary, prostate, skeletal muscle, brain, heart, lung, liver, pancreas, spleen, thymus, and testis. The functionally largely uncharacterized FOXO6 seems to be brain specific (Jacobs et al., 2003). FOXO1, 3 and 4 transcriptional activity is primarily regulated by the PI3K/Akt-kinase pathway while FOXO6 is not regulated by the PI3K/Akt signalling (Jacobs et al., 2003; van der Heide and Smidt, 2005). Upon PI3K activation, Akt kinase translocates into the nucleus and phosphorylates FOXOs at three main phosphorylation sites (Brunet et al., 1999; Nakae et al., 1999). Then, FOXOs bind to 14-3-3 proteins, shuttle out of the nucleus into cytoplasm, become ubiquitinated and are finally degraded by the proteasom (Arden and Biggs, 2002; Van Der Heide et al., 2004; van der Heide and Smidt, 2005). Gene targets of FOXO are involved in many processes such as inhibition of cell-cycle (*p21Cip1, p27Kip1, cyclinG2*), apoptosis (*Fasl, Bim, Bcl-6, Puma*), protection form oxidative stress (*MnSOD, Catalase*), DNA repair (*Ddb1, Gadd45a*) and cellular metabolism (*Pepck, G6pc*) (van der Horst and Burgering, 2007). FOXO transcription factors bind to the core DNA consensus sequence 5´-TTGTTTAC-3´ and can have redundant function (Furuyama et al., 2000; Biggs et al., 2001). Specificity in function of single FOXO members is supposed to be achieved through interaction with other transcriptional co-regulators. In response to oxidative stress, FOXO3 and 4 were shown to interact with the Wnt pathway downstream effector β-catenin (Essers et al., 2005; Almeida et

al., 2007). Intriguingly, in mammalian osteoblast cell lines, binding of FOXO3 to ß-catenin activates FOXO3 gene target transcription but inhibits Wnt gene targets (Almeida et al., 2007). In addition, several publications demonstrated that interaction of FOXO3 and FOXO4 with SIRT1 (sirtuin 1 ,silent mating type information regulation 2, homolog 1) upon oxidative stress differentially regulates expression of FOXO target genes (Brunet et al., 2004; Motta et al., 2004; van der Horst et al., 2004).

FOXO1, 3 and 4 also cooperate with several transcription factors such as STAT5 (signal transducer and activator of transcription 5), RUNX3 (runt related transcription factor 3), FOXG1, RBPJκ, SMAD3 (Mothers against decapentaplegic homolog 3) and SMAD4 (Bakker et al., 2004; Seoane et al., 2004; Yamamura et al., 2006; Kitamura et al., 2007). Seoane and colleagues (2004) demostrated that upon activation of TGFβ signalling the transcriptional effectors SMAD3 and SMAD4 form a complex with FOXOs to activate transcription of the cell cycle inhibitor *p21CIP1*. Furthermore, they indicated that binding of the transcription factor FOXG1 to the FOXO:SMAD complex inhibits its transcriptional activity. Finally, FOXO1 also has been described as an interactor of RBPJκ to induce *Hes1* expression in muscle stem and progenitor cells (Kitamura et al., 2007).

FOXO proteins have been implicated in maintenance of a number of stem cell populations such as hematopoietic stem cells, muscle stem- and progenitor cells, mouse spermatogonial stem cells, human embryonic stem cells and neural stem cells (Goertz et al. 2011; Zhang et al., 2011; Kitamura and Ido Kitamura, 2007; Miyamoto et al., 2007; Tothova et al., 2007; Paik et al., 2009; Renault et al., 2009). Work by Tothova and colleagues (2007) for example demonstrated that FOXO1, 3 and 4 triple conditional KO (cKO FOXO1/3/4) mice exhibit a significant decline in the long-term hematopoietic stem cell population. Paik and co-workers (2009) conditionally ablated FOXO1/3/4 in astrocytes and progenitor cells in the embryonic brain and observed less proliferation and decline of SOX2 positive cells in the adult SVZ. This finding was accompanied by another study where FOXO3 KO resulted in less cell proliferation in the adult dentate gyrus and less neurogenesis *in vitro* (Renault et al., 2009). In both studies, however, FOXOs ablation was already present during early development and was not confined to adult neural stem cells. Hence, the precise role of FOXO in adult neural stem cell maintenance remains to be determined.

3.5 TDP-43

TDP-43 (Tar DNA binding protein 43 kDa also known as TARDBP) is a highly conserved and ubiquitously expressed member of the heterogeneous nuclear ribonucleoprotein (hnRNP) family. Major attention was drawn on TDP-43 by the discovery of polyubiquitinated and hyperphosphorylated TDP-43 inclusions in frontotemporal lobar degeneration with ubiquitinated inclusions (FTLD-U) and amyotrophic lateral sclerosis (ALS) (Neumann et al., 2006). Studies of patients with familiar and sporadic ALS indicated several autosomal dominant mutations in TDP-43 (Lagier-Tourenne and Cleveland, 2009). Furthermore, TDP-43 mutations were also found in patients with Alzheimer disease as well as in Parkinson disease (Amador-Ortiz et al., 2007; Nakashima-Yasuda et al., 2007). TDP-43 protein has two main characteristics: the presence of two RNA recognition motifs (RRMs) and a glycine-rich domain on the C-terminus, which is important for protein-protein interactions e.g. with other hnRNP members (Buratti et al., 2001; Buratti et al., 2005; Maris et al., 2005). Intriguingly, C-terminal 25 kDa fragments of TDP-43 were found in inclusions in brains of ALS- and FTLD-U patients (Neumann et al., 2006). The C-terminal region also contains glutamine (Q) and asparagine (N) rich residues (Fuentealba et al. 2011; Udan and Baloh, 2011). These Q/N-rich domains are related to the prion domain of yeast, which is known to be involved in forming insoluble protein aggregates (Wickner et al., 2004). TDP-43 is mostly localized in the nucleus. However, TDP43 contains in addition to a nuclear localization signal (NLS) also a nuclear export signal (NES) and was shown to be capable to shuttle between nucleus and cytoplasm (Ayala et al., 2008).

G287S G298S G335D N352S A382T
G290A A315T M337V R361S A382P
N267S G294A A321G Q343R P363A I383V
G294V A321V N345K Y374X N390D
G295R Q331K G348C S379P N390S
K263E G295S S332N G348V S379C S393L

D169G

| NLS | | RRM1 | | RRM2 | NES | | Glycine-rich domain |

106   176   191   262 274   414
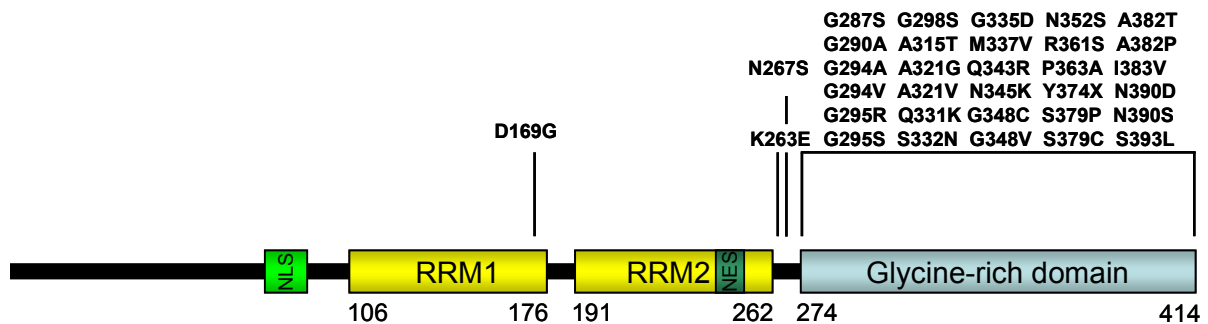
Fig. 3 Schematic representation of human TDP-43
TDP-43 belongs to the hnRNP family. It contains two RNA recognition motifs (RRM) and one glycine-rich domain, which is important for protein-protein interaction. Genetic mutations associated with Amyothropic lateral sclerosis (ALS) and frontotemporal lobar degeneration (FTLD) in human patient are mostly localized in the C-terminal glycine-rich domain. NES: nuclear export signal, NLS: Nuclear localization signal.

Consistent with the function of other hnRNP family members TDP-43 has been described to regulate splicing, such as splicing of human cystic fibrosis transmembrane conductance regulator (CFTR) (Buratti and Baralle, 2001), survival of motor neuron (SMN) (Bose et al., 2008), apolipoprotein A2 (APOA2) (Mercado et al., 2005) and serine/arginine-rich splicing factor 2 (also known as SC35) (Dreumont et al., 2010). Several studies demonstrated that TDP-43 preferentially binds UG-rich motifs near 5´splice sites (5´SS) of pre-mRNA to enhance exon excision (Tollervey et al., 2011; Buratti and Baralle, 2001; Buratti et al., 2001; Mercado et al., 2005). Work by Passoni and colleagues (2011), however, showed that TDP-43 binding to UG-rich sequences does not only activate but also inhibit recognition of the 5´SS by other splicing regulators (Passoni et al. 2011). Moreover, recent studies using high-throughput sequencing of RNA isolated by crosslinking immunoprecipitation (HITS-CLIP) indicated that TDP-43 also binds to non UG-rich repeats of multiple RNAs (more than 6000 RNAs including non-coding RNAs) (Polymenidou et al.; 2011 Tollervey et al., 2011). Interestingly, both studies indicate an enrichment of TDP-43 bound RNAs that are related to neuronal development and synaptic activity. In addition to its role in splicing, TDP-43 has been described to be involved in mRNA stabilization (Godena et al.; 2011 Strong et al., 2007). Godena et al., (2011) reported that binding of TDP-43 to the mRNA of microtubule-associated protein 1b (Map1b also known as futsch) is essential to prevent defects in synaptic microtubular organization in *Drosophila*. Apart from its function in mRNA processing, TDP-43 has also been suggested to be involved in the regulation of micro-RNA (miRNA)

biogenesis. The suggestion is mainly based on findings, which indicate that TDP-43 binds to the miRNA processing complex Drosha as well as that knockdown of TDP-43 alters the level of several miRNAs (Buratti and Baralle, 2011; Ling et al., 2010).

Aside its functions in RNA processing, TDP-43 has also been described as a DNA binding protein. Indeed, TDP-43 has been originally shown to bind the (poly) pyrimidine-rich region of the TAR DNA of the human immunodeficiency virus 1 gene (*Hiv1*) and to inhibit its transcription (Ou et al., 1995). More recently, Acharya and colleagues (2006) reported that TDP-43 can bind to the 5´-TGTGTG-3´ sequence in the murine *acrv1* (also known as SP10) promoter and that mutation of both binding sites led to premature transcription of *acrv1* in spermatocytes (Acharya et al., 2006). In this regard, a study by Lalmansingh and colleagues (2011) using chromatin immunoprecipitation (ChIP) assays indicated that TDP-43 directly interacts with the endogenous *acrv1* promoter in germ cells. Moreover, overexpression of TDP-43 inhibited the transcription of *acrv1* in reporter assays (Lalmansingh et al., 2011). The precise role of TDP-43 in transcriptional regulation, however, is not well characterized and the exact mechanisms how TDP-43 controls transcription of target genes remain to be deciphered.

3.6 Nuclear Factor 1 transcription factors

The <u>N</u>uclear <u>F</u>actor <u>I</u> (NFI) family of transcription factors (also known as <u>C</u>AAT box <u>t</u>ranscription <u>f</u>actor, CTF) was initially described in the context of *in vitro* replication of adenovirus (Nagata et al., 1982; Nagata et al., 1983). Later NFI were found to be key players involved in the regulation of a variety of important developmental genes in multiple vertebrate organs (Mason et al., 2009).

The vertebrate NFI family consists of four members: NFIA, NFIB, NFIC and NFIX. The NFI protein contains a conserved 220aa DNA binding and dimerization domain on the N-terminus and a highly variable proline rich C-terminal transactivation domain including a NLS (Mermod et al., 1989; Fletcher et al., 1999). NFI can bind as homo- or heterodimer to the palindromic consensus binding sequence 5´-TTGGCn^{5}GCCAA-3´ (das Neves et al., 1999; Gronostajski, 2000). However, it is not clear yet whether dimerization combinations display distinct target gene specificity. Furthermore, it was demonstrated that, although DNA binding is stronger when NFI bind to the palindromic site, it can also bind single site specific with lower binding affinity (Meisterernst et al., 1988). *Nfia*, *Nfib* and *Nfix* expression in embryonic- and postnatal

mouse brain, in particular in developing neocortex and midbrain, were first indicated by *in situ* hybridizations (Chaudhry et al., 1999). Immunohistochemistry staining in brain slices of P5 mice and in E16 cortical cultures showed expression of NFIA and NFIB in neurons as well as glia. In the adult brain, *in situ* hybridizations suggested *Nfia* and *Nfib* mRNA expression in both neurogenic niches. Intriguingly, *Nfib* mRNA was found to be enriched in neurogenic astrocytes from adult SVZ compared to non-neurogenic astrocytes from diencephalon (Beckervordersandforth et al., 2010). In contrast to the other members of NFI, only very little expression of *Nfic* mRNA in developing brain was found (Chaudhry et al., 1999). KO of NFIA and NFIB resulted in agenesis of the corpus callosum (ACC), enlarged lateral ventricles and reduced GFAP expression (das Neves et al., 1999; Shu et al., 2003; Steele-Perkins et al., 2005). Both KO mutants die at birth or perinatally. KO mutants of NFIX also revealed enlarged lateral ventricles but have normal lifespan if fed soft diet (Driller et al., 2007; Campbell et al., 2008).

NFI have been most prominently associated with the expression of glia-specific genes (Bisgrove et al., 2000; Cebolla and Vallejo, 2006). In chick embryonic spinal cord development, NFIA and NFIB were shown to regulate gliogenesis by up-regulation of the astrocytes-specific genes *Gfap* and *Glast* (also known as *Slc1a3*). Furthermore, it was suggested that NFIA is required for the continued inhibition of neurogenesis by inducing *Hes5* expression in VZ progenitors (Deneen et al., 2006). Interestingly, Namihira and colleagues (2009) demonstrated that activation of Notch pathway in neuronal precursor cells of E11.5 mice induces NFIA expression, which subsequently binds to the promoter of *Gfap* (Namihira et al., 2009). Strikingly, overexpression of NFIA resulted in demethylation of the STAT3 binding site on the *Gfap* promoter, thus allowing for its expression during astrocytic differentiation of embryonic neural stem cells. Recently, Piper and colleagues showed that differentiation of telencephalic ventricular zone progenitors is delayed in NFIA KO mice (Piper et al., 2010). Furthermore, transcriptome analysis of E16 hippocampal KO tissue revealed an up-regulation of Notch target genes *Hes1* and *Hes5* leading to the hypothesis that NFIA activation during embryogenesis inhibits Notch dependent progenitor self-renewal and induce gliogenesis (Piper et al., 2010). In this line, Subramanian et al., (2011) showed that in utero electroporation of full-length *Nfia*-GFP construct leads to massive astro-gliogenesis in developing hippocampus of the

embryos (Subramanian et al., 2011). Overall, these findings demonstrate an essential role of NFI in regulation of glia-specific genes and embryonic gliogenesis. Previous studies, however, also indicated that NFI mediate the expression of neuronal-specific genes. Wang and colleagues (2004) demonstrated binding of nuclear factors to the promoter of GABA type A receptor (*Gabra6*) and that ablation of NFIA greatly reduces GABRA6 expression *in vivo* (Wang et al., 2004). Moreover, Zheng et al., (2010) indicated a NMDA receptor activity dependent induction of *Nfia* expression and subsequent effect of NFIA on the survival of cortical primary neurons in culture (Zheng et al., 2010). So far, the exact role of NFI in adult brain, in particular in adult neurogenesis, has not been described.

3.7 Objectives of this study

There is increasing evidence that stem cell function may be controlled by a core transcriptional network which interacts on a biochemical level and cooperatively controls large sets of target genes (Boyer et al., 2005; Chen et al., 2008, van den Berg et al., 2010). The components of such regulatory network controlling adult hippocampal neural stem cell identity/function are largely unknown. Recent work by Ehm and colleagues (2010) demonstrated that Notch signalling and the transcriptional downstream effector RBPJκ are essential for neural stem cell maintenance in the adult hippocampus (Ehm et al., 2010). The overall aim of this work was to identify new candidate factors that regulate stem cell maintenance through cooperation with- or modulation of RBPJκ activity. To this end two experimental approaches were followed: a candidate approach and an unbiased approach. First I studied factors which have been demonstrated to play a role in stem cell maintenance of different stem cell systems. To gain more insight into a putative regulatory network and to decipher new candidates of Notch signalling mediated neural stem cell maintenance I performed mass spectrometry analyses of RBPJκ interacting proteins.

4 Results

4.1 Notch signalling pathway and FOXO

4.1.1 RBPJκ interacts with FOXO proteins

In the first set of experiments, I pursued a candidate approach. FOXO1, 3 and 4 transcription factors have recently been implicated in stem cell maintenance of various tissues and organs during embryogenesis as well as in the adult organism. Moreover, work in the myoblast cell line C2C12 indicated that FOXO1 and 3 can interact with RBPJκ and modulate the expression of Notch targets, raising the intriguing possibility that FOXO may cooperate with RBPJκ to modulate stem cell maintenance (Kitamura et al., 2007).

To further examine this possibility, the expression of FOXO1 and 3 in the adult mouse hippocampal neurogenic niche was studied using immunofluorescent staining against FOXO1 and 3. Analysis of these stainings in coronal brain slices of 8 week old mice revealed broad expression of FOXO1 and 3 in the dentate gyrus (Fig. 4). NSC in the adult hippocampus can be identified on the basis of SOX2 expression and the presence of a GFAP-positive radial process (Ferri et al., 2004). Using these criteria it was found that FOXO1 and 3 were indeed expressed in the hippocampal neural stem cell population (Fig. 4). Lack of suitable antibodies against FOXO4 precluded analysis of expression and further biochemical characterization of FOXO4.
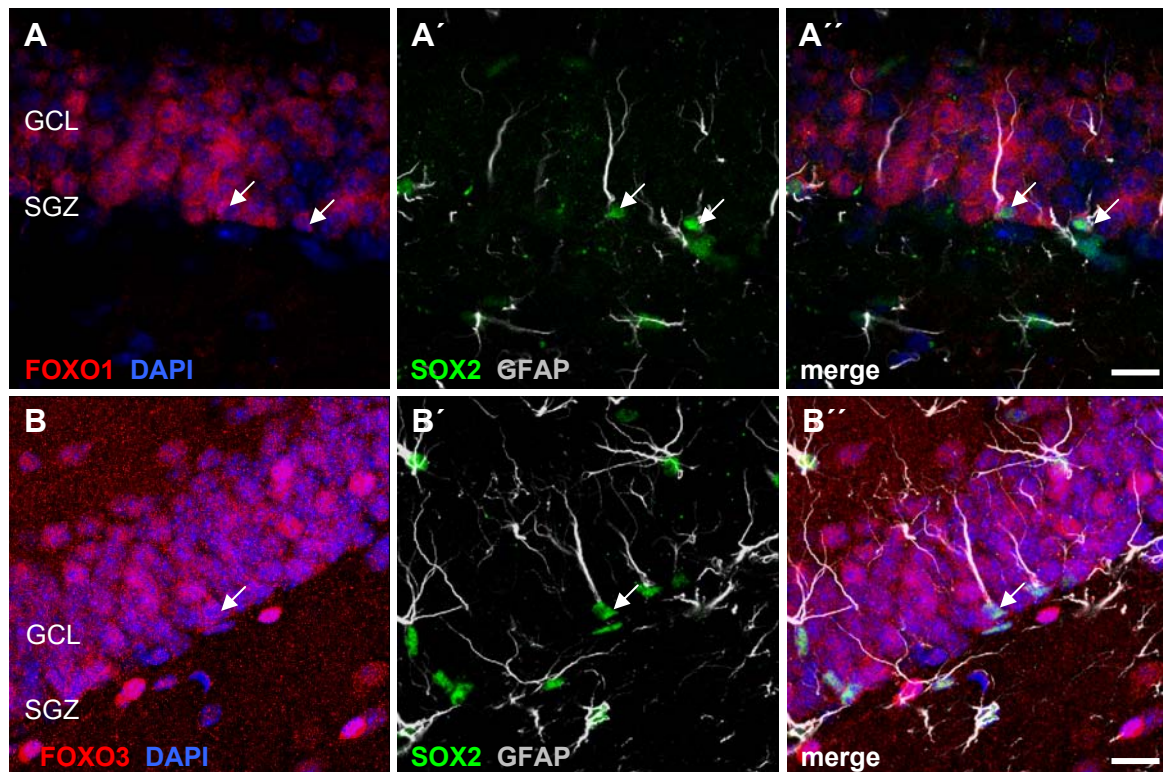
Fig. 4 FOXO1 and FOXO3 expression in the granular layer of dentate gyrus
Representative confocal images of immunofluorescent stainings of FOXO1 and
FOXO3. FOXO1 (red) **(A)** and FOXO3 (red) **(B)** are co-expressed with SOX2 (green)
and GFAP (grey) positive radial glia-like stem cells (arrows) in SGZ of DG. DAPI for
nuclear counterstain in blue, scale bars 20 µm, GCL Granular cell layer, SGZ
subgranular zone, DG dentate gyrus (data obtained in collaboration with Dr. Khan
Helmholtz Center Munich).

Next, I determined whether FOXO1 and 3 could interact with RBPJκ in adult neural
stem cells. To this end, nuclear protein extracts were prepared from neurospheres at
early passages, maintained under proliferative conditions. Co-immunoprecipitation
(CoIP) experiments were performed using antibodies directed against FOXO1, 3 or
non-immune IgGs as a control. Immunoprecipitated proteins were then separated by
SDS-PAGE and transferred to a PVDF membrane by immunoblotting. Membranes
were subsequently incubated with antibodies against RBPJκ. The result of the CoIP-
experiments (Fig. 5) shows the presence of interaction between FOXO1 as well as
FOXO3 and RBPJκ in the nuclei of adult neural stem cells.
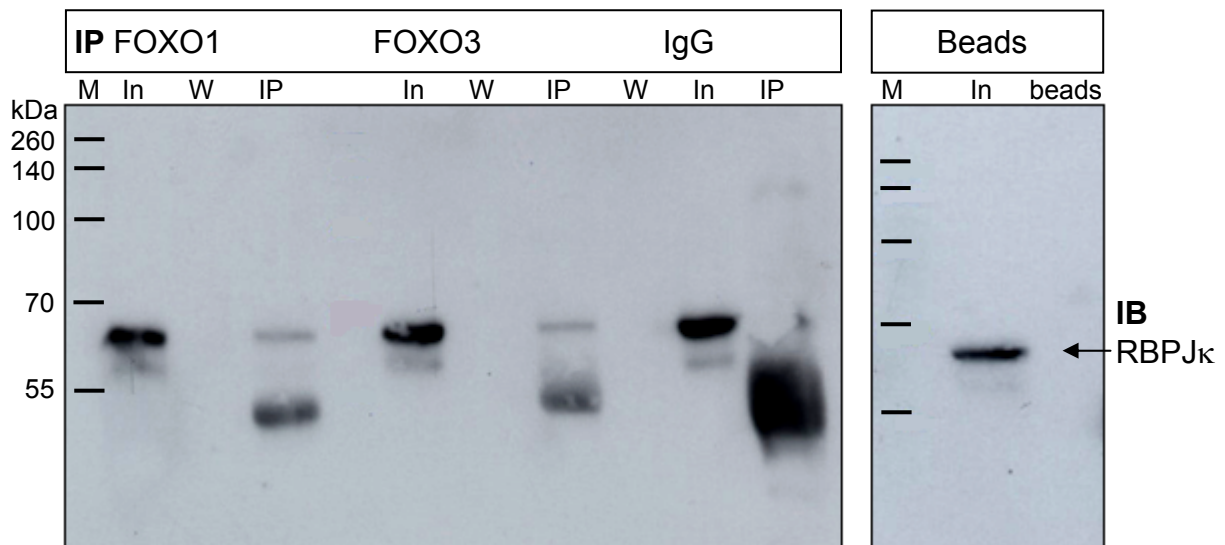
Fig. 5 FOXO1 and FOXO3 co-precipitate with RBPJκ

Representative immunoblot (IB) showing co-immunoprecipitation of FOXO1 and FOXO3 with RBPJκ. Nuclear protein extracts from SVZ neurospheres were incubated for 3 hours at 4°C with antibodies against FOXO1, FOXO3 or non-immune IgGs. Immunoprecipitates were separated by SDS-PAGE, proteins were then transferred to a PVDF membrane and hybridized with an antibody raised against RBPJκ. Non-immune IgGs or beads were used as a control to monitor unspecific binding. Input (In) resembles 5% of total nuclear protein used for IP. M: Molecular marker; W: supernatant of last washing step of Protein G Sepharose beads.

4.1.2 FOXO transcription factors modulate expression of the Notch target gene *Sox2*

The presence of FOXO1 and FOXO3 in SOX2 positive radial glia-like stem cells and their interaction with RBPJκ in isolated neural stem cells raised the question whether FOXO1 and 3 may modulate the expression of RBPJκ target *Sox2* in neural stem cells. Previous studies have shown that the 5 kb DNA region upstream of the transcription start site is important for *Sox2* expression in the telencephalon (Zappone et al., 2000). In silico analysis of this region using the Genomatix El Dorado suite and UCSD genome browser (www.genome.ucsc.edu) predicted one FOXO binding site on the sense (#1 -4833 nt to -4827 nt upstream of transcription start site) and three binding sites on the antisense strand (#2: -1981 nt to -1975 nt; #3: -1694 nt to -1688 nt and #4 -276 nt to -270 nt) of the *Sox2* promoter (Fig. 6).
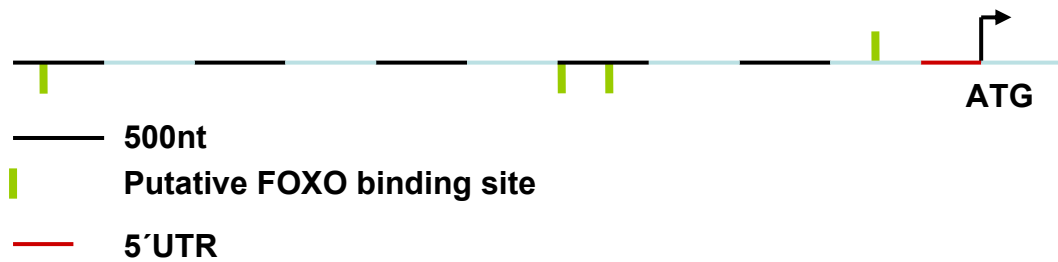
Fig. 6 Mouse *Sox2* promoter region
In silico analysis of 5 kb DNA region upstream of the transcription start site that has previously been shown to control *Sox2* expression. Predicted FOXO binding sites are shown as green bars. Locations of the putative binding sites are: #1: -4833 nt to -4827 nt; #2: -1981 nt to -1975 nt; #3: -1694 nt to -1688 nt; #4 -276 nt to -270 nt (values are referring to the position upstream of transcription start site). Black/grey bars represent 500 nt, red bar shows the 5´UTR, nt nucleotides.

To investigate, whether FOXOs might regulate *Sox2* expression, a *Sox2* promoter reporter construct was used, where the firefly luciferase gene is under the control of the 5,5 kb *Sox2* promoter (Ehm et al, 2010). HEK293T cells were transfected with constitutive active *Foxo1-ADA* (T24A, S253D and S316A; Nakae et al., 1999) and *Foxo3-A3* (T32A, S253A and S315A; Brunet et al., 1999) harbouring three mutations in the main phosphorylation sites of Akt kinase that inhibits nuclear export and thus are constitutively active. As control, expression plasmids containing *GFP* or dominant negative *Foxo1* (Nakae et al., 2001), which lacks the transactivation domain, were used. Luciferase activity was analysed 42h after transfection. Overexpression of FOXO1-ADA significantly increased *Sox2* promoter luciferase activity up to 7-fold. FOXO3-A3 overexpression significantly induced a 11,5-fold increase in promoter activity compared to GFP control. In contrast the dnFOXO1 did not result in *Sox2* promoter activation but rather appeared to decrease promoter activity (0.6-fold induction) (Fig. 7).
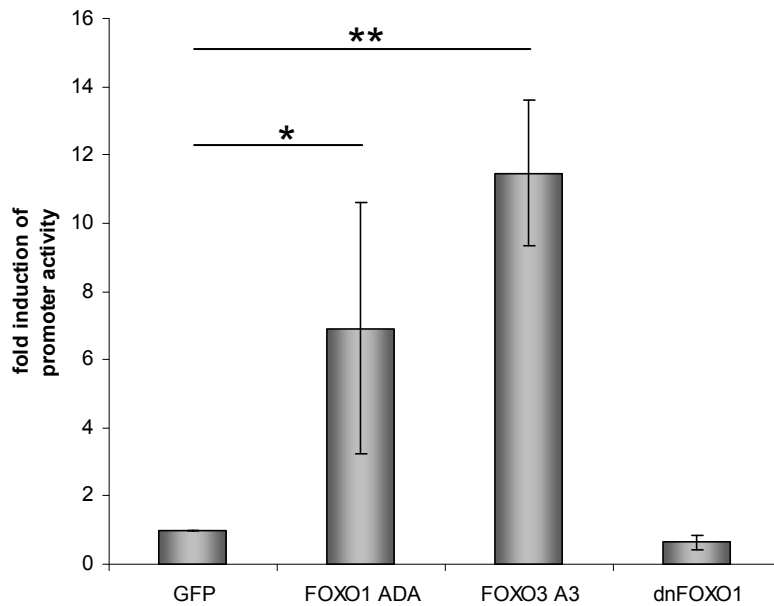
Fig. 7 FOXO1 and FOXO3 activate *Sox2* promoter driven luciferase expression
Luciferase reporter assays in HEK293T. Co-transfection of constitutively active
Foxo1-ADA (T24A, S253D, S316A) and *Foxo3*-A3 (T32A, S253A, S315A),
harbouring three mutations in the main phosphorylation sites of Akt kinase that
inhibits nuclear export, together with 5,5 kb *Sox2* promoter luciferase reporter
construct. Overexpression of FOXO1-ADA significantly increased *Sox2* promoter
luciferase activity up to 7-fold. FOXO3-A3 overexpression led to a significant 11,5-
fold increase. In contrast, dnFOXO1 which lacks the transactivation domain did not
enhance *Sox2* promoter activation (0.6-fold induction). Results represent the mean ±
SEM of 3 independent experiments performed in triplicate (*$p < 0.05$, **$p < 0.01$).

These results suggest that FOXO1 and FOXO3 modulate the expression of
Notch/RBPJκ targets in neural stem cells. Indeed, further analysis in Glast::CreER^{T2}
x Foxo1/3/4$^{loxP/loxP}$ x Rosa26::βGal mice, performed by Dr. Amir Khan (Helmholtz
Center Munich), revealed that conditional KO of FOXO1, 3 and 4 in adult
hippocampal NSCs led to a slowly progressive loss of NSC activity. To this end, the
expression pattern of glutamine synthetase (GS) in Nestin-GFP reporter mice, which
express GFP under the stem cell specific *Nestin* promoter, was studied. GS was
shown to be mainly expressed by astrocytes (Suarez et al., 2002). Analysis of GS
expression in coronal brain slices of 8 week old Nestin-GFP reporter mice
demonstrated that GS is expressed in radial glia-like cells, which are GFP negative.
This result indicated that GS is expressed in RG-like cells which are supposed to be
astrocytes lacking NSC activity (Fig. 8A). In this regard, GS expression was absent in
Nestin-GFP expressing RG-like stem cells (Fig. 8A). Subsequent analysis of the DG
of 8 month old FOXO1/3/4 conditional KO and control mice indicated a significant
increase of recombined β-galactosidase (β-Gal)- and GS positive RG-like cells

compared to all recombined RG-like cells suggesting a progressive loss of NSC activity in FOXO1/3/4 conditional KO mice (Fig. 8B,C,D). As a control, Glast::CreER^{T2} x Foxo1/3/4$^{loxP/+}$ x Rosa26::βGal mice, in which only one allele of each *Foxo*-gene is deleted upon induction of CRE mediated recombination, were used. Animals were analysed 8 month after induction of recombination with tamoxifen.
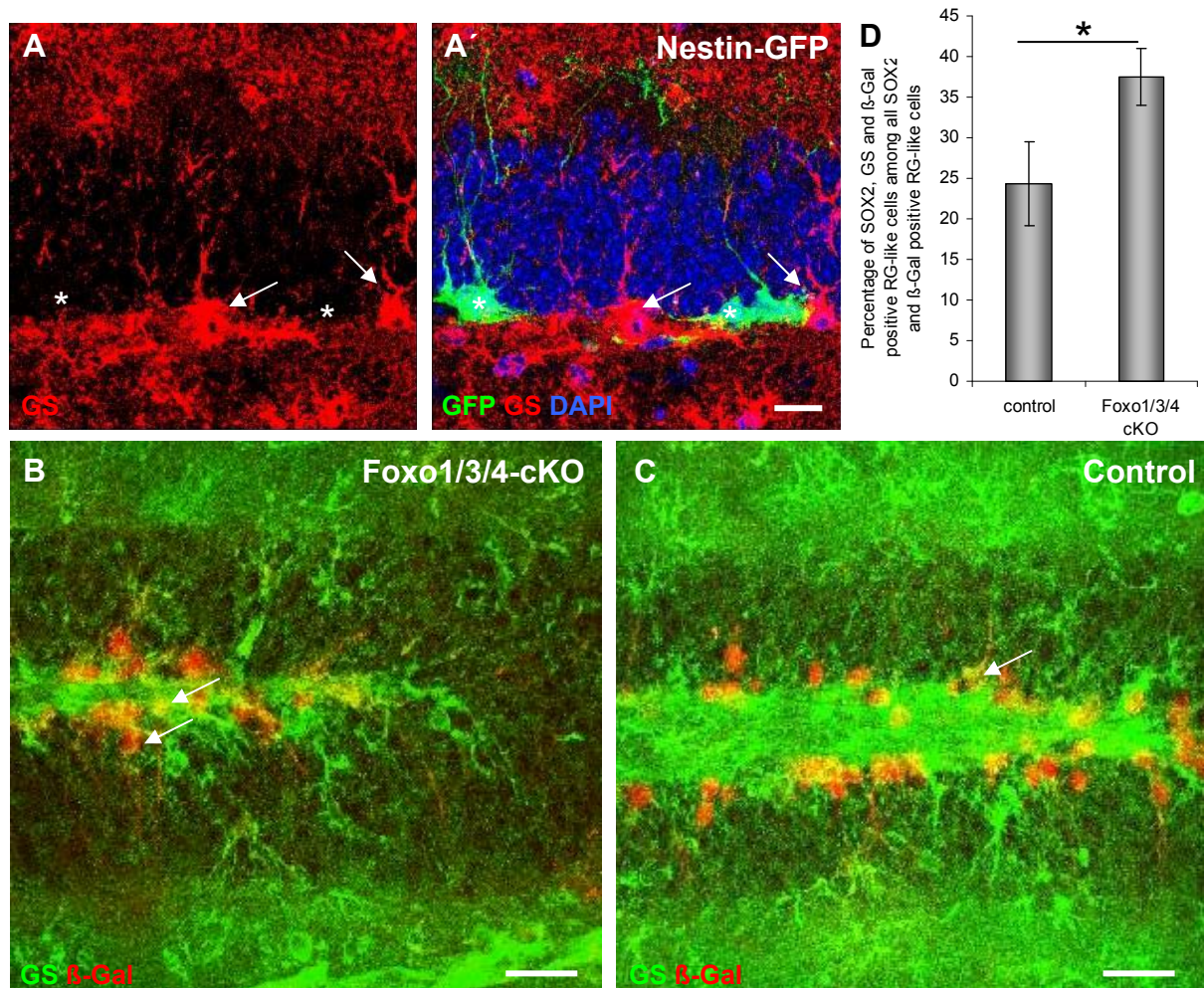
Fig. 8 Analysis of glutamine synthetase (GS) expression in RG-like stem cells in SGZ of *Foxo1/3/4*-cKO mice 8 months after induction of recombination
(A) Representative confocal images of Nestin-GFP reporter mice indicate GFP positive RG-like stem cells (green) that are GS (red) negative (asterisks). The presence of GS positive cells with RG-like morphology, that are GFP negative (arrows), might indicate the loss of stem cell identity. DAPI for nuclear counterstain in blue. **(B)** Analysis of *Foxo1/3/4*-cKO mice revealed an increase of recombined β-Gal positive (red) RG-like cells expressing GS (green) compared to **(C)** control mice, in which only one allele each of FOXO1/3/4 is deleted upon Cre-mediated recombination, suggesting less NSC activity in F*oxo1/3/4*-cKO mice. Scale bar (A) 20 µm, (B) 30 µm. **(D)** The percentage of GS positive SOX2 and β-Gal expressing recombined RG-like stem cells among all SOX2 and β-Gal expressing recombined RG-like stem cells is significantly increased in *Foxo1/3/4*-cKO. Results represent the mean ± SEM of 3 independent experiments (*p<0.05; data obtained in collaboration with Dr. Amir Khan, Helmholtz Center Munich).

Taken together, these results suggest that RBPJκ might cooperate with FOXO1 and FOXO3 in the regulation of adult neural stem cell maintenance. The interaction of Notch/RBPJκ signalling pathway and FOXO1/3 further raised the hypothesis that RBPJκ also might interact with other transcription factors in the control of aNCSs.

4.2 New regulators of adult neural stem cell maintenance

Next, I sought to identify new components of the transcriptional regulatory network underlying adult neural stem cells maintenance using an unbiased strategy. To this end, the proteome/interactome of RBPJκ in adult neural stem cells was analysed. NSCs were derived from SVZ of adult mouse brain and expanded in culture as free floating neurospheres. Nuclear protein extracts were prepared and co-immunoprecipitation experiments were performed using antibodies raised against RBPJκ or non-immune IgGs as a control. Immunoprecipitated proteins were then labelled with either heavy or light isotope labels (ICPL= isotope coded protein labelling), separated by SDS-PAGE and in-gel digested over night with trypsin. The resulting peptides were analysed by quantitative tandem mass spectrometry (MS/MS, LTQ-OrbiTrap).

4.2.1 Cross-linking of RBPJκ antibodies to Protein G Sepharose beads

As a first step different antibodies raised against RBPJκ were tested for their pull down efficiency (data not shown) and then chemically cross-linked with dimethyl pimelimidate (DMP) to Protein G Sepharose (PGS) beads to minimize the IgG background in adjacent MS/MS. The RBPJκ antibody clone 6E7 (obtained from Dr. Kremmer, Institute of Molecular Immunology Helmholtz Center Munich) recognized all three described mouse RBPJκ isoforms (data not shown; http://www.ncbi.nlm.nih.gov Gene ID: 19664; 54 kDa, 58 kDa and 68 kDa in SDS-PAGE) and was used for all subsequent experiments. Figure 9A displays the result of the cross-linking of the 6E7 clone of RBPJκ antibodies to PGS beads. To verify whether the cross-linked antibody was still capable of detecting RBPJκ, the cross-linked antibody was incubated with nuclear protein extracts (0,5 mg) from neurospheres or with IP buffer (Fig. 9B).
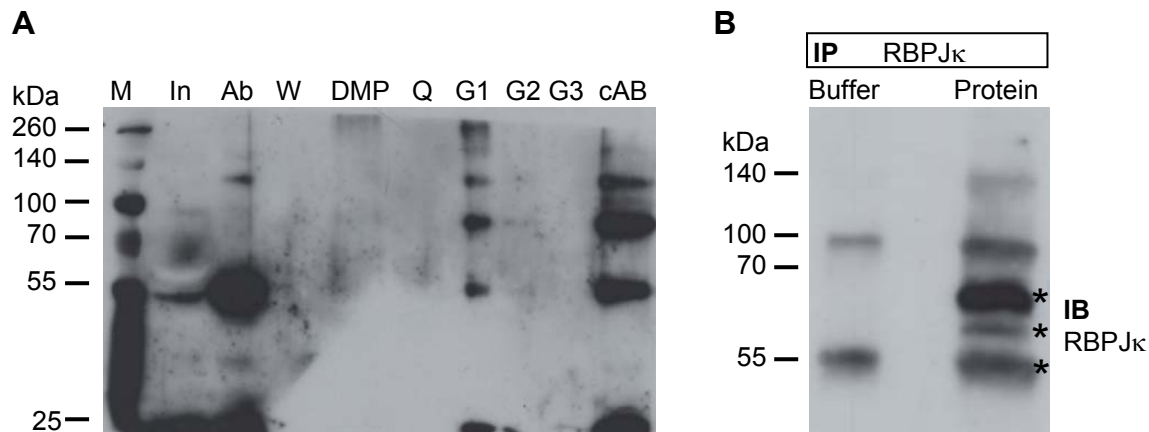
Fig. 9 Cross-linking of RBPJκ antibody and verification of functionality
(**A**) Cross-linking of RBPJκ 6E7 clone to Protein G Sepharose beads. After DMP cross-linking beads were washed 3 times with 100 mM glycine to eliminate non cross-linked IgGs and to minimize IgG background in tandem mass spectrometry analyses. (**B**) To verify of antibody activity, IP with protein or with control IP buffer was performed. Immunoprecipitations performed with cross-linked antibodies against RBPJκ recognized two known RBPJκ isoforms of 58 kDa and 68 kDa (upper two asterisks). The third isoform of 54 kDa (lower asterisk) is masked by antibody heavy-chains in western blot analysis. The lower band at 55 kDa is the heavy IgG chain and the upper ones at 100 and 140 kDa are cross-linked IgG chains. M: pre-stained protein marker; In: antibody input used for cross-linking; Ab: bound antibodies to beads; W: wash; DMP: supernatant after cross-linking; Q: quenching; G1-G3: glycine wash steps; cAb: cross-linked antibodies

4.2.2 Identification of proteins co-purified from RBPJκ immunoprecipitations in adult neural stem- and progenitor cells

Next, several non-quantitative MS/MS experiments were performed with different protein concentrations to determine under which conditions the best signal to noise ratio between specific and unspecific IgG background could be obtained. To ensure reproducibility and to enable the quantitative comparison of proteins specifically co-purified with RBPJκ antibodies, the isotope coded protein labeling (ICPL) approach (Schmidt et al., 2005) was used. For immunoprecipitation experiments, 12 mg of nuclear proteins isolated from neurospheres were used and incubated for 3h at 4°C with cross-linked antibodies raised against RBPJκ or non-specific IgGs. After IP proteins were labelled (ICPL) at their free amino groups either with heavy isotopes (RBPJκ IP) or with light isotopes (non-immune IgGs IP) and combined. The combined protein samples were separated by SDS-Page and subsequently in-gel digested with trypsin. After enzymatic cleavage, peptides were analysed with tandem

mass spectrometry (LTQ-Orbitrap) and the ratio of heavy to light isotopes was calculated by ICPL Quant software (Brunner et al., 2010).

471 proteins showed more than 2-fold enrichment in the RBPJκ immunoprecipitations relative to control (Table 1). Several interacting proteins of the already known RBPJκ transcriptional activator/repressor complex like Four and a half Lim domains (FHL1; Taniguchi et al., 1998), HDACs (Kao et al., 1998), CtBP (Oswald et al., 2005) and RBPJκ itself could be identified. These known RBPJκ interacting factors, however, were not labelled by ICPL (see discussion) and were therefore not included in the protein screen result (Table 1). To classify and group the identified factors Gene Ontology GO database analyses were performed.

Consistent with the previously described role of RBPJκ in gene expression (Tanigaki and Honjo) GO database analyses revealed enrichment in DNA binding proteins (101 genes) and proteins involved in transcription (83 genes). Interestingly, there was also extensive enrichment in RNA binding proteins (157 genes) and splicing factors (54 genes). Beside general roles in cell function, KEGG pathway analyses (http://www.genome.jp/kegg/pathway.html) also determined enrichment of co-purified proteins in neurodegenerative diseases such as Morbus Huntington (38 genes), Morbus Alzheimer (34 genes) and Morbus Parkinson (33 genes).
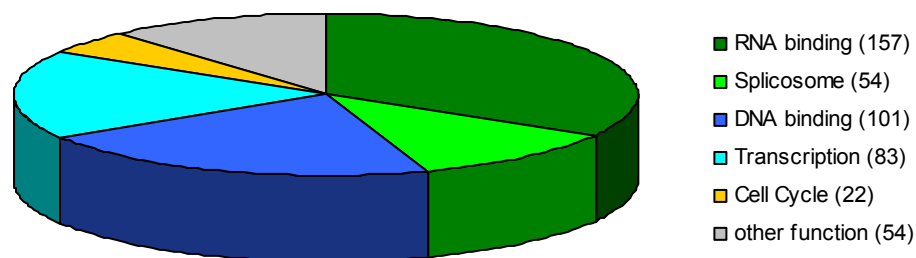
Fig.10 Gene ontology analyses of proteins co-purified with RBPJκ and identified by quantitative tandem mass spectrometry
GO analyses revealed enrichment in DNA binding proteins (101 genes) and proteins involved in transcription (83 genes). These findings could support previous studies that described a function of RBPJκ in gene expression. Moreover, there was also extensive enrichment in RNA binding proteins (157 genes) and splicing factors (54 genes).

Table 1. Co-purified proteins from RBPJκ immunoprecipitations in adult neural stem cells

Name	Symbol	Mw [kDa]	Accession	PSM	Peptides	Heavy/Light
MAGUK p55 subfamily member 2	Mpp2	61,5	Q9WV34	3	2	88,325
Cartilage acidic protein 1	Crac1	70,3	Q8R555	4	3	87,459
Protein phosphatase Slingshot homolog 2	Ssh2	158,1	Q5SW75	5	4	86,270
Cell death regulator Aven	Aven	37,2	Q9D9K3	3	2	81,733
SH3 domain-containing RING finger protein 3	Sh3rf3	93,1	Q8C120	4	1	80,385
Ig kappa chain V-V regions	Kv5ag	12,0	P01649	33	2	68,834
DNA damage-binding protein 1	Ddb1	126,8	Q3U1J4	6	4	55,770
Serologically defined colon cancer antigen 1 homolog	Sdccag1	121,1	Q8CCP0	2	2	51,230
Neuronal PAS domain-containing protein 3	Npas3	100,4	Q9QZQ0	9	6	46,290
Glycylpeptide N-tetradecanoyltransferase 1	Nmt1	56,9	O70310	1	1	44,974
Putative ATP-dependent RNA helicase DHX57	Dhx57	155,7	Q6P5D3	21	15	38,530
KRR1 small subunit processome component homolog	Krr1	43,5	Q8BGA5	3	3	32,690
ATP-binding cassette sub-family A member 13	Abca13	568,5	Q5SSE9	14	8	32,652
Constitutive coactivator of PPAR-gamma-like protein 1	Fam120a	121,6	Q6A0A9	17	9	29,740
ADP-ribosylation factor-like protein 8B	Arl8b	21,5	Q9CQW2	1	1	29,625
Pleckstrin homology domain-containing family H member 1	Plekhh 1	150,8	Q80TI1	6	5	27,010
Symplekin	Sympk	142,2	Q80X82	5	5	26,424
Regulator of differentiation 1	Rod1	56,7	Q8BHD7	10	5	26,038
Probable ATP-dependent RNA helicase DDX47	Ddx47	50,6	Q9CWX9	18	6	24,955
Superkiller viralicidic activity 2-like 2	Skiv2l2	117,6	Q9CZU3	3	3	23,784
Protein disulfide-isomerase TMX3	Tmx3	51,8	Q8BXZ1	2	2	23,039
Transcription factor SOX-1	Sox1	39,2	P53783	7	3	19,613
SRA stem-loop-interacting RNA-binding protein	Slirp	12,6	Q9D8T7	4	3	19,424
Nuclear cap-binding protein subunit 1	Ncbp1	91,9	Q3UYV9	12	9	19,327
Probable ATP-dependent RNA helicase DHX36	Dhx36	113,8	Q8VHK9	22	12	19,307
Putative Polycomb group protein ASXL2	Asxl2	147,0	Q8BZ32	18	3	19,082
Probable saccharopine dehydrogenase	Sccpdh	47,1	Q8R127	1	1	18,980
WD40 repeat-containing protein SMU1	Smu1	57,5	Q3UKJ7	10	7	18,903

Table 1.   continued

Name	Symbol	Mw [kDa]	Accession	PSM	Peptides	Heavy/Light
Probable ATP-dependent RNA helicase YTHDC2	Ythdc2	161,0	B2RR83	22	16	18,761
Nicalin	Ndn	62,9	Q8VCM8	7	6	18,743
FACT complex subunit SPT16	Supt16h	119,7	Q920B9	9	7	18,465
AP-2 complex subunit mu	Ap2m1	49,6	P84091	2	2	18,385
Dedicator of cytokinesis protein 1	Dock1	214,9	Q8BUR4	14	10	17,819
Ras-related protein Rab-5C	Rab5c	23,4	P35278	8	3	17,722
Eukaryotic translation initiation factor 2 subunit 3, X-linked	Eif2s3x	51,0	Q9Z0N1	8	7	16,989
Endoplasmin	Hsp90b1	92,4	P08113	21	5	16,928
ATP-dependent RNA helicase A	Dhx9	149,4	O70133	239	34	16,927
T-complex protein 1 subunit theta	Cct8	59,5	P42932	5	4	16,454
Pre-mRNA-processing factor 6	Prpf6	106,7	Q91YR7	10	9	15,570
Nucleolar protein 56	Nop56	64,4	Q9D6Z1	3	3	15,392
Cell growth-regulating nucleolar protein	Lyar	43,7	Q08288	19	4	15,384
Leucine-rich repeat-containing protein 6	Lrrc6	55,0	O88978	6	3	14,817
Multivesicular body subunit 12A	Fam125a	28,7	Q78HU3	4	2	14,676
Pre-mRNA-processing-splicing factor 8	Prpf8	273,4	Q99PV0	35	21	14,640
Pre-mRNA-splicing factor 38B	Prpf38b	63,7	Q80SY5	5	3	14,153
Ras-related protein Rab-3B	Rab3b	24,7	Q9CZT8	2	1	14,087
Transmembrane emp24 domain-containing protein 10	Tmed10	24,9	Q9D1D4	2	2	14,015
Lipase maturation factor 1	Lmf1	65,8	Q3U3R4	3	3	13,463
116 kDa U5 small nuclear ribonucleoprotein component	Eftud2	109,3	O08810	11	7	13,439
Cohesin subunit SA-1	Stag1	144,6	Q9D3E6	4	4	13,403
T-complex protein 1 subunit eta	Cct7	59,6	P80313	14	6	13,114
Transmembrane 9 superfamily member 2	Tm9sf2	75,3	P58021	1	1	12,896
Pre-mRNA-processing factor 19	Prpf19	55,2	Q99KP6	12	4	12,830
Fermitin family homolog 2	Fermt2	77,8	Q8CIB5	5	2	12,753
Cullin-associated NEDD8-dissociated protein 1	Cand1	136,2	Q6ZQ38	7	6	12,737
6.8 kDa mitochondrial proteolipid	Mp68	6,7	P56379	9	1	12,615

Table 1. continued

Name	Symbol	Mw [kDa]	Accession	PSM	Peptides	Heavy/Light
Splicing factor 3B subunit 1	Sf3b1	145,7	Q99NB9	37	19	12,603
Epoxide hydrolase 1	Ephx1	52,5	Q9D379	20	5	12,396
Rho guanine nucleotide exchange factor 2	Arhgef2	111,9	Q60875	11	6	12,369
Long-chain fatty acid transport protein 1	Slc27a1	71,2	Q60714	5	5	12,222
Cytoplasmic FMR1-interacting protein 1	Cyfip1	145,1	Q7TMB8	23	13	12,161
Metastasis-associated protein MTA2	Mta2	75,0	Q9R190	4	3	12,086
Clathrin heavy chain 1	Cltc	191,4	Q68FD5	15	10	12,063
Ras-related protein Rab-2A	Rab2a	23,5	P53994	2	2	12,027
Protein argonaute-2	Eif2c2	97,3	Q8CJG0	18	10	11,870
UPF0389 protein FAM162A	Fam126a	17,7	Q9D6U8	9	5	11,626
Sorting nexin-9	Snx9	66,5	Q91VH2	4	3	11,603
Tyrosine-protein kinase BAZ1B	Baz1b	170,5	Q9Z277	9	6	11,557
Structural maintenance of chromosomes flexible hinge domain-containing protein1	Smchd1	225,5	Q6P5D8	8	6	11,335
Traf2 and NCK-interacting protein kinase	Tnik	150,3	P83510	16	8	11,263
Acidic leucine-rich nuclear phosphoprotein 32 family member E	Anp32e	29,6	P97822	8	2	11,210
Amine oxidase [flavin-containing] A	Maoa	59,5	Q64133	6	3	11,082
Ras-related protein Rab-35	Rab35	23,0	Q6PHN9	2	1	11,020
Sphingosine-1-phosphate lyase 1	Sgpl1	63,6	Q8R0X7	3	2	10,964
Nck-associated protein 1	Nckap1	128,7	P28660	5	3	10,678
Splicing factor 3B subunit 3	Sf3b3	135,5	Q921M3	22	11	10,485
4F2 cell-surface antigen heavy chain	4F2	58,3	P10852	12	5	10,455
Sideroflexin-5	Sfxn5	37,3	Q925N0	3	3	10,278
Leucine-rich repeat-containing protein 47	Lrrc47	63,6	Q505F5	6	6	10,230
Serine/threonine-protein kinase SRPK1	Srpk1	73,0	O70551	10	5	10,179
Signal recognition particle 68 kDa protein	Srp68	70,6	Q8BMA6	6	4	10,059
B-cell receptor-associated protein 31	Bap31	27,9	Q61335	2	1	9,949
T-complex protein 1 subunit delta	Cct4	58,0	P80315	9	6	9,947

Table 1. continued

Name	Symbol	Mw [kDa]	Accession	PSM	Peptides	Heavy/Light
Constitutive coactivator of PPAR-gamma-like protein 2	Fam120c	119,7	Q8C3F2	16	8	9,795
Ras-related protein Rab-10	Rab10	22,5	P61027	4	3	9,702
E3 ubiquitin-protein ligase UHRF1	Uhrf1	88,2	Q8VDF2	7	5	9,682
Alpha-parvin	Parva	42,3	Q9EPC1	2	2	9,414
Peroxiredoxin-1	Prdx1	22,2	P35700	1	1	9,288
Mitogen-activated protein kinase kinase kinase kinase 4	Map4k4	140,5	P97820	21	9	9,206
Trinucleotide repeat-containing gene 6A protein	Tnrc6a	203,1	Q3UHK8	2	2	8,873
Putative ATP-dependent RNA helicase DHX30	Dhx30	136,6	Q99PU8	29	18	8,837
Neurocan core protein	Ncan	137,1	P55066	6	5	8,506
T-complex protein 1 subunit beta	Cct2	57,4	P80314	7	5	8,479
Nuclear factor 1 B-type	Nfib	63,5	P97863	44	6	8,404
RNA-binding protein 42	Rbm42	49,8	Q91V81	10	7	8,267
RNA-binding protein 14	Rbm14	69,4	Q8C2Q3	46	12	8,236
Cold shock domain-containing protein E1	Csde1	88,7	Q91W50	9	6	8,093
PHD finger-like domain-containing protein 5A	Phf5a	12,4	P83870	4	2	7,995
Elongation factor 2	Ef2	95,3	P58252	35	16	7,986
Nucleolysin TIA-1	Tia1	42,8	P52912	52	4	7,953
Nuclear pore complex protein Nup160	Nup160	158,1	Q9Z0W3	5	5	7,884
Pre-mRNA-splicing factor CWC22 homolog	Cwc22	104,7	Q8C5N3	23	6	7,830
DnaJ homolog subfamily C member 10	Dnajc10	90,5	Q9DC23	5	4	7,786
Nuclear pore complex protein Nup155	Nup155	155,0	Q99P88	6	5	7,761
Mortality factor 4-like protein 1	Morf4l1	41,5	P60762	3	2	7,739
Ras-related protein Rap-1b	Rap1b	20,8	Q99JI6	4	2	7,714
Coronin-1B	Coro1b	53,9	Q9WUM3	4	3	7,690
Interleukin enhancer-binding factor 2	Ilf2	43,0	Q9CXY6	37	7	7,688
Coatomer subunit alpha	Copa	138,4	Q8CIE6	7	3	7,670
SWI/SNF-related matrix-associated actin-dependent regulator of chromatin subfamily A member 5	Smarca5	121,6	Q91ZW3	26	17	7,667

Table 1. continued

Name	Symbol	Mw [kDa]	Accession	PSM	Peptides	Heavy/Light
Phosphatidylinositol-binding clathrin assembly protein	Picalm	71,5	Q7M6Y3	2	2	7,634
CCR4-NOT transcription complex subunit 1	Cnot1	266,6	Q6ZQ08	11	4	7,478
Metastasis-associated protein MTA1	Mta1	80,7	Q8K4B0	2	2	7,411
Nucleoporin NUP188 homolog	Nup188	196,6	Q6ZQH8	5	5	7,363
Transforming protein RhoA	Rhoa	21,8	Q9QUI0	6	3	7,348
Protein disulfide-isomerase A5	Pdia5	59,2	Q921X9	3	2	7,253
Ras-related C3 botulinum toxin substrate 1	Rac1	21,4	P63001	3	2	7,253
ADP-ribosylation factor-like protein 6-interacting protein 1	Arl6ip1	23,4	Q9JKW0	5	3	7,251
Zinc finger RNA-binding protein	Zfr	116,8	O88532	48	17	7,202
Leucine-rich PPR motif-containing protein, mitochondrial	Lpprc	156,5	Q6PB66	3	2	7,136
Vesicle-associated membrane protein-associated protein A	Vapa	27,8	Q9WV55	10	5	7,110
Putative adenosylhomocysteinase 2	Ahcyl1	58,9	Q80SW1	2	2	7,089
Protein ERGIC-53	Lamn1	57,8	Q9D0F3	5	4	7,081
Luc7-like protein 3	Luc7l3	51,4	Q5SUF2	12	3	7,077
Excitatory amino acid transporter 2	Slc1a2	62,0	P43006	5	2	7,047
Splicing factor 1	Sf1	70,4	Q64213	3	3	7,043
Transmembrane protein 43	Tmem43	44,8	Q9DBS1	3	2	6,962
U1 small nuclear ribonucleoprotein C	Snrpc	17,4	Q62241	3	1	6,934
UPF0681 protein KIAA1033	Kiaa1033	136,3	Q3UMB9	15	3	6,896
Tight junction protein ZO-2	Zo2	131,2	Q9Z0U1	6	6	6,882
Hepatocyte cell adhesion molecule	Hepacam	46,3	Q640R3	9	4	6,866
Ankyrin-2	Ank2	426,0	Q8C8R3	16	8	6,833
Protein FAM50B	Fam50b	39,6	Q9WTJ8	4	2	6,831
Protein RRP5 homolog	Pdcd11	207,6	Q6NS46	9	8	6,831
Meiosis-specific nuclear structural protein 1	Mns1	60,2	Q61884	7	5	6,821
Alpha-(1,6)-fucosyltransferase	Fut8	66,5	Q9WTS2	4	4	6,802
Transmembrane 9 superfamily member 3	Tm9sf3	67,5	Q9ET30	7	4	6,796
Vigilin	Vigln	141,7	Q8VDJ3	132	36	6,708

Table 1. continued

Name	Symbol	Mw [kDa]	Accession	PSM	Peptides	Heavy/Light
A-kinase anchor protein 8	Akap8	76,2	Q9DBR0	4	2	6,697
ATP-dependent RNA helicase DDX3X	Ddx3x	73,1	Q62167	490	23	6,624
Heterogeneous nuclear ribonucleoprotein A/B	Hnrnpab	30,8	Q99020	113	3	6,615
Uncharacterized protein KIAA0090	Kiaa0090	111,5	Q8C7X2	5	5	6,581
Nucleosome assembly protein 1-like 1	Nap1l1	45,3	P28656	2	2	6,526
Centlein	Cntln	160,6	A2AM05	5	4	6,516
Elongation factor 1-gamma	EF1g	50,0	Q9D8N0	14	7	6,502
Dedicator of cytokinesis protein 7	Dock7	241,3	Q8R1A4	12	5	6,494
Protein disulfide-isomerase A4	Pdia4	71,9	P08003	3	2	6,460
Far upstream element-binding protein 2	Fubp2	76,8	Q3U0V1	43	10	6,453
Dihydropyrimidinase-related protein 2	Dpyl2	62,2	O08553	3	2	6,329
Heterogeneous nuclear ribonucleoprotein U-like protein 2	Hnrnpul2	84,9	Q00PI9	97	14	6,291
Transforming acidic coiled-coil-containing protein 3	Tacc3	70,6	Q9JJ11	4	2	6,289
Eukaryotic translation initiation factor 5B	IF2p	137,5	Q05D44	8	6	6,257
ATP-dependent RNA helicase DDX3Y	Ddx3y	73,4	Q62095	379	23	6,159
Abnormal spindle-like microcephaly-associated protein homolog	Aspm	363,9	Q8CJ27	9	9	6,116
Putative pre-mRNA-splicing factor ATP-dependent RNA helicase DHX15	Dhx15	90,9	O35286	26	12	6,064
Disco-interacting protein 2 homolog A	Dip2a	165,2	Q8BWT5	5	5	6,053
Translocation protein SEC63 homolog	Sec63	87,8	Q8VHE0	2	2	6,048
Dynein heavy chain 8, axonemal	Dnahc8	540,9	Q91XQ0	13	6	6,033
S1 RNA-binding domain-containing protein 1	Srbp1	114,0	Q497V5	9	7	6,032
Heterogeneous nuclear ribonucleoprotein L	Hnrnpl	63,9	Q8R081	118	11	6,028
Heterogeneous nuclear ribonucleoprotein H2	Hnrnph2	49,2	P70333	230	14	5,984
Nuclear factor 1 X-type	Nfix	53,4	P70257	36	6	5,972
Regulator of nonsense transcripts 1	Rent1	123,9	Q9EPU0	16	11	5,955
Serrate RNA effector molecule homolog	Srrt	100,4	Q99MR6	27	15	5,897
Leucine-rich repeat-containing protein 59	Lrrc59	34,9	Q922Q8	18	7	5,803
Transcriptional repressor CTCF	Ctcf	83,7	Q61164	5	4	5,799

Table 1. continued

Name	Symbol	Mw [kDa]	Accession	PSM	Peptides	Heavy/Light
Heterogeneous nuclear ribonucleoprotein H	Hnrnph1	49,2	O35737	245	13	5,788
U2-associated protein SR140	Sr140	118,2	Q6NV83	26	12	5,784
DAZ-associated protein 1 GN=Dazap1 SV=2 - [DAZP1]	Dazap1	43,2	Q9JII5	55	7	5,760
Histidine triad nucleotide-binding protein 1	Hint1	13,8	P70349	1	1	5,726
Heterogeneous nuclear ribonucleoprotein U	Hnrnpu	87,9	Q8VEK3	472	18	5,721
Protein FRG1	Frg1	29,1	P97376	2	2	5,713
Calcium/calmodulin-dependent protein kinase type II beta chain	Camk2b	60,4	P28652	24	7	5,713
Transmembrane and coiled-coil domain-containing protein 1	Tmco1	21,2	Q921L3	2	2	5,708
Transcription elongation factor A protein 1	Tcea1	33,9	P10711	4	3	5,702
Guanine nucleotide-binding protein subunit beta-2-like 1	Gblp	35,1	P68040	183	8	5,700
Uncharacterized protein CXorf65 homolog	Cx065	21,6	Q3V2K1	15	1	5,694
Protein RCC2	Rcc2	55,9	Q8BK67	17	6	5,691
Heterogeneous nuclear ribonucleoproteins A2/B1	Hnrnpa2b1	37,4	O88569	1020	13	5,659
Protein quaking	Qki	37,6	Q9QYS9	17	7	5,617
Peptidyl-prolyl cis-trans isomerase NIMA-interacting 4	Pin4	13,8	Q9CWW6	5	2	5,614
La-related protein 7	Larp7	64,8	Q05CL8	7	4	5,596
Poly(U)-binding-splicing factor PUF60	Puf60	60,2	Q3UEB3	4	3	5,595
Excitatory amino acid transporter 1	Eaa1	59,6	P56564	4	2	5,585
Nuclear cap-binding protein subunit 2	Ncbp2	18,0	Q9CQ49	3	3	5,578
Destrin	Dest	18,5	Q9R0P5	3	2	5,577
Serine/arginine repetitive matrix protein 2	Srrm2	294,5	Q8BTI8	17	8	5,489
UPF0027 protein C22orf28 homolog	CV028	55,2	Q99LF4	30	5	5,472
Interleukin enhancer-binding factor 3	Ilf3	96,0	Q9Z1X4	62	10	5,466
RNA-binding protein 10	Rbm10	103,4	Q99KG3	18	10	5,449
Cleavage and polyadenylation specificity factor subunit 5	Nudt21	26,2	Q9CQF3	17	6	5,448
14-3-3 protein theta	Ywhaq	27,8	P68254	2	2	5,444
Small nuclear ribonucleoprotein Sm D1	Snrpd1	13,3	P62315	25	2	5,431
Pleckstrin homology-like domain family A member 3	Phla3	13,7	Q9WV95	2	2	5,425

Table 1. continued

Name	Symbol	Mw [kDa]	Accession	PSM	Peptides	Heavy/Light
Myosin-binding protein C, cardiac-type	Mybp3	140,5	O70468	8	4	5,415
Splicing factor 3 subunit 1	Sf3a1	88,5	Q8K4Z5	9	3	5,404
Splicing factor U2AF 35 kDa subunit	U2af1	27,8	Q9D883	18	5	5,400
Heterogeneous nuclear ribonucleoprotein F	Hnrnpf	45,7	Q9Z2X1	144	13	5,394
Heterogeneous nuclear ribonucleoprotein A3	Hnrnpa3	39,6	Q8BG05	875	12	5,375
CUG-BP- and ETR-3-like factor 1	Cugbp1	52,1	P28659	7	5	5,374
Far upstream element-binding protein 1	Fubp1	68,5	Q91WJ8	69	12	5,357
Probable ATP-dependent RNA helicase DDX17	Ddx17	72,4	Q501J6	500	31	5,357
Heterogeneous nuclear ribonucleoprotein Q	Hnrnpq	69,6	Q7TMK9	233	13	5,336
Splicing factor, arginine/serine-rich 4	Sfrs4	55,9	Q8VE97	29	10	5,336
Protein KIAA0649	Kiaa0649	124,9	Q6A025	9	3	5,322
PDZ domain-containing protein GIPC1	Gipc1	36,1	Q9Z0G0	10	8	5,322
KH domain-containing, RNA-binding, signal transduction-associated protein 3	Khdr3	38,8	Q9R226	24	5	5,299
Forty-two-three domain-containing protein 1	Fyttd1	35,9	Q91Z49	4	4	5,296
Heterogeneous nuclear ribonucleoprotein G	Hnrpg	42,2	O35479	21	4	5,287
Heterogeneous nuclear ribonucleoprotein D-like	Hrnpdl	33,5	Q9Z130	125	4	5,287
DNA (cytosine-5)-methyltransferase 1	Dnmt1	183,1	P13864	15	12	5,265
Coiled-coil domain-containing protein 109A	C109A	39,7	Q3UMR5	4	4	5,258
Glutamate receptor, ionotropic kainate 5	Grik5	109,2	Q61626	4	3	5,250
Cell division cycle and apoptosis regulator protein 1	Ccar1	132,0	Q8CH18	11	6	5,248
Spliceosome RNA helicase Bat1	Bat1	49,0	Q9Z1N5	51	10	5,220
Low-density lipoprotein receptor-related protein 4	Lrp4	211,8	Q8VI56	2	2	5,218
Nucleolysin TIAR	Tiar	43,4	P70318	92	7	5,193
Eukaryotic translation initiation factor 2A	Eif2a	64,4	Q8BJW6	9	3	5,160
Nuclear factor 1 A-type	Nfia	58,5	Q02780	46	8	5,154
Eukaryotic translation initiation factor 3 subunit A	Eif3a	161,8	P23116	19	15	5,146
Plakophilin-1	Pkp1	80,8	P97350	6	4	5,113
Thioredoxin-related transmembrane protein 2	Tmx2	33,9	Q9D710	3	1	5,101

Table 1. continued

Name	Symbol	Mw [kDa]	Accession	PSM	Peptides	Heavy/Light
T-complex protein 1 subunit alpha B	Tcpa2	60,4	P11983	10	3	5,089
Staphylococcal nuclease domain-containing protein 1	Snd1	102,0	Q78PY7	48	15	5,054
Adenomatous polyposis coli protein	Apc	310,9	Q61315	10	6	5,046
Plasminogen activator inhibitor 1 RNA-binding protein	Serbp1	44,7	Q9CY58	72	9	5,038
Splicing factor, arginine/serine-rich 7	Srfr7	30,8	Q8BL97	60	9	5,031
Heterogeneous nuclear ribonucleoprotein D0	Hnrnpd	38,3	Q60668	69	3	4,999
Myb-binding protein 1A	Mybbpia	151,9	Q7TPV4	39	18	4,990
G/T mismatch-specific thymine DNA glycosylase	Tdg	44,1	P56581	2	2	4,988
Ribosomal protein S6 kinase alpha-2	Rps6ka2	83,1	Q9WUT3	4	4	4,970
Heterogeneous nuclear ribonucleoproteins C1/C2	Hnrnpc	34,4	Q9Z204	40	3	4,961
YTH domain family protein 1	Ythdf1	60,8	P59326	22	2	4,949
Splicing factor, arginine/serine-rich 3	Sfrs3	19,3	P84104	39	6	4,940
Phosphoglycerate mutase 1	Pgam1	28,8	Q9DBJ1	9	5	4,933
ATP-dependent RNA helicase DDX1	Ddx1	82,4	Q91VR5	41	13	4,923
T-complex protein 1 subunit epsilon	Cct5	59,6	P80316	7	4	4,899
Heterogeneous nuclear ribonucleoprotein A1	Hnrnpa1	34,2	P49312	699	13	4,893
TBC1 domain family member 10A	Tb10a	56,2	P58802	4	3	4,881
Splicing factor, arginine/serine-rich 2	Sfrs2	25,5	Q62093	43	7	4,877
Cytoskeleton-associated protein 5	Ckap5	225,5	A2AGT5	23	8	4,866
Tight junction protein ZO-1	Zo1	194,6	P39447	44	18	4,866
TAR DNA-binding protein 43	TARDBP	44,5	Q921F2	135	8	4,864
Triosephosphate isomerase	Tpi1	26,7	P17751	2	1	4,843
SAP domain-containing ribonucleoprotein	Sarnp	23,5	Q9D1J3	8	4	4,838
E3 SUMO-protein ligase RanBP2	Ranbp2	340,9	Q9ERU9	11	7	4,832
Eukaryotic translation initiation factor 3 subunit D	Eif3d	63,9	O70194	3	3	4,830
Small nuclear ribonucleoprotein E	Snrpe	10,8	P62305	64	3	4,818
Coiled-coil-helix-coiled-coil-helix domain-containing protein 1	Chchd1	13,6	Q9CQA6	3	1	4,806
Splicing factor, arginine/serine-rich 13A	Sfrs13a	31,3	Q9R0U0	33	8	4,806

Table 1. continued

Name	Symbol	Mw [kDa]	Accession	PSM	Peptides	Heavy/Light
mRNA export factor	Rae1	40,9	Q8C570	8	5	4,780
U2 small nuclear ribonucleoprotein B''	Snrpb2	25,3	Q9CQI7	1	1	4,777
Splicing factor, arginine/serine-rich 1	Sfrs1	27,7	Q6PDM2	251	19	4,765
ELAV-like protein 1	Elav1	36,0	P70372	77	8	4,754
Heterogeneous nuclear ribonucleoprotein K	Hnrnpk	50,9	P61979	324	13	4,753
Spectrin beta chain, brain 1	Sptbn1	274,1	Q62261	24	18	4,726
Alpha-actinin-4	Actn4	104,9	P57780	9	5	4,716
YLP motif-containing protein 1	Ylpm1	155,0	Q9R0I7	10	6	4,713
Moesin	Msn	67,7	P26041	85	20	4,706
Lupus La protein homolog	Ssb	47,7	P32067	38	8	4,703
Surfeit locus protein 4	Surf4	30,4	Q64310	2	1	4,703
RNA-binding protein Musashi homolog 2	Msi2	36,9	Q920Q6	9	2	4,684
Microtubule-actin cross-linking factor 1	MAcf1	607,6	Q9QXZ0	35	17	4,679
Probable ATP-dependent RNA helicase DDX5	Ddx5	69,3	Q61656	635	24	4,654
ATP-binding cassette sub-family E member 1	Abce1	67,3	P61222	2	2	4,651
RNA-binding protein Raly	Raly	33,1	Q64012	17	6	4,639
Septin-7	Sep 17	50,5	O55131	14	4	4,622
Small nuclear ribonucleoprotein-associated protein N	Snrpn	24,6	P63163	103	8	4,617
Septin-11	Sep 11	49,7	Q8C1B7	5	3	4,599
Polyadenylate-binding protein 1	Pabp1	70,6	P29341	108	18	4,595
AP-2 complex subunit alpha-1	Ap2a1	107,6	P17426	11	6	4,562
PHD finger protein 6	Phf6	41,1	Q9D4J7	4	3	4,557
Transcription intermediary factor 1-beta	Trim28	88,8	Q62318	21	6	4,554
Small nuclear ribonucleoprotein Sm D2	Snrpd2	13,5	P62317	132	9	4,527
Z-DNA-binding protein 1	Zbp1	44,3	Q9QY24	2	1	4,525
DNA-(apurinic or apyrimidinic site) lyase	Apex1	35,5	P28352	15	6	4,520
Structural maintenance of chromosomes protein 2	Smc2	134,2	Q8CG48	11	6	4,511
Septin-8	Sep 08	49,8	Q8CHH9	6	3	4,499

Table 1.   continued

Name	Symbol	Mw [kDa]	Accession	PSM	Peptides	Heavy/Light
Splicing factor U2AF 65 kDa subunit	U2af2	53,5	P26369	18	4	4,494
Chromodomain-helicase-DNA-binding protein 4	Chd4	217,6	Q6PDQ2	44	30	4,441
2-5A-dependent ribonuclease	Rnasel	83,2	Q05921	11	4	4,432
Protein disulfide-isomerase A3	Pdia3	56,6	P27773	12	5	4,424
Radixin	Rdx	68,6	P26043	42	11	4,418
Putative oxidoreductase GLYR1	Glyr1	59,7	Q922P9	25	7	4,415
Protein DJ-1	Park7 /DJ1	20,0	Q99LX0	1	1	4,409
Zinc finger protein 326	Znf326	65,2	O88291	6	3	4,400
Protein FAM98A	Fam98a	55,0	Q3TJZ6	14	7	4,395
Putative RNA-binding protein Luc7-like 2	Luc7l2	46,6	Q7TNC4	5	5	4,394
U1 small nuclear ribonucleoprotein 70 kDa	Snrnp70	52,0	Q62376	278	21	4,384
Flap endonuclease 1	Fen1	42,3	P39749	7	5	4,370
T-complex protein 1 subunit gamma	Cct3	60,6	P80318	8	5	4,365
U1 small nuclear ribonucleoprotein A	Snrpa	31,8	Q62189	212	7	4,359
Protein FAM98B	Fam98b	45,3	Q80VD1	12	6	4,357
DNA replication licensing factor MCM4	Mcm4	96,7	P49717	4	4	4,344
Spermatid perinuclear RNA-binding protein	Strbp	73,7	Q91WM1	28	4	4,342
Cellular nucleic acid-binding protein	Cnbp	19,6	P53996	1	1	4,322
Heterogeneous nuclear ribonucleoprotein L-like	Hnrpll	64,1	Q921F4	11	3	4,304
Acyl-CoA desaturase 1	Scd1	41,0	P13516	1	1	4,302
Small nuclear ribonucleoprotein Sm D3	Snrp3	13,9	P62320	52	4	4,302
FK506-binding protein 2	Fkbp2	15,3	P45878	3	1	4,298
Peptidyl-prolyl cis-trans isomerase A	Ppia	18,0	P17742	42	4	4,294
Nuclease-sensitive element-binding protein 1	Ybx1	35,7	P62960	55	7	4,293
Kinesin-like protein KIF26A	Kif26a	196,2	Q52KG5	11	8	4,285
Trinucleotide repeat-containing gene 6B protein	Tnrc6b	191,8	Q8BKI2	6	5	4,277
U2 small nuclear ribonucleoprotein A'	Snrpa1	28,3	P57784	21	10	4,270
RNA-binding protein EWS	Ews	68,4	Q61545	48	9	4,253

Table 1. continued

Name	Symbol	Mw [kDa]	Accession	PSM	Peptides	Heavy/Light
Transcription factor SOX-3	Sox3	37,8	P53784	11	4	4,237
Splicing factor, arginine/serine-rich 5	Sfrs5	30,9	O35326	43	7	4,236
Translationally-controlled tumor protein	Tpt1	19,4	P63028	2	1	4,216
Pinin	Pnn	82,4	O35691	9	8	4,192
Alpha-enolase	Eno1	47,1	P17182	27	5	4,182
Transcription factor Sp3	Sp3	82,3	O70494	5	1	4,182
Peptidyl-prolyl cis-trans isomerase G	Ppig	88,3	A2AR02	12	5	4,177
U5 small nuclear ribonucleoprotein 40 kDa protein	Snrnp40	39,3	Q6PE01	4	3	4,176
Eukaryotic translation initiation factor 4 gamma 3	Eif4g3	174,8	Q80XI3	9	5	4,170
Transcriptional activator protein Pur-alpha	Pura	34,9	P42669	37	9	4,167
UPF0568 protein C14orf166 homolog	Cn166	28,1	Q9CQE8	21	6	4,145
N-acylneuraminate cytidylyltransferase	Neua	48,0	Q99KK2	12	5	4,145
Transcription elongation regulator 1	Tcerg1	123,7	Q8CGF7	33	16	4,142
Splicing factor, arginine/serine-rich 9	Sfrs9	25,6	Q9D0B0	25	3	4,129
Microtubule-associated protein 1S	Map1s	102,9	Q8C052	10	5	4,120
Neuronal pentraxin-1	Nptx1	47,1	Q62443	4	4	4,115
Galectin-1	Leg1	14,9	P16045	2	2	4,104
Zinc finger protein 638	Znf638	218,0	Q61464	13	10	4,101
Septin-9	Sep 09	65,5	Q80UG5	42	11	4,099
Nuclear RNA export factor 1	Nfx1	70,3	Q99JX7	17	11	4,096
Pre-mRNA-splicing factor SYF1	Syf1	99,9	Q9DCD2	4	3	4,075
Septin-2	Sept2	41,5	P42208	31	9	4,073
Spectrin alpha chain, brain	Sptan1	284,4	P16546	35	27	4,057
Pre-mRNA-processing factor 40 homolog A	Prpf40a	108,4	Q9R1C7	12	5	4,051
Protein SON	Son	261,3	Q9QX47	7	4	4,032
Ubiquitin	Ubiq	8,6	P62991	17	2	3,996
Actin, alpha cardiac muscle 1	Actc	42,0	P68033	163	5	3,959
KH domain-containing, RNA-binding, signal transduction-associated protein 1	Khdr1	48,3	Q60749	39	4	3,952

Table 1. continued

Name	Symbol	Mw [kDa]	Accession	PSM	Peptides	Heavy/Light
Rho GDP-dissociation inhibitor 1	Gdir1	23,4	Q99PT1	2	2	3,941
Peptidyl-prolyl cis-trans isomerase H	Ppih	20,5	Q9D868	1	1	3,919
Cofilin-1	Cof1	18,5	P18760	9	2	3,881
Microtubule-associated protein RP/EB family member 1	Mare1	30,0	Q61166	5	2	3,859
RNA-binding protein FUS	Fus	52,6	P56959	174	6	3,855
Creatine kinase B-type	Kcrb	42,7	Q04447	158	12	3,852
Apoptotic chromatin condensation inducer in the nucleus	Acin1	150,6	Q9JIX8	10	5	3,849
Heterogeneous nuclear ribonucleoprotein U-like protein 1	Hnrnpul1	95,9	Q8VDM6	151	17	3,841
Methyl-CpG-binding protein 2	Mecp2	52,3	Q9Z2D6	5	4	3,832
Eukaryotic initiation factor 4A-III	Eif4a3	46,8	Q91VC3	35	10	3,831
MOSC domain-containing protein 2, mitochondrial	Mosc2	38,2	Q922Q1	11	6	3,820
High mobility group protein B2	Hmbg2	24,1	P30681	8	3	3,793
Zinc finger protein 771	Znf771	35,7	Q8BJ90	3	3	3,788
Ras GTPase-activating protein-binding protein 1	G3bp1	51,8	P97855	14	8	3,787
TNF receptor-associated factor 3	Traf3	64,2	Q60803	6	4	3,785
Small nuclear ribonucleoprotein-associated protein B	Snrpb	23,6	P27048	133	7	3,783
Protein SEC13 homolog	Sec13	35,5	Q9D1M0	9	3	3,778
Transcriptional activator protein Pur-beta	Purb	33,9	O35295	49	11	3,734
Stromal cell-derived factor 2	Sdf2	23,1	Q9DCT5	1	1	3,719
Kinesin-like protein KIF21A	Kif21a	186,4	Q9QXL2	12	7	3,708
Ubiquitin-conjugating enzyme E2 N	Ube2n	17,1	P61089	3	2	3,700
La-related protein 1	Larp1	121,1	Q6ZQ58	11	9	3,693
Low molecular weight phosphotyrosine protein phosphatase	Acp1	18,2	Q9D358	2	2	3,686
Matrin-3	Matr3	94,6	Q8K310	87	19	3,671
Protein syndesmos	Sdos	23,4	Q8VHN8	7	6	3,606
Pre-B-cell leukemia transcription factor 3	Pbx3	47,2	O35317	2	2	3,592
Arginine and glutamate-rich protein 1	Arglu1	32,9	Q3UL36	11	6	3,589
Signal recognition particle 14 kDa protein	Srp14	12,5	P16254	1	1	3,583

Table 1. continued

Name	Symbol	Mw [kDa]	Accession	PSM	Peptides	Heavy/Light
14-3-3 protein beta/alpha	Ywahb	28,1	Q9CQV8	3	2	3,567
SAFB-like transcription modulator	Sltm	116,8	Q8CH25	19	12	3,562
Transcription factor A, mitochondrial	Tfam	28,0	P40630	3	2	3,556
Elongation factor 1-delta	Ef1d	31,3	P57776	6	5	3,548
WD repeat-containing protein 82	Wdr82	35,1	Q8BFQ4	5	5	3,542
Chromobox protein homolog 8	Cbx8	39,8	Q9QXV1	10	7	3,521
SWI/SNF complex subunit SMARCC2	Smarcc2	132,5	Q6PDG5	13	7	3,519
MORC family CW-type zinc finger protein 2A	Morc2a	117,3	Q69ZX6	6	5	3,502
78 kDa glucose-regulated protein	Hspa5	72,4	P20029	22	6	3,494
Tubulin gamma-1 chain	Tubg1	51,1	P83887	3	2	3,483
Fatty acid-binding protein, brain	Fabp7	14,9	P51880	4	2	3,480
Rab GDP dissociation inhibitor alpha	Gdia	50,5	P50396	5	2	3,472
Actin-like protein 6A	Actl6a	47,4	Q9Z2N8	4	3	3,465
Uncharacterized protein C1orf77 homolog	Ca077	26,6	Q9CY57	16	5	3,460
Dynactin subunit 1	Dctn1	141,6	O08788	18	9	3,455
Eukaryotic translation initiation factor 2 subunit 1	Eif2s1	36,1	Q6ZWX6	21	10	3,454
Peptidyl-prolyl cis-trans isomerase B	Ppib	23,7	P24369	32	3	3,452
Nucleoside diphosphate kinase A	Nme1	17,2	P15532	7	2	3,438
RNA-binding protein Musashi homolog 1	Msi1	39,1	Q61474	6	2	3,433
Methionine aminopeptidase 2	Metap2	52,9	O08663	3	1	3,413
Protein DEK	Dek	43,1	Q7TNV0	10	5	3,398
Serine/threonine-protein kinase TAO1	Taok1	116,0	Q5F2E8	8	4	3,385
GTP-binding nuclear protein Ran	Ran	24,4	P62827	13	2	3,366
General transcription factor II-I	Gtf2ci	112,2	Q9ESZ8	62	14	3,355
Polyhomeotic-like protein 2	Phc2	89,7	Q9QWH1	2	1	3,353
Myosin-Va	Myo5a	215,5	Q99104	18	8	3,342
Selenoprotein H	Selh	13,0	Q3UQA7	11	7	3,315
Regulator of chromosome condensation	Rcc1	44,9	Q8VE37	3	3	3,310

Table 1. continued

Name	Symbol	Mw [kDa]	Accession	PSM	Peptides	Heavy/Light
Alba-like protein C9orf23 homolog	Ci023	17,7	Q99JH1	1	1	3,305
Ribosome-binding protein 1	Rrpb1	172,8	Q99PL5	26	13	3,249
SWI/SNF complex subunit SMARCC1	Smarcc1	122,8	P97496	17	8	3,246
RNA-binding protein 39	Rbm39	59,5	Q8VH51	23	10	3,214
Paraspeckle component 1	Pspc1	58,7	Q8R326	37	11	3,209
Proliferation-associated protein 2G4	Pa2g4	43,7	P50580	25	8	3,192
Protein dpy-19 homolog 4	Dpy19l4	83,5	A2AJQ3	3	3	3,174
ATP-binding cassette sub-family D member 3	Abcd3	75,4	P55096	19	10	3,145
Dedicator of cytokinesis protein 10	Dock10	245,6	Q8BZN6	7	6	3,140
Glia-derived nexin	GDN	44,2	Q07235	27	5	3,123
Serologically defined colon cancer antigen 8 homolog	Sdccag8	82,9	Q80UF4	11	5	3,113
Sideroflexin-1	Sfxn1	35,6	Q99JR1	13	5	3,107
Microtubule-associated protein 2	Map2	198,9	P20357	38	8	3,098
THO complex subunit 4	Thoc4	26,9	O08583	31	6	3,065
ATP-dependent RNA helicase DDX19A	Ddx19a	53,9	Q61655	2	2	3,050
Ras GTPase-activating protein-binding protein 2	G3bp2	54,1	P97379	5	4	3,032
Nestin	Nes	207,0	Q6P5H2	54	26	2,982
Nucleolar transcription factor 1	Ubf1	89,5	P25976	10	6	2,922
Transformer-2 protein homolog alpha	Tra2a	32,3	Q6PFR5	15	5	2,919
Zinc finger protein 22	Znf22	27,3	Q9ERU3	25	7	2,913
Catenin delta-1	Ctnnd1	104,9	P30999	12	5	2,897
Poly(rC)-binding protein 2	Pcbp2	38,2	Q61990	33	5	2,870
14-3-3 protein epsilon	Ywhae	29,2	P62259	6	2	2,860
Polypyrimidine tract-binding protein 2	Ptbp2	57,5	Q91Z31	14	2	2,836
Eukaryotic translation initiation factor 2 subunit 2	Eif2s2	38,1	Q99L45	30	9	2,825
Peroxiredoxin-6	Prdx6	24,9	O08709	2	2	2,824
FACT complex subunit SSRP1	Ssrp1	80,8	Q08943	5	5	2,821
Myosin-10	Myh10	228,9	Q61879	26	15	2,769

Table 1. continued

Name	Symbol	Mw [kDa]	Accession	PSM	Peptides	Heavy/Light
Kinesin-like protein KIF2A	Kif2a	79,7	P28740	9	7	2,766
Nucleolin	Ncl	76,7	P09405	19	3	2,765
Tubulin beta-5 chain	Tubb5	49,6	P99024	95	11	2,752
Histone H1.4	Hist1h1e	22,0	P43274	104	2	2,741
Golgi phosphoprotein 3	Golp3	33,7	Q9CRA5	1	1	2,741
Elongation factor Tu	Eftu	49,5	Q8BFR5	11	5	2,690
Thyroid hormone receptor-associated protein 3	Thrap3	108,1	Q569Z6	27	12	2,643
F-box/LRR-repeat protein 14	Fbxl14	43,8	Q8BID8	5	3	2,636
Histone H3.1	Hist1h3a	15,4	P68433	105	9	2,624
Histone H4	Hist1h4a	11,4	P62806	97	8	2,595
Histone H1.1	Hist1h1a	21,8	P43275	19	2	2,581
Interferon-inducible double stranded RNA-dependent protein kinase activator A	Prkra	34,3	Q9WTX2	9	3	2,573
Eukaryotic initiation factor 4A-I	Eif4a1	46,1	P60843	49	8	2,571
Serine/threonine-protein kinase VRK1	Vrk1	49,7	Q80X41	10	7	2,562
DNA2-like helicase	Dna2	119,4	Q6ZQJ5	8	5	2,560
Scaffold attachment factor B2	Safb2	111,8	Q80YR5	14	11	2,560
Elongation factor 1-alpha 1	Ef1a1	50,1	P10126	275	6	2,542
Myosin-VI	Myo6	146,3	Q64331	10	8	2,532
Vimentin	Vim	53,7	P20152	327	22	2,522
Actin, cytoplasmic 1	Actb	41,7	P60710	239	8	2,508
Rho guanine nucleotide exchange factor 1	Arhgef1	102,7	Q61210	6	3	2,485
Coronin-1C	Cor1c	53,1	Q9WUM4	13	5	2,484
Histone H3.3	H3f3a	15,3	P84244	98	9	2,473
Histone H1.0	H1f0	20,8	P10922	1	1	2,464
Calpain-9	Can9	78,9	Q9D805	10	3	2,460
Poly(rC)-binding protein 1	Pcbp1	37,5	P60335	27	6	2,457
TNF receptor-associated factor 4	Traf4	53,4	Q61382	5	2	2,447
Histone H3.2	Hist1h3b	15,4	P84228	108	9	2,418

Table 1. continued
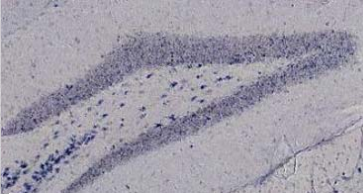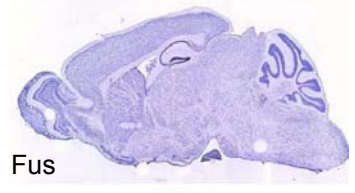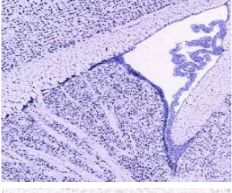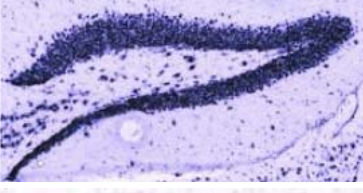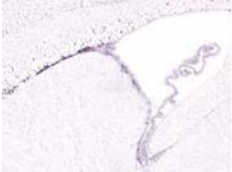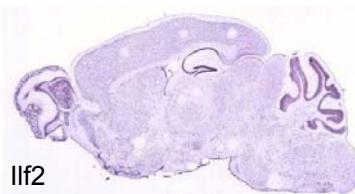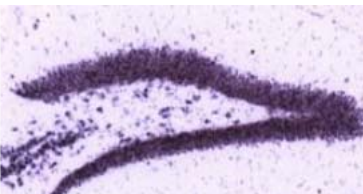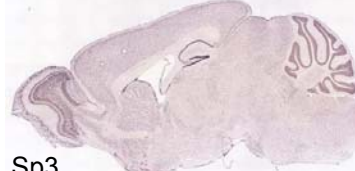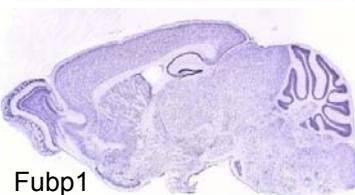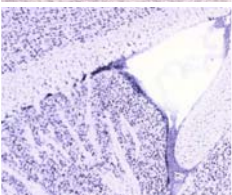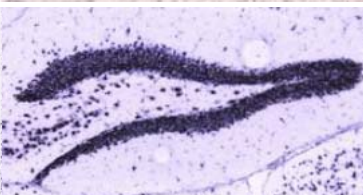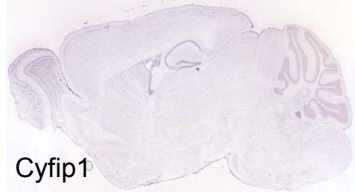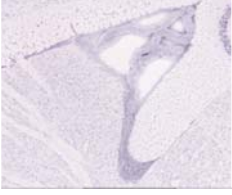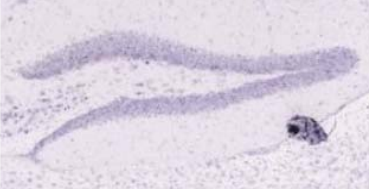
Name	Symbol	Mw [kDa]	Accession	PSM	Peptides	Heavy/Light
SET-binding protein	Setbp1	168,0	Q9Z180	4	3	2,405
Heterochromatin protein 1-binding protein 3	Hp1b3	60,8	Q3TEA8	51	10	2,384
Structural maintenance of chromosomes protein 1A	Smc1a	143,1	Q9CU62	24	14	2,375
Protein polybromo-1	Pbrm1	187,1	Q8BSQ9	26	11	2,371
Histone H1.5	Hist1h1b	22,6	P43276	85	2	2,355
PC4 and SFRS1-interacting protein	Psip1	59,7	Q99JF8	17	6	2,313
3'-5' exoribonuclease 1	Eri1	39,5	Q7TMF2	4	3	2,297
Histone H2B type 1-K	Hist1h2bk	13,9	Q8CGP1	4	3	2,296
Histone H2A type 3	Hist3h2a	14,1	Q8BFU2	33	5	2,256
Single-stranded DNA-binding protein, mitochondrial	Ssbp	17,3	Q9CYR0	3	3	2,255
Tubulin beta-2A chain	Tubb2a	49,9	Q7TMM9	95	11	2,247
Serpin H1	Serph	46,6	P19324	8	5	2,230
Fragile X mental retardation protein 1 homolog	Fmr1	68,9	P35922	7	5	2,221
Pleiotropic regulator 1	Plrg1	56,9	Q922V4	16	4	2,205
Zinc finger protein 22	Tubb2b	49,9	Q9CWF2	95	11	2,162
Non-POU domain-containing octamer-binding protein	Nono	54,5	Q99K48	210	18	2,133
DNA topoisomerase 1	Top1	90,8	Q04750	127	23	2,099
RuvB-like 2	Ruvb2	51,1	Q9WTM5	15	7	2,098
Protein disulfide-isomerase	Pdia1	57,1	P09103	5	2	2,098
Microtubule-associated protein 4	Map4	117,4	P27546	95	9	2,077
Polypyrimidine tract-binding protein 1	Ptbp1	56,4	P17225	29	6	2,071
Splicing factor, proline- and glutamine-rich	Sfpg	75,4	Q8VIJ6	195	19	2,066
Tubulin beta-2C chain	Tubb2c	49,8	P68372	83	11	2,061
MTSS1-like protein	Mtss1	76,8	Q6P9S0	5	2	2,031
NHP2-like protein 1	Nhp2l1	14,2	Q9D0T1	3	1	2,024

4.2.3 Validation of proteins co-purified with RBPJκ and identified by MS/MS

The proteomic analysis revealed a high number of potential interactors of RBPJκ in adult NSCs. Given the aim of this study, i.e. to identify candidates that modulate RBPJκ-dependent stem cell function through interaction on the transcriptional level, I first identified proteins with function in transcriptional and stem cell regulation by gene ontology, KEGG pathway analyses and data mining of scientific literature analyses. Next, I examined the expression patterns of those genes by studying literature and public databases for expression patterns (Allen Brain Atlas, Gensat Org). Further analyses were then focusing on TFs with a strong expression in SVZ of the lateral ventricles or SGZ of the dentate gyrus, as these proteins were the most likely candidates for interaction with RBPJκ in adult neural stem cells. TFs which showed no expression in SVZ or the DG were excluded from further analysis.

Fig.11 (following page) Allen Brain Atlas *in situ* hybridisations further validated proteins co-purified in RBPJκ immunoprecipitations in adult neural stem and progenitor cells
Allen Brain Atlas, a genome-wide comprehensive ISH database for identifying anatomically gene expression patterns in the adult mouse brain was used for further validation of around 50 candidates identified by data mining of scientific literature, gene ontology and KEGG pathway analyses, involved in stem cell and transcriptional regulation. Afterwards, the number of putative candidates interacting with RBPJκ was narrowed down to 30. Pictures depicted here show *In situ* hybridisations of some of these candidates on sagittal adult brain sections; rostral is to the left. Blue staining demonstrates gene expression in an overview of adult mouse brain. Candidates such as Cyfip1 (last row), which showed no expression in SVZ or DG were excluded from further analysis. Pictures shown are available from: https//mouse.brain-map.org.

Overview	SVZ	DG
Fhl1		
Fus		
Nfia		
Nfib		
Ilf2		
Sp3		
Fubp1		
Cyfip1		

4.2.4 Confirmation of RBPJκ interacting proteins

Proteins which were found to be expressed in the adult neurogenic niches were further validated for interaction with RBPJκ. Two independent strategies were pursued: a) conventional CoIP, b) IP for RBPJκ and subsequent quantitative tandem MS/MS analysis under highly stringent conditions. Conventional CoIP analysis of nuclear extracts from neurospheres demonstrated interaction of RBPJκ with the transcriptional repressor and insulator protein CTCF, Fused in sarcoma (FUS/TLS), NFIA and TDP-43.

The interaction of RBPJκ and TDP-43 in adult neural stem cells will be discussed more in detail in a later section of this work.
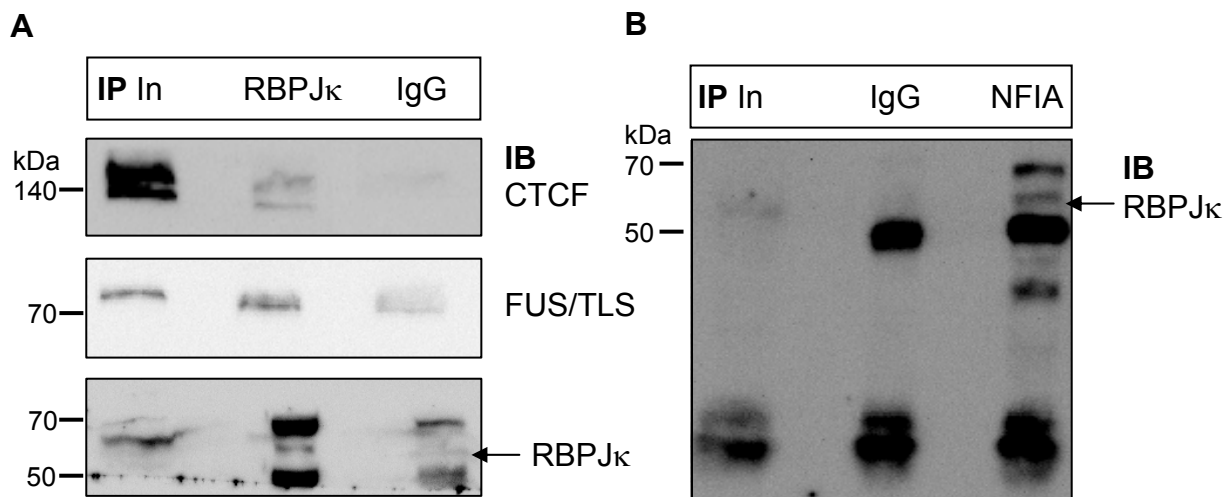

Fig. 12 Western blot analysis for candidate validation of MS/MS results
(A) Representative western blots of immunoprecipitation of nuclear protein extracts from neurospheres with antibodies raised against RBPJκ confirmed interaction with CTCF (upper blot) and FUS/TLS proteins (middle blot). Antibodies were stripped from PVDF membranes and membranes were incubated with antibodies raised against RBPJκ to validate the presence of RBPJκ in the IP (lower blot). **(B)** IP with antibodies raised against NFIA show co-precipitation of NFIA with RBPJκ proteins.

In a second approach, IPs were performed under high salt concentration conditions (stringent conditions) to further characterize proteins that strongly interact with RBPJκ in adult NSCs. To this end, salt concentration of the IP buffer was increased up to 4x reaching a final concentration of 480 mM KCl. Under such high stringency only proteins that are strongly bound to RBPJκ will be co-precipitated with RBPJκ. Proteins were quantitatively labelled by ICPL and analysed by tandem MS/MS.

Proteins showing more than 1.5-fold enrichment were considered as specific interactors of RBPJκ. Using this criterion, 14 proteins were found to strongly interact with RBPJκ in adult neural stem cells. Again, RNA-binding and RNA-splicing factors were found to co-immunoprecipitate with RBPJκ, strongly suggesting that RBPJκ may indeed influence RNA metabolism. Moreover, two factors with transcriptional activity, i.e., ILF3 and TDP43 were also found to strongly interact with RBPJκ even under stringent IP-conditions.

Table 2.   Copurified proteins from high stringent RBPJk immunoprecipitations in aNSCs

name	symbol	mw [kDa]	peptides	aa	heavy/light
ATP-dependent RNA helicase DDX3X	Ddx3	73,1	21	662	4,525
Heat shock cognate 71 kDa protein	Hspa8	70,8	2	646	3,606
Elongation factor 1-alpha 1	Eef1a1	50,1	4	462	2,457
ATP synthase subunit alpha, mitochondrial	Atp5a1	59,7	5	553	2,333
Probable ATP-dependent RNA helicase DDX17	Ddx17	72,4	27	650	2,164
Heterogeneous nuclear ribonucleoprotein U-like protein 1	Hnrnpul1	95,9	15	859	2,149
Small nuclear ribonucleoprotein Sm D1	Snrpd1	13,3	4	119	2,065
Splicing factor, arginine/serine-rich 2	Sfrs2	25,5	5	221	1,988
Probable ATP-dependent RNA helicase DDX5	Ddx5	69,3	38	614	1,931
TAR DNA-binding protein 43	Tardbp	44,5	5	414	1,868
Interleukin enhancer-binding factor 3	Ilf3	96,0	3	898	1,841
Peptidyl-prolyl cis-trans isomerase B	Ppib	23,7	1	216	1,711
Microtubule-associated protein 4	Map4	117,4	5	1125	1,657
Heterogeneous nuclear ribonucleoprotein Q	Syncrip	69,6	11	623	1,609

Table2. Mass spectrometry results of immunoprecipitations under high stringent conditions
MS/MS of high stringent immunoprecipitations demonstrated strong interactions of RBPJκ with RNA binding proteins and the transcription factors TDP-43 and ILF3.

In the following experiments I focused on the potential interaction of RBPJκ with TDP-43 and NFIA in adult neural stem cells.

4.3 Notch signalling pathway and TDP-43

4.3.1 RBPJκ interacts with TDP-43

First, I investigated the potential function of TDP-43 in Notch/RBPJκ signalling. TDP-43 is a 43 kDa protein which was originally identified as a transcriptional repressor of HIV-1 (Ou et al., 1995) and later on shown to be a regulator of mRNA splicing (Buratti and Baralle, 2010). In recent years TDP-43 gained major attention due to the finding that mutations in TDP-43 cause neurodegenerative diseases such as FTLD-U and ALS and that TDP-43 shows abnormal distribution and aggregation in several neurodegenerative diseases.

A detailed expression pattern for TDP-43 in adult neurogenic niches *in vivo* has not been determined yet, in particular its expression in neural stem cells is unknown. Analyses of 8 week old mice brains showed ubiquitous expression of TDP-43 in the dentate gyrus and CA regions of the hippocampal formation (Fig. 13B,D). Using different adult neurogenesis markers it was found that TDP-43 is co-localized with SOX2 positive cells in the SVZ (Fig. 13C). To investigate possible expression of TDP-43 in radial glia-like stem cells in the DG Nestin-GFP mice were analysed. In these Nestin-GFP reporter mice TDP-43 co-localized with SOX2 and GFP in the SGZ of the DG (Fig. 13D), indicating that TDP-43 is indeed expressed in adult neural stem cells.

Currently available antibodies against RBPJκ are not suitable for staining of adult brain slices. Hence, immunohistochemical analysis for co-expression of TDP-43 and RBPJκ in neural stem cells of the adult brain was not possible. Yet, given the expression of RBPJκ RNA throughout the neurogenic niches (Breunig et al. 2007), the activity of Notch/RBPJκ signalling reporter (Duncan et al., 2005; Mizutani et al., 2007) in neural stem cells (Ehm et al., 2010, Imayoshi et al, 2010, Lugert et al. 2010), and direct function of RBPJκ function in neural stem cell maintenance in vivo (Ehm et al., 2010, Imayoshi et al, 2010) it can be assumed that RBPJκ and TDP-43 are co-expressed in neural stem cells.
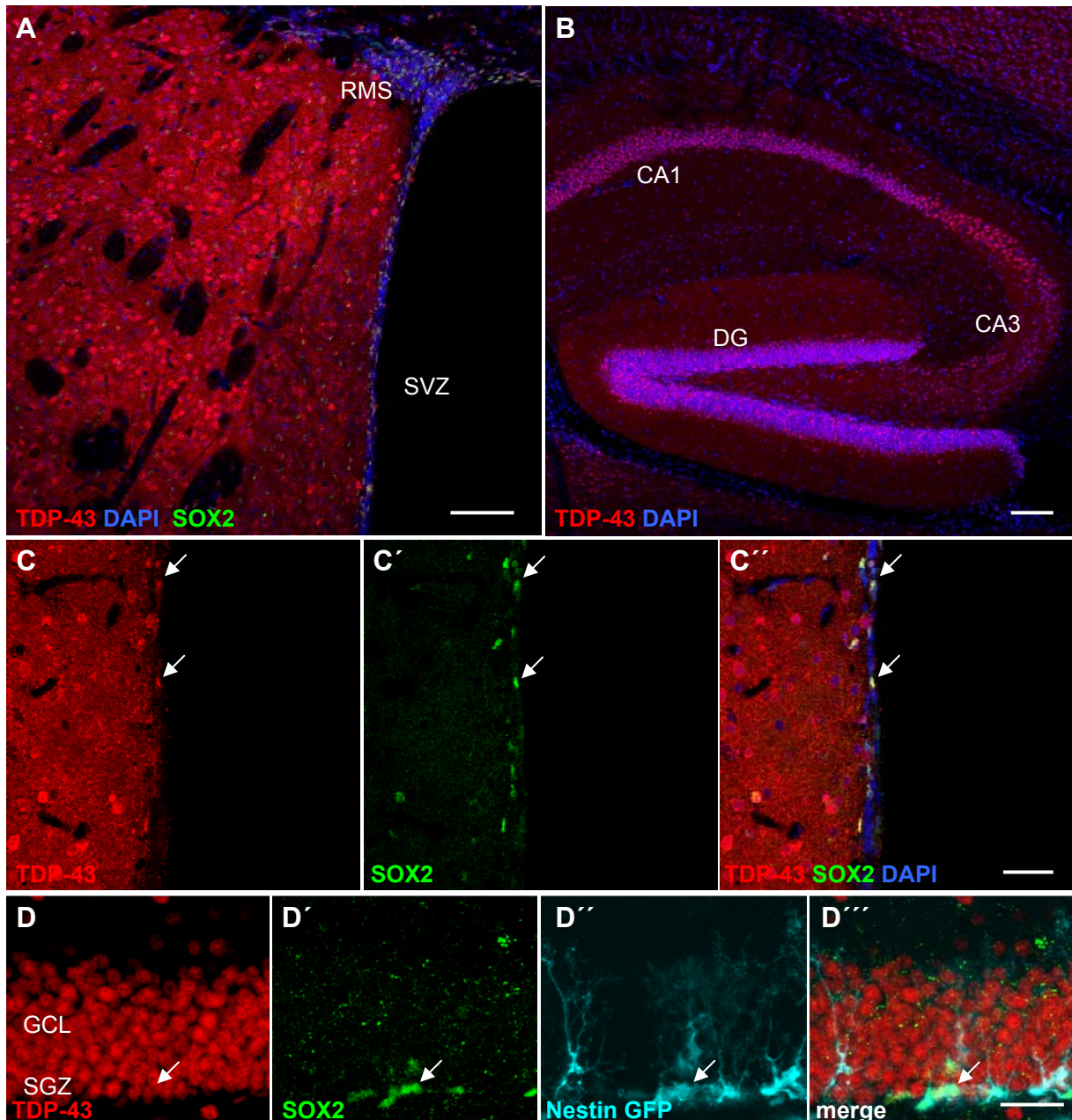
Fig.13 TDP- 43 expression in the adult SVZ zone and dentate gyrus
Representative confocal images of immunofluorescent stainings of brain slices from 8 week old mice. **(A-B)** Overview images of TDP-43 (red) showing expression in SVZ and DG in 8 w old mouse brain section. DAPI for nuclear counterstain in blue, scale bars (A,B), 100 µm. **(C)** Use of different adult neurogenesis markers indicated that TDP-43 co-localizes with SOX2 positive cells (green) in the SVZ. **(D)** Analysis of Nestin-GFP mice, demonstrate co-localization of TDP-43 with GFP (light blue) and SOX2 (green) (arrow). Scale bars (C, D), 30 µm. CA cornus ammonis of the hippocampus, GCL granular cell layer, DG dentate gyrus, RMS rostral migratory stream, SGZ subgranular zone, SVZ subventricular zone.

CoIP assays indicated that RBPJκ and TDP-43 strongly interact in adult neural stem cells (Table 1 and 2). To determine, whether the interaction of RBPJκ with TDP-43 is dependent on the presence of RNA and/or DNA, IPs with RBPJκ antibodies or non-immune IgGs were performed in the presence and/or absence of the endonuclease benzonase. Nucleic acids were digested for 3 hours with benzonase (200 U/mg protein) during IPs under physiological conditions (100 mM KCl). DNA was isolated from the unbound protein supernatants by chloroform/methanol precipitation, subjected to gel electrophoresis, and visualized using EtBr. In the absence of benzonase, samples showed an enrichment of DNA fragments in the size of 2- and 2,5-kb. In addition, a smear of DNA from 3- to 10-kb was found in RBPJκ− as well as in non-immune IgGs IPs. In benzonase-treated samples no DNA was visualized by EtBr, demonstrating that benzonase treatment resulted in efficient digestion of nucleic acids (Fig. 14b).

Western blot analyses of the immunoprecipitated proteins showed that RBPJκ and TDP43 co-immunoprecipitated even in the presence of benzonase, indicating that interaction of RBPJκ and TDP43 does not require the presence of DNA or RNA (Fig. 14a).
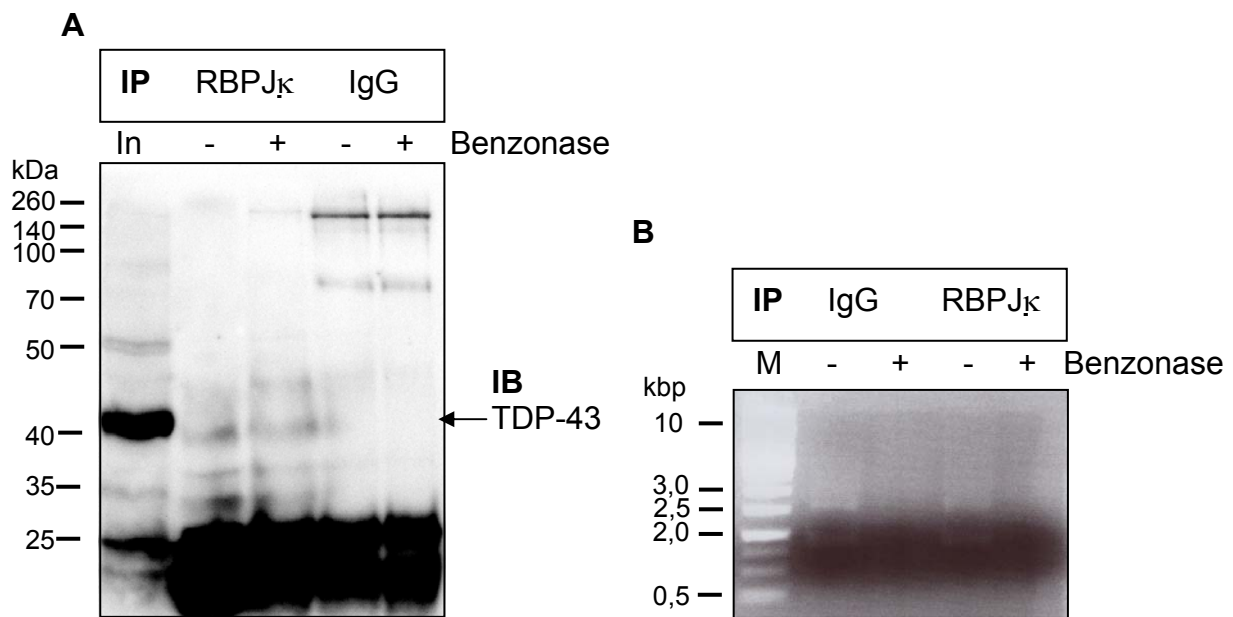
Fig.14 RBPJκ interacts with TDP-43 independent of the presence of DNA and/or RNA

(A) Nuclear proteins were isolated from neurospheres and subjected to immunoprecipitations with antibodies raised against RBPJκ or non-immune IgGs. IPs were performed for 3 h in the presence or absence of the endonuclease benzonase (200 U/mg protein). Representative WB shows DNA/RNA independent interaction of RBPJκ with TDP-43. **(B)** DNA was isolated from supernatants of IPs, subjected to gel electrophoresis and visualized using EtBr. In the absence of benzonase, samples showed an enrichment of DNA fragments in the size of 2 and 2,5-kb. Moreover, a smear of DNA from 3 up to 10-kb in RBPJκ as well as in non-immune IgGs immunoprecipitations was observed as well. In benzonase treated samples no DNA was visualized by EtBr, demonstrating efficient enzymatic digestion of DNA.

4.3.2 TDP-43 enhances Notch signalling mediated *Hes1* promoter activity

The observed expression pattern *in vivo* and the strong interaction of TDP-43 with RBPJk found in nuclear extracts of adult neural stem cells *in vitro* suggested a possible role of TDP-43 in the modulation of Notch/RBPJκ-dependent gene expression. To investigate this hypothesis, I focused on the effects of TDP-43 on Notch/RBPJκ target promoters *Hes1* and *Hes5*. The activity of the *Hes1* and *Hes5* promoters was studied using *Hes1*- and *Hes5* luciferase reporter assays in HEK293T cells, respectively. Activation of the Notch-signalling pathway was achieved through transient transfection of the cells with an expression vector encoding for the Notch intracellular domain (NICD). Increasing amounts of *Nicd*-cDNA (0,1 ng – 320 ng)

were co-transfected together with *Hes1* (160 ng) and/or *Hes5* (160 ng) luciferase promoter reporter constructs (data not shown). The amount of *Nicd*-cDNA (40 ng), which increased *Hes1* or *Hes5* luciferase promoter activity in the submaximal range was subsequently used to test the effects of co-transfection with *Tdp-43*-cDNA. To this purpose, increasing amounts of *Tdp-43* cDNA (0,1 ng – 320 ng) were transiently co-transfected with *Nicd*-cDNA (data not shown).

Overexpression of NICD resulted in a significant 50-fold increase of *Hes1* promoter luciferase activity while TDP-43 (80 ng) alone significantly stimulated luciferase activity up to 3.8-fold (Fig. 15A). Co-expression of NICD with TDP-43 significantly enhanced *Hes1* promoter activity and resulted in 350-fold induction. In contrast, TDP-43 had no effect on NICD-induced *Hes5* luciferase promoter activity (Fig. 15B).
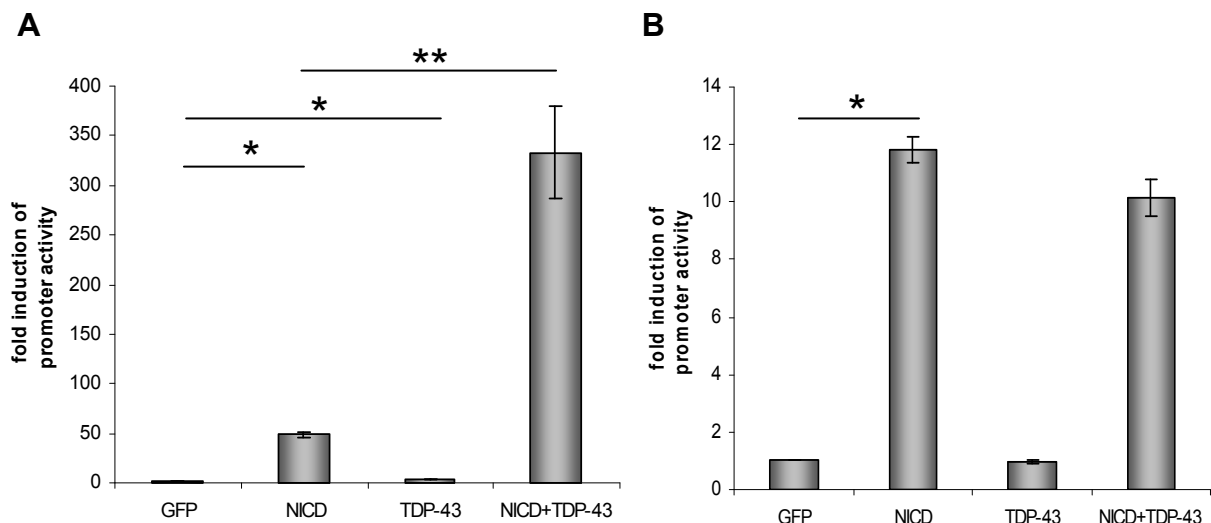

Fig.15 TDP-43 increases Notch signalling mediated activation of *Hes1* but not of *Hes5* promoter luciferase reporter.
Luciferase reporter assays in HEK293T cells. HEK293T cells were transiently transfected either with the cDNA of the Notch intracellular domain *Nicd* or with *Tdp-43* alone or with both, *Nicd* and *Tdp-43* in combination. *Hes* promoter luciferase reporter activity was assayed 48h after transfection. **(A)** Overexpression of NICD resulted in a significant 50-fold increase of *Hes1* promoter luciferase activity while TDP-43 alone significantly increased luciferase activity 3.8-fold. Co-expression of NICD and TDP-43 significantly increased Notch signalling mediated *Hes1* promoter activation up to 350-fold. **(B)** Overexpression of NICD significantly enhanced *Hes5* promoter activity by 12-fold. In contrast to the *Hes1* promoter TDP-43 had no effect on *Hes5* promoter activity. Moreover, co-expression of TDP-43 and NICD had no promoting effect of Notch signalling on *Hes5* promoter activity. Results represent the mean ± SEM of three independent experiments performed in triplicate (*p<0.05; **p<0.01).

The next important question was to verify whether TDP-43 specifically cooperates with RBPJk in activating target genes of the Notch signalling pathway or whether TDP-43 enhances transcriptional activation induced by other signalling pathways as well. To this end, I examined whether TDP-43 modulates the activation of a Wnt-signalling dependent reporter construct, i.e. the Super 8xTOPFLASH (TCF reporter plasmid) luciferase reporter (Korinek et al., 1997). The Super 8xTOPFLASH promoter luciferase construct contains 8 TCF/LEF binding sites and can be activated by the constitutive active form of the Wnt signalling mediator β-catenin, which contains a mutated (S33Y) phosphorylation site and cannot be phosphorylated and excluded from the nucleus (Lie et al., 2005). Activity of the Super 8xTOPFLASH promoter (160 ng) could be increased over a wide range (5- to 2000-fold) by increasing amounts of *β-catenin* cDNA (0,1 ng – 250 ng). Submaximal activation (350-fold) was observed with a *β-catenin* cDNA concentration of 12,5 ng. To determine whether TDP-43 could modulate β-catenin-induced activation of Super 8xTOPFLASH promoter activity, increasing amounts of *Tdp-43* cDNA were co-transfected with *β-catenin* cDNA (12,5 ng). Overexpression of *β-catenin S33Y* resulted in a 350-fold increase of the Super 8xTOPFLASH promoter luciferase while TDP-43 alone increased promoter activity up to 7-fold (Fig. 16). Co-expression of β-catenin and TDP-43 could not significantly enhance the effect of β-catenin alone on Super 8xTOPFLASH promoter activity.
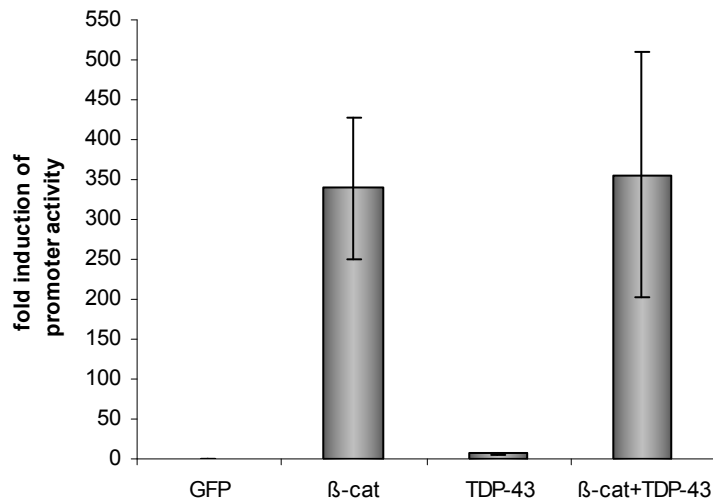
Fig. 16 TDP-43 does not enhance β-catenin induced activation of Super 8xTOPFLASH promoter reporter construct
Luciferase reporter assays in HEK293T cells. HEK293T cells were transiently transfected with the constitutive active form of *β-catenin* which contains a mutated (S33Y) phosphorylation site and cannot be phosphorylated and excluded from nucleus, with *Tdp-43* alone or in combination with *β-catenin*. Super 8xTOPFLASH promoter luciferase reporter activity was assayed 48 h after transfection. Overexpression of β-catenin resulted in a 350-fold increase of Super 8xTOPFLASH promoter luciferase activity while TDP-43 stimulated luciferase activity up to 7 -fold. Coexpression of β-catenin and TDP-43 could not significantly increase β-catenin mediated activation of Super 8xTOPFLASH luciferase reporter. Results represent the mean ± SEM of 3 independent experiments performed in triplicate.

Work by Acharya et al., 2006 and by Lalmansingh et al., 2011 indicated that TDP-43 modulates transcription through binding to the consensus sequence 5′-GTGTGT-3′. In silico analyses of the 1100 bp region, upstream (-) of both *Hes1* and *Hes5* transcription start site (TSS), which was shown to contain the promoters (Beatus et al., 1999), predicted the presence of two binding sites for TDP-43 on *Hes1* -and none on the *Hes5* promoter (Fig. 17). The binding sites on *Hes1* promoter mapped at position -61 nt to -56 nt (1#) and a second one around the TSS -2 nt to +4 nt (2#). These putative binding sites were conserved in the *Hes1* promoter luciferase reporter construct used in the above described transfection experiments.
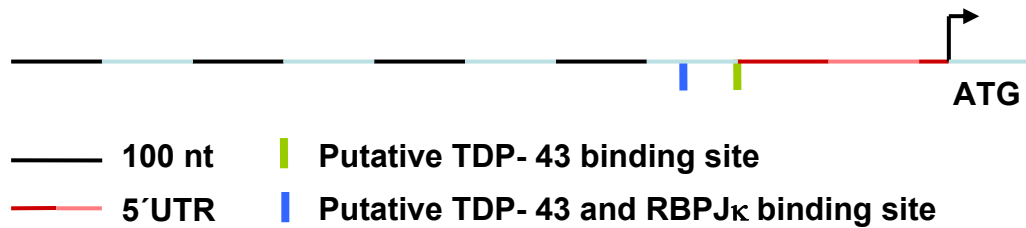
Fig.17 Schematic representation of the mouse *Hes1*-gene promoter
In silico analysis predicted the presence of two putative binding sites for TDP-43 on *Hes1* promoter containing the consensus sequence 5′-GTGTGT-3′: 1#, -61 nt to -56 nt, which is overlapping with a putative RBPJκ binding site with the consensus sequence 5′-CGTGTGAA-3′ (blue bar) and 2#, -2 nt to +4 nt, here depicted in green, on the antisense strand of the mouse *Hes1* promoter. These binding sites were conserved in the *Hes1* promoter luciferase reporter construct used in the above described transfection experiments. Nt: number of nucleotides upstream (-) or downstream (+) of the transcription start site.

This led to the assumption that TDP-43 might modulate *Hes1* luciferase reporter activity through binding to these consensus sequences. To investigate this hypothesis both binding sites 5′-GTGTGT-3′ were point mutated individually to 5′GTAAAT3′. Activation of the mutated *Hes1* luciferase reporter by TDP-43 and NICD was then tested in transient transfection assays in HEK293T cells.

When the putative binding site 1# was mutated, overexpression of NICD resulted in a 2,8-fold increase of *Hes1* luciferase activity, while TDP-43 alone significantly stimulated luciferase activity up to 4.8–fold (Fig. 18A). Co-expression of NICD with TDP-43 significantly enhanced *Hes1* promoter activity to 19.8-fold. The decreased activation of mutant 1# by NICD is likely due to the fact that the mutated putative TDP-43 binding site (-61 nt to -56 nt with respect to the transcriptional start site) is overlapping with an RBPJκ binding site 5′-CGTGTGAA-3′ on the antisense strand.

In contrast, mutation of the putative binding site 2#: resulted in a significant 40-fold increase of *Hes1* promoter luciferase following overexpression of NICD, whereas TDP-43 significantly increased luciferase activity by 3.2-fold. Again, co-expression of NICD with TDP-43 significantly enhanced *Hes1* promoter activity up to 389-fold (Fig. 18B).

Mutation of both putative binding sites together further reduced stimulation of *Hes1* promoter luciferase activity by overexpression of NICD (1,6-fold) while TDP-43 alone significantly induced luciferase activity up to 3.4-fold. Co-expression of NICD with TDP-43 could significantly enhance *Hes1* promoter activity by 8.6-fold (Fig. 18C).
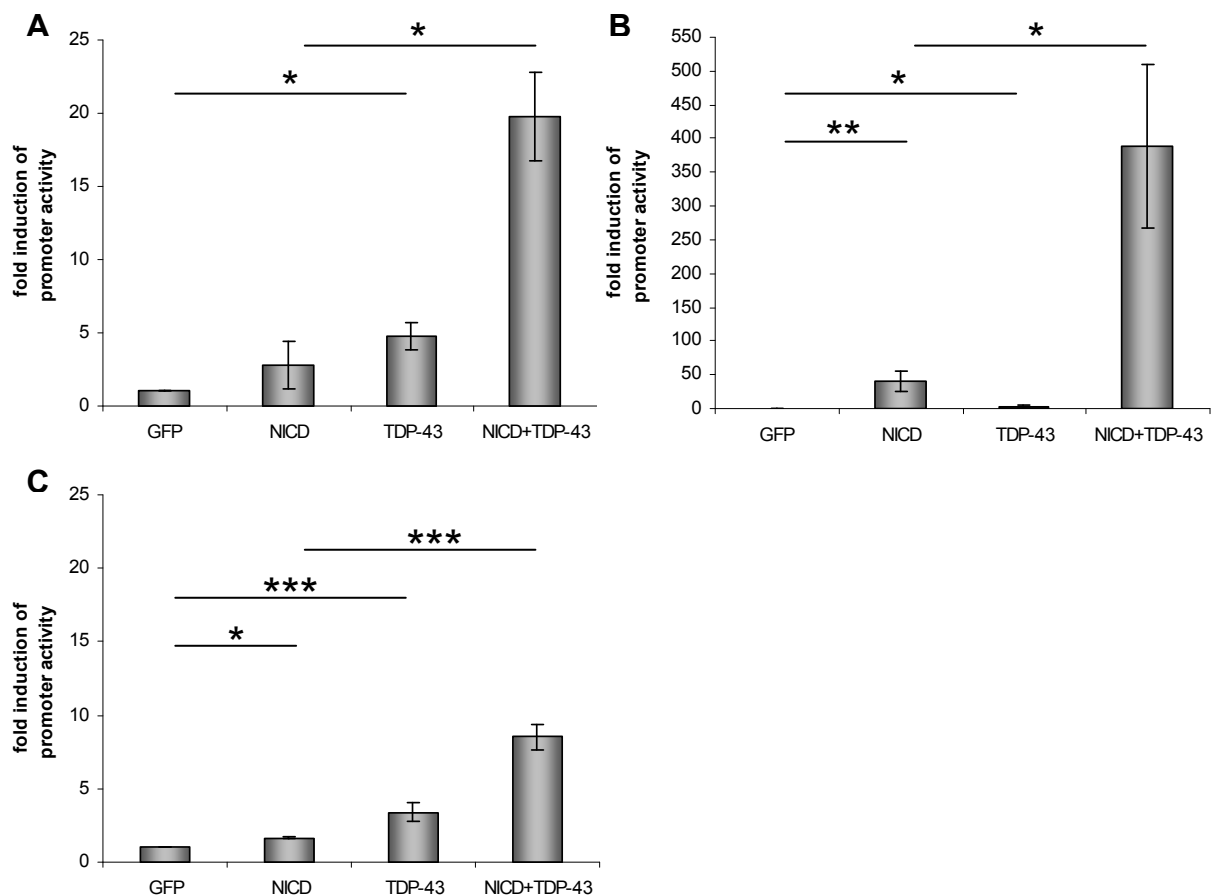
Fig. 18 Luciferase assays using *Hes1* promoter luciferase reporters with mutations in the putative binding sites for TDP-43

HEK293T cells were transiently transfected with *Hes1* promoter luciferase reporter constructs where the predicted DNA binding sites for TDP-43 were mutated. **(A)** Mutation of the predicted TDP-43 binding site 1# (-61nt to -56nt upstream of transcription start), which is overlapping with an RBPJκ binding site on the antisense strand led to a decreased activation by NICD (2,8-fold). Overexpression of TDP-43 significantly induced *Hes1* promoter activation of 4.8-fold and co-expression of TDP-43 and NICD together significantly increased luciferase activity up to 20-fold. **(B)** Mutation of the predicted TDP-43 binding site 2# (-4nt to +2nt around transcription start). Overexpression of NICD resulted in a significant 40-fold induction of *Hes1* promoter luciferase activity while TDP-43 significantly induced luciferase activity to 3.2 -fold. Co-expression of NICD and TDP-43 resulted in a significant 400-fold induction of *Hes1* promoter activity. **(C)** Mutation of both predicted TDP-43 binding sites. Overexpression of NICD resulted in a significant 1,6-fold induction on *Hes1* promoter luciferase activity while TDP-43 significantly enhanced luciferase activity 3.4-fold. Induction of *Hes1* luciferase reporter activity after co-expression of NICD and TDP-43 was significantly increased to 9.6-fold. Results represent the mean ± SEM of 3 independent experiments performed in triplicate (*$p < 0.05$, **$p < 0.01$, ***$p < 0.001$).

4.3.3 A TDP-43 (A315T) mutant associated with ALS and FTLD-U induces lower activation of *Hes1* promoter

TDP-43 contains two RNA recognition motifs and one glycine-rich domain, which is important for protein-protein interaction. Point-mutations in the glycine-rich domain have been causally linked to ALS and FTDL-U in humans (Neumann et al., 2006; Pesiridis et al., 2009). Since the glycine-rich domain is important for protein interaction and TDP-43 still enhanced Notch signalling mediated activation of the *Hes1* luciferase promoter construct after mutation of the predicted DNA binding sites, an interesting question was whether Notch signalling might be disturbed by A315T mutations that are associated with ALS and FTDL-U. To this end I compared the effect of the A315T mutation in TDP-43 to WT TDP-43 in *Hes1* promoter luciferase reporter assays.

Overexpression of NICD (40 ng) resulted in a significant 49 -fold increase of *Hes1* promoter-driven luciferase (Fig. 19A). TDP-43 (80 ng) alone significantly induced 3.8-fold luciferase activity while the A315T TDP-43 mutant (80 ng) increased *Hes1* promoter activity only 2,7-fold. Co-expression of NICD with TDP-43 significantly enhanced *Hes1* promoter activity up to 333-fold. In contrast, overexpression of NICD together with the A315T TDP-43 mutant resulted in 162-fold induction of *Hes1* promoter activity. Concentrations of DNA plasmids used for this experiment were measured using a NanoDrop and controlled by gel electrophoresis and EtBr incorporation after enzymatic digestion of 1µg plasmid DNA by 1U SFiI for one hour at 37°C. Western blot analysis was used to ensure that equal amount of protein product was obtained after transfection of HEK293T cells with controlled/equal DNA amount for WT TDP-43 and A315T TDP-43 mutant (Fig. 19B).
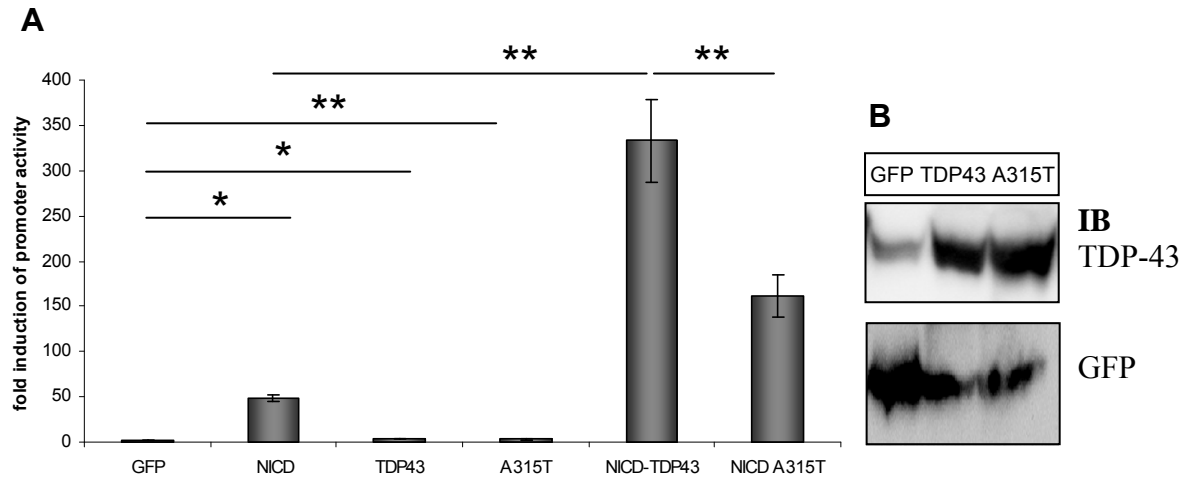
Fig. 19 Comparison of the effect of WT TDP-43 and the mutant A315T TDP-43 on *Hes1* promoter luciferase activity
(A) Transient transfection of *Nicd*, *Tdp-43*, *A315T Tdp-43*, *Nicd* and *Tdp-43* and *Nicd* together with *A315T Tdp-43* in HEK293T cells. Overexpression of NICD resulted in a significant 49-fold increase of *Hes1* promoter luciferase activity. TDP-43 alone significantly induced 3.8-fold luciferase activity while A315T TDP-43 increased *Hes1* promoter activity up to 2,7-fold. Co-expression of NICD with TDP-43 significantly enhanced *Hes1* promoter activity by 333-fold. Overexpression of NICD together with A315T TDP-43 resulted in a significant 162-fold induction of *Hes1* promoter activity. Comparison of co-expression of NICD and TDP-43 versus NICD and A315T TDP-43 indicated significantly less *Hes1* promoter activity induction by NICD and A315T TDP-43. Results represent the mean ± SEM of 3 independent experiments performed in triplicate (*$p<0.05$, **$p<0.01$ **(B)** Western blot analysis was used to ensure that equal amount of protein product was obtained after transfection of HEK293T cells with controlled/equal TDP-43 and A315T TDP-43 DNA amount. GFP was used as loading control.

4.3.4 TDP-43 promotes expression of endogenous *Hes1*

To test whether TDP-43 and A315T TDP-43 could increase expression of endogenous *Hes1*, HEK293T cells were transiently transfected with same amounts of plasmid DNA (2 µg DNA for 14cm^2 confluent HEK293T cell dish) for TDP-43 or A315T TDP-43. 84 hours after transfection nuclear proteins were isolated and subjected to western blot analysis (20 µg of nuclear protein were loaded on gel). Both overexpression of WT TDP-43 and of A315T TDP-43 increased the expression of endogenous *Hes1* in HEK293Tcells as revealed by increased amounts of HES1 protein in Western Blot (Fig. 20A).

However, HES1 protein levels following overexpression of mutant TDP-43 were lower compared to the HES1 protein levels observed in the context of WT TDP-43 overexpression.
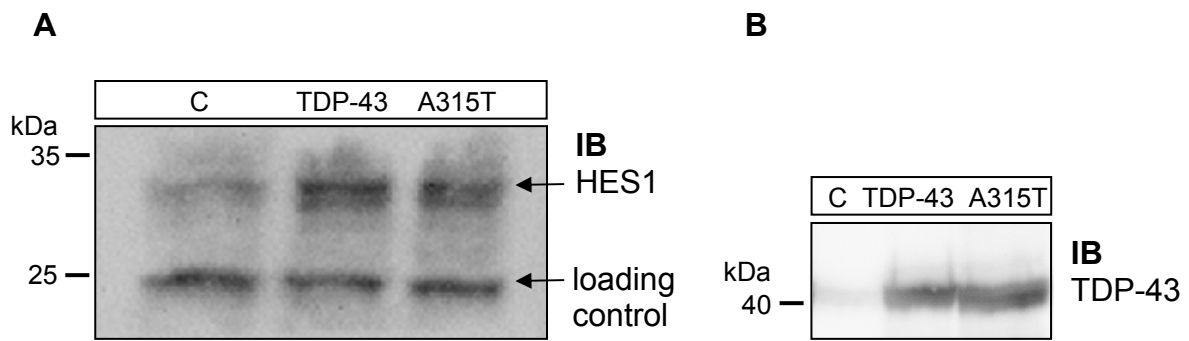
Fig. 20 TDP-43 promotes expression of endogenous *Hes1* in HEK293 cells
HEK293T cells were transiently transfected with cDNA of *Tdp-43* or the mutant *A315T Tdp-43*. Nuclear proteins were purified 84 hs after transfection and subjected to western blot analyses. **(A)** This representative WB shows up-regulation of endogenous HES1 protein (band at approximately 30 kDa) after overexpression of TDP43 or A315T. The HES-1 antibody detects also an unspecific protein band at around 25 kDa which was used as loading control. Bands represent 20 µg nuclear protein. **(B)** For transfection control, western blot membrane was stripped and re-incubated with antibodies raised against TDP-43.

Taken together, the present study identified TDP-43 as a novel and strong interactor of RBPJκ. In addition my data suggests TDP-43 as an important contributor to the regulation of stem cell maintenance through the modulation of Notch/RBPJκ signalling. Moreover, the data also describes that disease associated TDP-43 mutant A315T has a decreased potential to enhance Notch signalling.

4.4 Notch signalling pathway and NFIA

4.4.1 RBPJκ interacts with NFIA

In the second part of my work, I focused on the function of Nuclear factor 1a (NFIA) in Notch/RBPJκ signalling. NFIA has been associated with glial fate specification during embryonic spinal cord and neocortical development (Deneen et al., 2006; Namihira et al., 2009). Work by Piper et al. (2010) indicated that NFIA represses *Hes1* expression in embryonic telencephalic progenitor cell and might act as a switch from stem cell quiescence to astrogenesis. The physiological function of NFIA in adult neurogenesis is largely unknown. A detailed expression pattern for NFIA in adult neurogenic niches has not been determined, in particular, its expression in neural stem cells *in vivo* is unknown. Analyses of 8 week old mice brains revealed the presence of NFIA in the subgranular zone of the dentate gyrus (Fig. 21A). To investigate possible expression of NFIA in radial glia-like stem cells, Nestin-GFP reporter mice were analysed. NFIA colocalized with SOX2 and GFP in the SGZ of the DG (Fig. 21B). Using antibodies against doublecortin (DCX) it was found that NFIA is also expressed in immature neurons in SGZ of DG (Fig. 21C). Analyses of the subventricular zone of the lateral ventricles indicated expression of NFIA in SOX2 positive cells. Co-staining with DCX antibodies demonstrated expression of NFIA in migrating neuroblasts in the rostral migratory stream (RMS) (Fig. 22).

Based on previous analyses that determined the presence and function of RBPJk and Notch signalling in neural stem cells (for further explanation see p.56 line 20-29) and also based on NFIA expression pattern *in vivo*, it can be assumed, that RBPJκ and NFIA are co-expressed in the neural stem cell population.

It is, however, noteworthy, that NFIA levels in neuroblasts appear to be much higher than NFIA levels in neural stem cells.
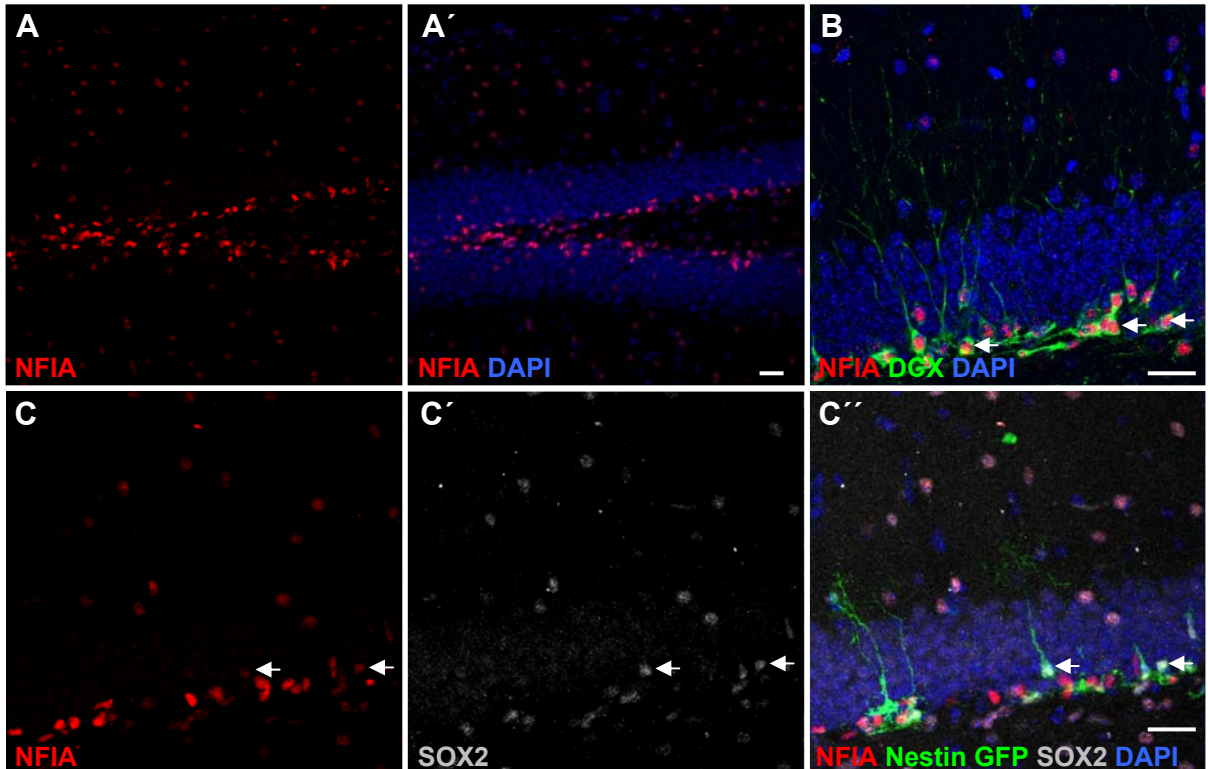
Fig. 21 NFIA expression in the subgranular zone of the adult dentate gyrus
Representative confocal images of immunofluorescent stainings of brain slices from
8 week old mice. **(A)** Overview of NFIA expression (red) in the dentate gyrus, DAPI
for nuclear counterstain in blue. **(B)** NFIA is expressed in DCX-positive immature
neurons in the SGZ (arrows). **(C)** Analyses of Nestin-GFP mice demonstrate
colocalisation of NFIA with GFP (green) and SOX2 (grey) (arrows) indicating NFIA
expression in radial glia-like stem cells in DG. DG dentate gyrus, SGZ subgranular
zone, Scale bars 40 μm.
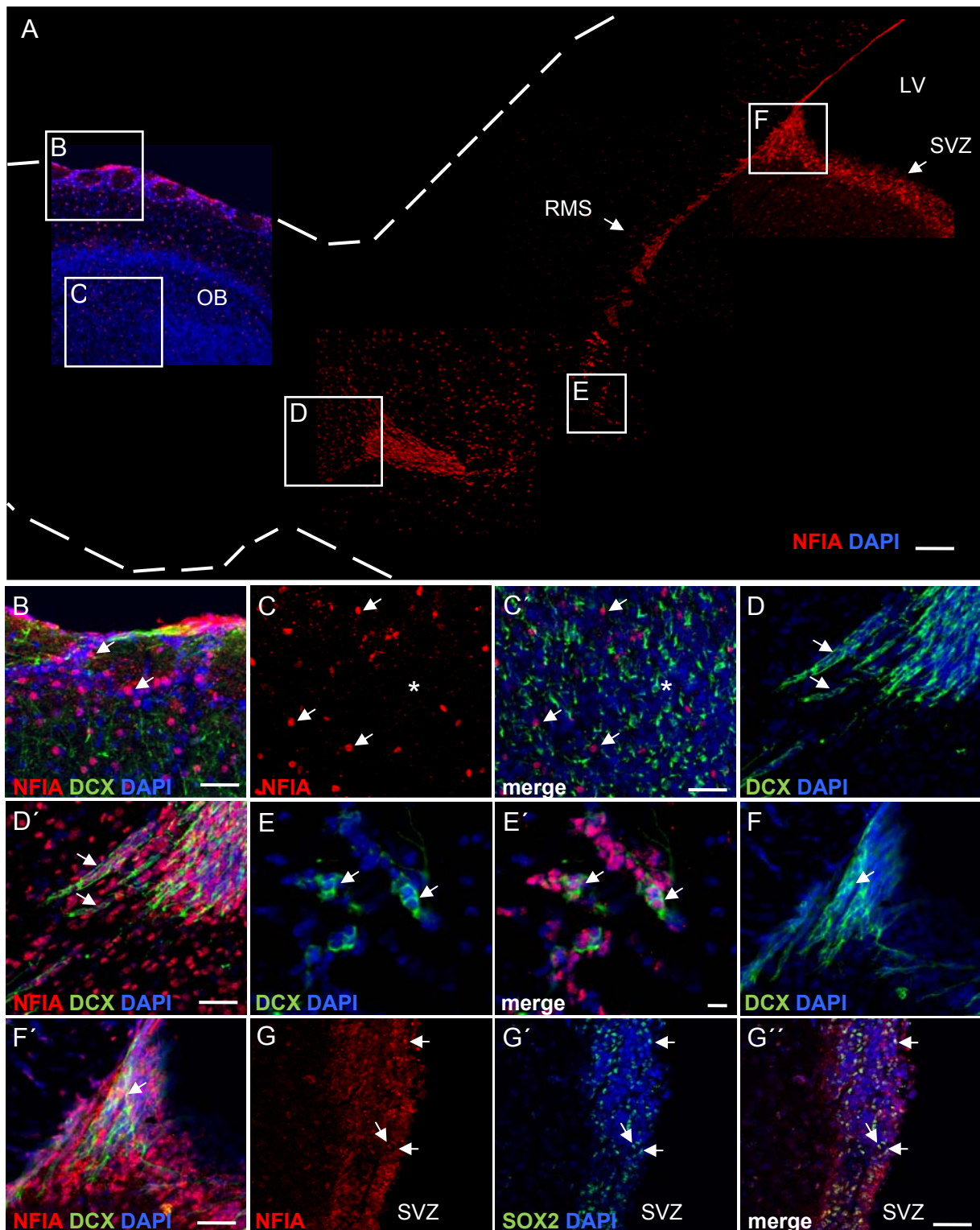
Fig.22 NFIA expression in the subventricular zone of the lateral ventricle, the rostral migratory stream and olfactory bulb

Representative confocal images of immunofluorescent stainings of brain slices from 8 week old mice **(A)** Overview of NFIA expression (red) in SVZ, RMS and OB. DAPI for nuclear counterstain in blue. **(B)** NFIA expression in periglomerular cells (arrows) of the OB. **(C)** NFIA (red, arrows) does not co-localize with DCX positive cells (green, asterisk) (arrows) in the OB. **(D-F)** NFIA expression in migrating DCX positive neuroblasts (arrows) throughout the RMS. **(G)** NFIA co-localizes with SOX2 positive cells (arrows) in SVZ. Scale bars (A) 75 µm, (B,C,D,F,G) 50µm, (E) 20 µm. OB

olfactory bulb, LV Lateral ventricle, RMS rostral migratory stream, SVZ subventricular zone.

Co-immunoprecipitation assays indicated that RBPJκ and NFIA interacted in adult neural stem cells (Fig. 12B). To determine whether the interaction of RBPJκ with NFIA was dependent on the presence of RNA/DNA, immunoprecipitation with antibodies raised against RBPJκ or non-immune IgGs were performed in the presence and absence of endonuclease (benzonase). Western blot analyses of the immunoprecipitated proteins showed that RBPJκ and NFIA interaction requires the presence of DNA or RNA (Fig. 23).
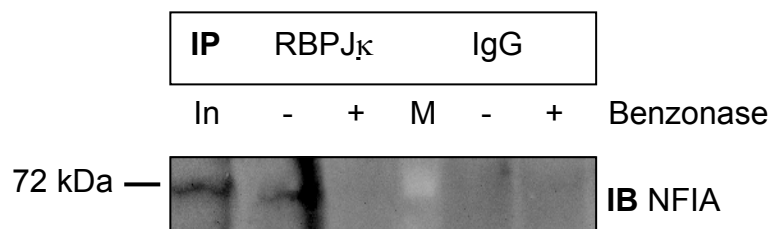
Fig. 23 RBPJκ interaction with NFIA requires the presence of DNA and/or RNA
Representative western blot of RBPJκ and NFIA co-immunoprecipitation. Interaction of RBPJκ and NFIA (- Benzonase lane) is lost after digestion of DNA/RNA during IP (+ Benzonase lane). Nuclear proteins were isolated from neurospheres and subjected to immunoprecipitation with antibodies raised against RBPJκ or with non-immune IgGs. IPs were performed for 3 h in the presence or absence of the endonuclease benzonase. Input (In) represents 5% of protein used for IP. M: marker.

4.4.2 NFIA inhibits Notch signalling-mediated *Hes1* and *Hes5* promoter activation

The expression pattern of NFIA in mouse adult brain and the fact that NFIA and RBPJκ interact in the presence of DNA/RNA in adult neural stem cells led to the hypothesis that NFIA could have a role in the modulation of Notch/RBPJκ-dependent gene expression. To prove this hypothesis, the effects of NFIA on Notch/RBPJκ target promoter were investigated. To this end, the promoters of the canonical Notch/RBPJκ gene targets *Hes1* and *Hes5* were used. Their activity was studied using *Hes1* and *Hes5* luciferase reporter assays in HEK293T cells. Activation of the

Notch-signalling pathway was achieved through transfection with an expression vector encoding for NICD. Increasing amounts of *Nicd*-cDNA were co-transfected together with the *Hes1* and/or the *Hes5* luciferase promoter reporter constructs (data not shown). The amount of *Nicd*-cDNA (40 ng), which increased *Hes* luciferase promoter activity in the submaximal range, was subsequently used to test the effects of co-transfection with different amounts of NFIA (0,1 ng – 250 ng) on *Hes* promoter activity.

Overexpression of NICD resulted in a significant 45-fold increase of *Hes1* promoter luciferase. In contrast, NFIA alone inhibited luciferase activity to 0,54-fold (Fig. 24A). Expression of a dominant negative constructs of *Nfia* (*dnNfia*), which contains the DNA binding- but misses the transactivation domain (Namihira et al., 2009) resulted in 0,9-fold induction of *Hes1* promoter activity. Co-expression of NFIA with NICD significantly decreased NICD-induced *Hes1* promoter activity to 2,75-fold. In contrast, dnNFIA not only did not decrease NICD-induced *Hes1* luciferase promoter activity but it even slightly improved it (51-fold induction).

NICD alone significantly increased *Hes5* promoter luciferase activity by 13-fold while NFIA significantly inhibited promoter activity to 0,06-fold (Fig. 24B). Expression of the *dnNfia* construct alone resulted in 1,21-fold induction. Co-expression of NFIA and NICD significantly inhibited NICD-induced *Hes5* promoter activity (0,76-fold induction). In contrast, co-expression of dnNFIA with NICD did not inhibit NICD induced *Hes5* luciferase promoter activity but it even slightly improved it (17-fold induction).
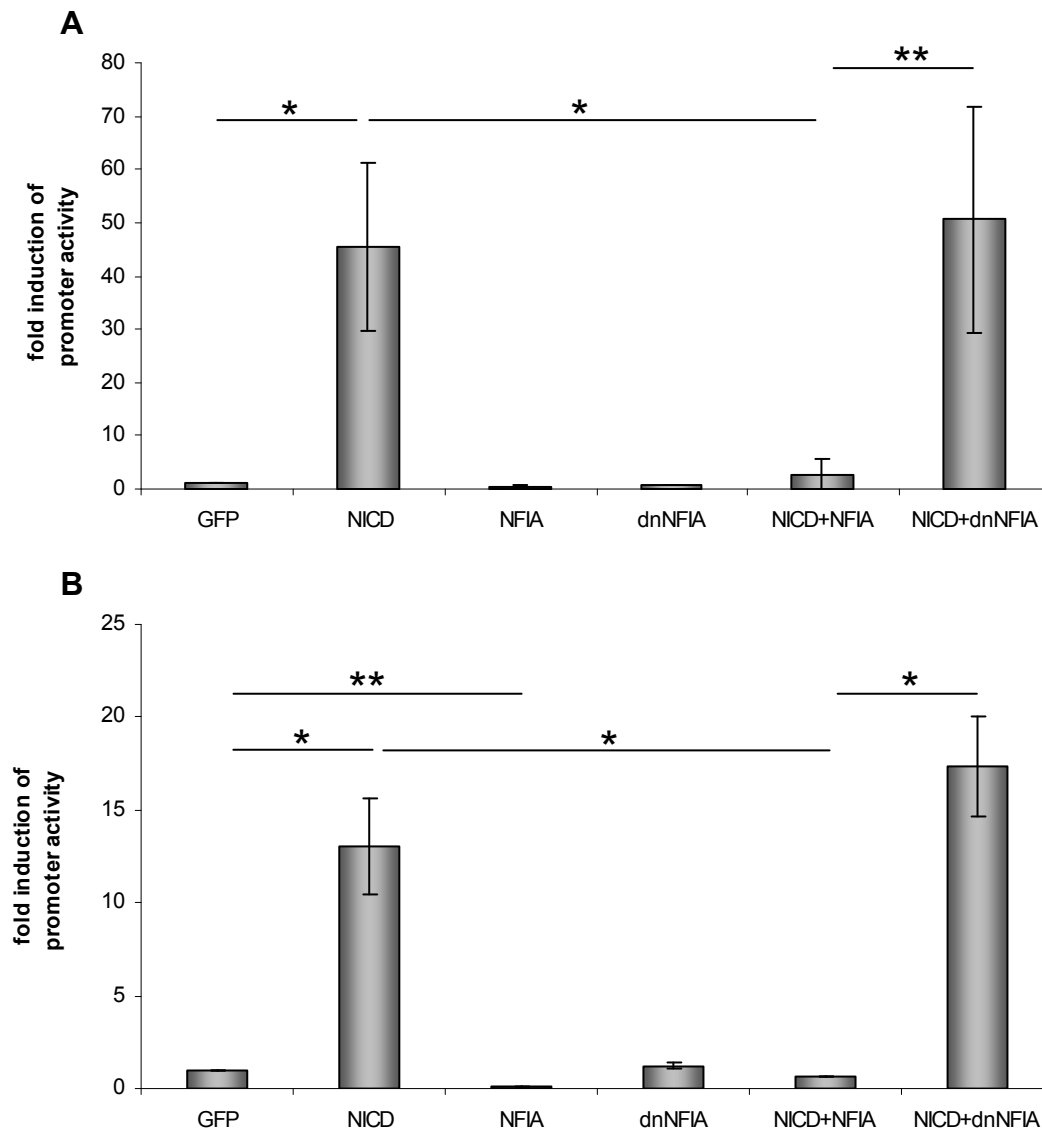
Fig. 24 NFIA inhibits Notch signalling mediated *Hes1* and *Hes5* luciferase activation

Luciferase reporter assays in HEK293T cells. HEK293T cells were transiently transfected either with the cDNA of *Nicd*, *Nfia*, *dnNfia* alone,or *Nicd* in combination with *Nfia* or *dnNfia*. *Hes* promoter luciferase reporter activity was assayed 48h after transfection. **(A)** Effect on *Hes1* promoter luciferase activity. Overexpression of NICD resulted in a significant 45-fold increase of *Hes1* promoter luciferase activity. NFIA decreased luciferase activity to 0,54-fold while the dnNFIA, which contains only the DNA binding but not the transactivation domain, showed almost no effect (0,9-fold) on promoter activity. Co-expression of NFIA together with NICD significantly inhibited NICD-induced *Hes1* promoter activity to 2,75-fold. dnNFIA did not inhibit NICD induced *Hes1* promoter activity but slightly increased it (51-fold). **(B)** Effect on *Hes5* promoter luciferase activity. Overexpression of NICD resulted in a significant 13-fold increase of *Hes5* promoter activity. NFIA significantly decreased luciferase activity to 0,06-fold while dnNfia showed no effect (1,2-fold) on promoter activity. Co-expression of NFIA significantly inhibited NICD induced *Hes5* promoter activity to 0,66-fold induction. Again, dnNFIA did not interfere with NICD dependent induction of *Hes5* promoter activity. Results represent the mean ± SEM of 3 independent experiments performed in triplicate (*p<0.05, **p<0.01).

4.4.3 RBPJκ conditional knockout mice display increased NFIA expression in the dentate gyrus

Active Notch/RBPJκ signalling is essential for adult hippocampal neural stem cell maintenance *in vivo* (Ehm et al., 2010). I found that NFIA is highly represented in SGZ of the dentate gyrus in immature neuroblasts (Fig 21. C) and to a lower extent in neural stem cells (Fig. 21B). Further, my results and the study by Piper et al., (2010) indicate that NFIA inhibits active Notch signalling.

How inhibition of Notch-signalling on the other hand affects NFIA expression is currently unknown.

To investigate the effect of RBPJκ loss of function on NFIA expression, I examined Glast::CreER^{T2} x RBPJκ$^{loxP/loxP}$ x R26::EYFP (RBPJκ cKO) mice (Ehm et al., 2010). In these mice, RBPJκ is conditionally ablated in radial glia-like stem cells and in a subset of non-neurogenic astrocytes (Ehm et al., 2010). For control, Glast::CreER^{T2} x RBPJκ$^{loxP/+}$ x R26::EYFP mice, in which only one RBPJκ allele is deleted upon CRE mediated recombination, were used.

It was previously shown that RBPJκ cKO mice exhibit increased stem cell differentiation 3 weeks after Tamoxifen induced recombination (Ehm et al., 2010). Intriguingly, I found that at this time-point recombined cells exhibited an increased NFIA immuno-reactivity signal (Fig. 25B). Because all confocal images were taken with same settings and laser intensities the observed increase in NFIA immunoreactivity signal is likely to reflect increased NFIA expression. This observation suggests that NFIA expression may be negatively controlled by Notch/RBPJκ signalling.

Further examinations 8 weeks after induction of recombination resulted in a virtual loss of NFIA expression in the SGZ of dentate gyrus (Fig. 25D). This result, together with my findings that NFIA is expressed in new-born neurons is in line with data of Ehm and colleagues (2010) indicating that ablation of RBPJk led to the loss of neurogenesis (Ehm et al., 2010).

Overall my findings suggest that expression of NFIA and Notch/RBPJκ signalling activity are connected and that the interplay between NFIA and Notch/RBPJκ signalling may significantly contribute to the balance of stem cell maintenance and differentiation in adult neurogenesis.
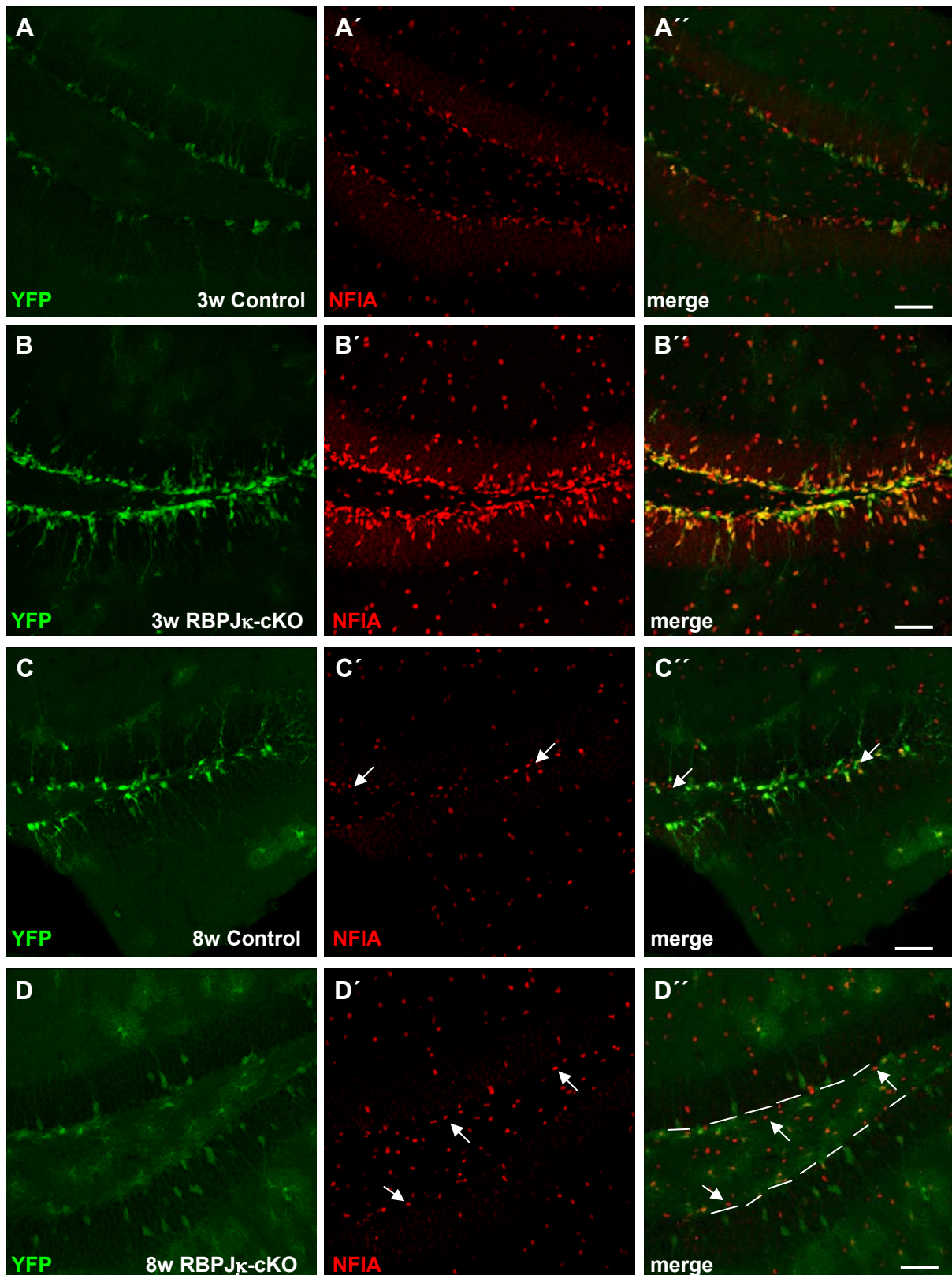
Fig. 25 Loss of RBPJκ in radial glia-like stem cells increases NFIA expression 3 weeks after induction of recombination. 8 weeks after recombination NFIA expression is virtually absent in the SGZ.

Representative confocal images of immunofluorescent stainings of brain slices from RBPJκ cKO and control mice. All images were taken with same confocal microscopy settings. **(A)** 3 weeks after recombination, control heterozygous Glast::CreER^{T2} x

RBPJκ^loxP/+ x R26::EYFP mice (RBPJκ+/-), in which only one RBPJκ allele is deleted upon Cre-mediated recombination, showed less NFIA staining intensity compared to RBPJκ cKO mice **(B)** that exhibited an up-regulation in NFIA expression in YFP positive cells. (C-D) Analyses of brain slices 8 weeks after recombination. Control mice **(C)** display NFIA positive cells in the SGZ (arrows) while NFIA positive cells are strongly reduced in the SGZ but still present in the hilus (arrows) of RBPJκ cKO mice **(D)**. DG: dentate gyrus; SGZ: subgranular zone; Scale bars 50 µm.

5 Discussion

The generation of new born neurons in the neurogenic niches of the adult brain significantly contributes to hippocampus dependent learning and mood regulation (Shors et al., 2001; Saxe et al., 2006; Dupret et al., 2008; Imayoshi et al., 2008; Zhang et al., 2008; Clelland et al., 2009; Deng et al., 2009; Garthe et al., 2009; Kitamura et al., 2009, Sahay et al., 2011). Maintaining adult neurogenesis throughout lifetime and balancing neural stem cell maintenance and differentiation to new neurons therefore is essential to ensure optimal hippocampal function. Several studies indicate that aging strongly reduces the generation of new neurons in adult hippocampus in rodents and primates (Kuhn et al., 1996; Kempermann et al., 1998; Gould et al., 1999; Drapeau et al., 2003; van Praag et al., 2005; Kronenberg et al., 2006; Rao et al., 2006; Villeda et al., 2011). Intriguingly, age-associated decline of cognitive function was found to correlate with a decreasing rate of adult hippocampal neurogenesis (Drapeau et al., 2003; van Praag et al., 2005). Whether decreasing neurogenesis is due to impaired stem cell maintenance or due to an increase of quiescent stem cells is not fully understood yet (Lugert et al., 2010; Manganas et al., 2007; Walker et al., 2008; Aizawa et al., 2009).

The aim of this work was to identify new regulators of neural stem cell maintenance. This was pursued using a candidate and an unbiased approach. New candidate regulators of stem cell maintenance were identified on the basis of their interaction with RBPJκ, the only known transcriptional downstream effector of Notch signalling. Such approach was based on the finding that RBPJκ is essential for stem cell maintenance (Ehm et al., 2010; Imayoshi et al., 2010).

5.1 Interaction of the Notch signalling pathway with FOXOs

In the candidate approach FOXO transcription factors (TF) were analysed. FOXO TFs have previously been found to control cellular homeostasis and proliferative activity through the regulation of genes involved in cell cycle regulation (*p21*, *p27*, *cyclin2*), apoptosis (*Fasl, Bim, Bcl-6, Puma*), detoxification (*MnSOD, Catalase*), DNA repair (*Ddb1, Gadd45a*) and cellular metabolism (*Pepck, G6pc*) (van der Horst and Burgering, 2007). Numerous studies demonstrated a fundamental role of FOXO in regulation of maintenance of various stem cells, such as hematopoietic stem cells, muscle stem- and progenitor cells, mouse spermatogonial stem cells, human

embryonic stem cells and neural stem cells (Goertz et al., 2011; Kitamura et al., 2007; Miyamoto et al., 2007; Paik et al., 2009; Renault et al., 2009; Tothova et al., 2009; Zhang et al., 2011). Paik and co-workers (2009) conditionally ablated FOXO1/3/4 in astrocytes and progenitor cells in the embryonic mouse brain and observed decreased proliferation and decline of SOX2 positive cells in the adult SVZ. This finding was accompanied by another study where *Foxo3*-gene knockout resulted in less cell proliferation in the adult dentate gyrus and impaired neurogenesis *in vitro* (Renault et al., 2009). In both studies, however, FOXO TFs were ablated from early development on and not confined to adult neural stem cells. Hence, the precise role of FOXO1, 3 and 4 in adult neural stem cell maintenance remained to be determined.

FOXO1 and FOXO3 transcription factors have been described previously to modulate the expression of the Notch downstream target *Hes1* in muscle stem- and progenitor cells through interaction with RBPJκ (Kitamura et al., 2007). In this work, I found FOXO1 and FOXO3 expression in GFAP and SOX2 positive cells in the dentate gyrus (see Fig. 4). This further confirmed in situ hybridisation analysis by Hoekman et al., (2006) that described *Foxo1* and *Foxo3* mRNA expression in the neurogenic niches as well as findings by Renault et al. (2009) that showed FOXO1 and FOXO3 expression in SOX2 positive progenitor cells in SGZ of dentate gyrus (Hoekman et al., 2006; Renauld et al., 2009). On the basis of this result, I analysed the possibility that RBPJκ might interact with FOXO1 and FOXO3 in adult neural stem cells as previously described in muscle stem cells (Kitamura et al. 2007). Indeed, FOXO1 and FOXO3 co-immunoprecipitated with RBPJκ in nuclear extracts from adult NSCs (see Fig. 5). At present, it remains to be determined whether this CoIP reflects direct physical interaction or whether FOXO1 and 3 binding to RBPJk is mediated by other proteins as well. Moreover, since FOXO1/3 and RBPJκ could co-target promoter regions in close proximity on a number of promoters and since protein extracts were not pre-treated with DNA/RNAse in these experiments, it cannot be ruled out that DNA acts as a bridging factor leading to CoIP of FOXO1/3 and RBPJκ.

Regardless of whether the interaction between RBPJκ and FOXO1/3 is direct or mediated via nucleic acids, the CoIP data raised the possibility that FOXO1/3 and RBPJκ converge on same gene targets in adult NSCs. Ehm and colleagues (2010) previously reported that active Notch signalling is transcriptionally activating *Sox2-*

gene expression through RBPJκ in adult neural stem cells. Moreover, a recent publication demonstrated that *Foxo1* siRNA-mediated knockdown decreases *Sox2* expression in human ESCs (Zhang et al., 2011). Consistent with a direct regulation of *Sox2*-gene expression by FOXO1, in silico analysis of the *Sox2*-gene promoter predicted four putative FOXO binding sites (see Fig. 6). Moreover, overexpression of constitutive active *Foxo1*- and *Foxo3* cDNA in luciferase assays resulted in an increase of *Sox2* promoter activity (see Fig. 7). Unpublished data from Dr. A. Khan and I. Schäffner (personal communication, Helmholtz Center Munich) further demonstrate promoting effect of FOXO1 and FOXO3 on Notch target promoters *Hes1* and *Hes5* in luciferase assays. In addition, they found that conditional knockout of FOXO1/3/4 in adult neural stem cells led to an increase of glutamine syntethase positive recombined RG-like stem cells indicating a progressive loss of NSC activity and therefore impaired stem cell maintenance *in vivo* (see Fig. 8). Collectively these data suggest that FOXO1 and FOXO3 directly control adult neural stem cell maintenance, potentially through cooperation with and modulation of the Notch/RBPJκ signalling pathway.

It would be interesting to investigate whether FOXOs also interact with Notch/RBPJκ signalling at later time points during neuronal differentiation. In this regard, FOXO1/3 was also found to be expressed in DCX positive immature and Calbindin positive mature neurons (unpublished data in cooperation with Dr. A. Khan and I. Schäffner, Helmholtz Center Munich). A potential function of FOXOs in later stages during the development of new neurons is suggested by the finding of Torre-Ubieta and colleagues (2010), who showed that FOXOs control neuronal polarity and dendritic development of primary hippocampal granule neurons *in vitro* (de la Torre-Ubieta et al., 2010). Intriguingly, Notch signalling has also been shown to be active in scattered cells in DG (Ehm et al., 2010) and moreover has been linked to the control of dendritic growth and polarity of newborn neurons in the adult DG (Breunig et al., 2007) and cortical neurons, respectively (Sestan et al., 1999; Redmond et al., 2000). Hence, interaction of FOXOs and Notch signalling might control major developmental processes in adult neurogenesis and may indeed extend to other cell systems.

5.2 Core transcriptional network in stem cell maintenance

Regulation of stem cell maintenance is likely to be a complex mechanism and previous studies indicated a vast number of factors as putative modifiers. How all these signals get integrated to faithfully maintain the stem cell pool and elicit an optimal balance between proliferation and quiescence is still unknown (Schwarz et al., 2012 in press). One possible explanation for how this might be achieved comes from ESC studies that indicated that several essentiall transcription factor, such as Octamer binding protein 4 OCT4, SOX2 and NANOG physically interact to regulate gene programs for the maintenance of ESC pluripotency (Ambrosetti et al., 1997; Ambrosetti et al., 2000; Boiani and Scholer, 2005; Chew et al., 2005; Rodda et al., 2005; Wang et al., 2006). In this line, numerous reports demonstrated that the precise regulation of the expression of OCT4, NANOG and SOX2 is essential for ESC identity (Nichols et al., 1998; Niwa et al., 2000; Masui et al., 2005; Chambers et al., 2007; Masui et al., 2007; Kopp et al., 2008). Interestingly, all three transcription factors modulate each others expression in a feedback system which keeps their expression at the appropriate levels needed to maintain pluripotency (Gonzales and Ng; Boyer et al., 2005; Pan et al., 2006). Strikingly, genome-scale and ChIP-seq analyses revealed co-binding of OCT4, NANOG and SOX2 to numerous targets, which encode for secondary transcription factors involved in maintaining ESC identity (Boyer et al., 2005; Loh et al., 2006). These initial findings established the idea that cell maintenance is regulated by a core network of essential transcription factors interacting and integrating signals to fine-tune ESC identity in precise manner (Ng and Surani; Boyer et al., 2005; Chen et al., 2008).
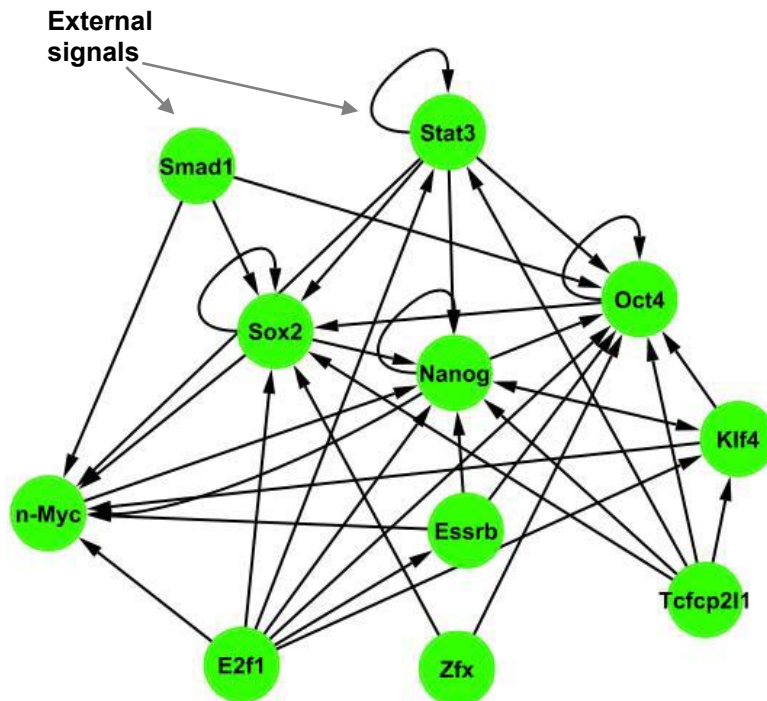
Fig. 26 Core network of interacting transcription factors in the regulation of embryonic stem cell maintenance
ESCs have been shown to contain several essential transcription factors, which are interacting on the same gene targets, thereby controlling ESC identity in precise manner. Transcription factors (green nodes) and interactions shown here were determined by ChIP-seq binding assays (Ivanova et al., 2006; Zhou et al., 2007). Arrows indicate interacting proteins and point of direction shows gene target.

Subsequent detailed MS/MS analysis of protein complexes of NANOG and OCT4 demonstrated extensive protein-protein interactions of multiple transcription factors, which might explain their colocalisation on same gene target promoters (Pardo et al., 2010; van den Berg et al., 2010; Wang et al., 2006; Liang et al., 2008).

The existence and identity of such core transcriptional regulatory network in adult neural stem cells remains largely unexplored. RBPJκ is an essential transcriptional regulator of stem cell identity and stem cell function which operates upstream of *Hes1, Hes5* and *Sox2* (Ehm et al., 2010; Zhang et al., 2011), that are all considered to be essential for stem cell self-renewal and multipotency (Favaro et al., 2009; Imayoshi et al.2010). Moreover, van den Berg and colleagues (2010) demonstrated that RBPJk also binds to OCT4 in ESCs and might be part of an ESC core network. Thus, RBPJκ was assumed as a good candidate acting in the core transcriptional regulatory network controlling NSC maintenance. Indeed, the RBPJκ interacting

proteins FOXO1 and FOXO3 were found to modify long-term maintenance of the stem cell population (see Fig. 8).

To identify new factors modulating Notch signalling and adult neural stem cell maintenance, the RBPJκ interactome in adult NSCs was investigated through an unbiased protein screening approach. ICPL analysis indicated 471 proteins as more than 2 fold enriched in RBPJκ IP (see Table 1). However, this list of interactors is likely to overestimate the number of putative protein-protein interactors, since IPs were not treated with benzonase and thus DNA and RNA could act as a matrix leading to bridging effects and therefore co-purification of proteins in RBPJκ IPs. Indeed, preliminary MS/MS analyses to determine the protein interactome of RBPJκ in ESC detected 166 candidates in IPs with antibodies against RBPJκ that were treated with DNAse and thus diminished DNA mediated interactions but left RNA mediated interactions intact. Moreover, when RBPJκ IPs were treated with benzonase and DNA as well as RNA were digested, MS/MS detected only 15 candidate interactors of RBPJk.

Several known RBPJκ interactors such as FHL1, HDAC, CtBP and RBPJκ itself could be identified in the protein screen but were not labelled by ICPL. Lack of ICPL labelling may be the consequence of low lysine/arginine content of proteins that can be therefore labelled by ICPL-tags only with low efficiency. One possible solution to circumvent this problem in future experiments could be SILAC (stable isotope coded labelling with amino acids in culture). SILAC is an alternative method for quantitative MS/MS in which proteins get metabolically labelled by incorporation of amino acid isotopes during cell culture (Ong et al., 2002; Ong et al., 2003). Presence of isotope coded lysine and arginine in cell culture medium could increase incorporation and therefore increases the chance of labelling and detection of proteins with low Arg/Lys content.

To further determine strong protein-protein interactions, immunoprecipitation experiments were performed under high salt conditions and RBPJκ protein complexes subsequent analysed by MS/MS. As expected high stringency resulted in a reduction of proteins co-immunoprecipitating with RBPJκ (see Table 2). IPs repeated in the presence of benzonase further confined putative protein interactors of RBPJκ. In parallel, factors known to be involved in transcriptional or stem cell regulation were also screened for their expression pattern. This combinatorial

screening approach drove attention on two proteins, TDP-43 and NFIA. TDP-43 was found to strongly bind to RBPJκ by protein-protein interaction even under high stringency conditions (see Table 2 and Fig. 14). The importance of TDP-43 and RBPJκ interaction was additionally supported by my findings in ESC where the physical interaction of both proteins also exists (data not shown).

Given the novel potential link between TDP-43 and Notch signaling as well as the genetic evidence for a causative role of TDP-43 in the neurodegenerative disease FTLD-U, the possible function of TDP-43 in Notch signaling was examined more in detail.

As a second candidate, the transcription factor NFIA was chosen. Interestingly, NFIA was found to be highly expressed specifically in SGZ of the dentate gyrus (see Fig. 21) as well as in SVZ of the lateral ventricles and RMS (see Fig. 22). NFIA was previously described as an essential regulator for gliogenesis during embryonic development possibly interacting with the Notch pathway (Namhihira et al., 2009; Piper et al., 2010).

5.3 Interaction of the Notch signalling pathway with TDP-43

TDP-43 was originally identified as a transcriptional repressor of HIV1 (Ou et al., 1995) and more recent work also indicated an inhibitory effect of TDP-43 on Acrv1 gene expression (Archarya et al., 2006; Lalmansingh et al., 2011). The physiological function of TDP-43, however, is largely unknown. The strong binding of TDP-43 to RBPJκ suggested a putative interaction on the modulation of Notch signalling. In contrary to data in the literature, that describes TDP-43 as a transcriptional repressor (Archarya et al., 2006; Lalmansingh et al., 2011; Ou et al., 1995), TDP-43 was found to activate transcription of a *Hes1* promoter luciferase reporter (see Fig. 15A). In addition, TDP-43 overexpression also increased endogenous levels of HES1 protein, indicating that artificial effects due to the presence of the luciferase gene can be excluded (see Fig. 20). Intriguingly, the promoting effect of TDP-43 on Notch signalling induced promoter activity was observed only in the context of the *Hes1* promoter, whereas TDP-43 did not alter the activity of the *Hes5* promoter, another canonical Notch target (see Fig. 15B). The specific effect of TDP-43 on *Hes1* promoter suggested that TDP-43 could act as a transcriptional cofactor for *Hes1* expression. Indeed, bioinformatics analysis of the 1,1 kb DNA sequence upstream of the transcription start site (TSS) indicated two putative binding sites for TDP-43

(Archarya et al., 2006; Lalmansingh et al., 2011) in the *Hes1* but not in *Hes5* gene promoter (see Fig. 17). Mutation of both binding sites, however, still resulted in activation of the mutated *Hes1* promoter luciferase by TDP-43 (see Fig. 18C). This might indicate that TDP-43 can also bind to another DNA consensus sequence present in *Hes1-* but not in *Hes5* promoter. Alternatively this could indicate that TDP-43 modulates Notch/RBPJ*k* dependent transcription without binding directly to *Hes1* promoter. Future experiments such as DNA foot printing or electrophoretic mobility shift assay (EMSA) should be performed to investigate the presence of other putative consensus sequences.

I also studied the effect of TDP-43 on Wnt signalling to investigate whether TDP-43 specifically enhances Notch signalling or is rather a general transcriptional cofactor recruited by several signalling pathways. Interestingly, TDP-43 alone increased activity of TOPFlash, a synthetic Wnt target promoter, but did not enhance β-catenin mediated activation of Super8x TOPFLASH luciferase reporter (see Fig. 16). This might suggest that, although TDP-43 can act as a transcriptional modulator on both *Hes1-* and Super8x TOPFLASH promoter, it can only enhance Notch signalling on *Hes1* promoter by interacting with RBPJκ. In this line, further analysis by means of ChIP/EMSA needs to determine whether TDP-43 enhances the activation of *Hes1* promoter by direct binding to the promoter.

5.4 Interaction of the Notch signalling pathway with an ALS and FTLD-U associated TDP-43 mutant

Major attention was drawn on TDP-43 after the discovery of polyubiquitinated and hyperphosphorylated TDP-43 inclusions in frontotemporal lobar degenerations (FTLD-U) and amyotrophe lateral sclerosis (ALS) (Neumann et al., 2006). Further studies revealed that many ALS or FTLD-U patients carry characteristic point-mutations in the TDP-43 gene. Interestingly, all but one point-mutation are located in the glycine rich domain which is predicted to mediate protein-protein interactions (Pesiridis et al., 2009). The relevance of these point-mutations in TDP-43 function, however, is not fully understood yet. The results presented in this study indicating that TDP-43 interacts with RBPJκ and modulates the transcriptional output of the Notch signalling pathway, raised the intriguing question whether Notch signalling is disturbed by disease-associated TDP-43 mutations. Indeed, overexpression of a disease-associated TDP-43 mutant, TDP-43 A315T, which contains a mutation in the

glycine-rich protein-protein interaction domain (see Fig. 3) resulted in decreased effect on Notch-induced *Hes1* promoter activity as well as on endogenous HES1 expression (see Fig. 19 and 20A). DNA and protein levels of WT and A315T mutant were comparable in these experiments. Furthermore both WT and A315T mutant were localized to the nucleus of transfected cells (see Fig. 20). If and how the A315T point-mutation leads to disturbed binding to RBPJκ and therefore to less enhancement of Notch pathway needs to be investigated in future. Using a tandem purification approach, for example (Gloeckner et al., 2009), tagged WT TDP-43 and A315T TDP-43 proteins could be purified and binding capability to RBPJκ could be compared by IP and subsequent western blot analysis. Moreover, the possibility that the A315T mutation of TDP-43 could change the conformation of the protein and/or increase polyubiquitination needs to be examined. These changes could also lead to a different protein half-life and function, which might not be detectable by western blot analyses and might explain the differences between WT and mutant in *Hes1* promoter activation.

Taken together, it will be fascinating to examine in future, whether misregulation of TDP-43 affects Notch signalling and therefore adult hippocampal neurogenesis. In this regard, very recent data by Swarup and colleagues (2011), indicating that mice overexpressing WT TDP-43 exhibited significant spatial learning impairment in the Barnes maze test at 10 months of age, might support the importance of TDP-43 for adult neurogenesis (Swarup et al., 2011). Whether Notch signalling and therefore adult hippocampal neurogenesis as well is affected in these mice, however, still needs to be determined.

5.5 Interaction of the Notch signalling pathway and NFIA

The second protein candidate I analysed in this work was the transcription factor NFIA, which belongs to the nuclear transcription factor family 1 (NFI). NFIs were originally linked to CNS development and brain function because of the striking phenotype of *Nfia* knockout mice that display agenesis of the corpus callosum (ACC), hydrocephalus and reduced *Gfap*-gene expression (das Neves et al., 1999). Further studies indicated a promoting effect of NFIA in glial fate specification during embryonic spinal cord and neocortical development (Deneen et al., 2006; Namihira et al., 2009). The physiological function of NFIA in adult neurogenesis is currently unknown.

Strikingly, NFIA was found to be highly and specifically expressed in SVZ and SGZ of dentate gyrus (see Fig. 21 and 22). Moreover, the results indicated that NFIA is expressed in Nestin-GFP and SOX2 positive cells as well as strongly in DCX positive immature neurons compared to SOX2 positive cells in DG. In previous studies NFIA expression in the developing brain was not only detected in astrocytes but also in neurons (Piper et al., 2010; Plachez et al., 2008). Interestingly, by in silico analyses I found a perfect palindromic consensus NFI binding sequence (Gronostajski, 2000) on the neuron specific DCX promoter (data not shown). Wang and colleagues (2004) demonstrated binding of NFI to the promoter of GABA A receptor (*Gabra6*) by ChIP and EMSA assays, suggesting an active role for this protein family in transcription of neuron specific gene targets. Work by Zheng et al., (2010) indicated a NMDA receptor activity-dependent induction of *Nfia* expression and subsequent effect of NFIA on the survival of cortical primary neurons in culture. Together with my finding that NFIA is expressed in immature neurons and periglomerular interneurons in the OB, this might indicate that NFIA could play an important role not only in astrogenesis during embryonic development but also in adult neurogenesis.

Furthermore, I found that NFIA could inhibit Notch signalling mediated activation of *Hes1* (see Fig. 24A) and *Hes5* promoter luciferase activity (see Fig. 24B). This is consistent with recent work by Piper et al., (2010) who showed an up-regulation of *Hes1/5* expression in micro-arrays of hippocampal tissue from *Nfia* knockout mice. Considering the high expression in immature neurons and the inhibiting effect of NFIA on Notch signalling, NFIA might act as a switch from stem cell maintenance to neuronal fate committment. Intriguingly, I found that NFIA expression is up-regulated in RBPJκ cKO mice 3 weeks after recombination (see Fig. 25B). This finding is in strong contrast to the data of Namihira et al., (2009), who showed that RBPJκ is bound to NFIA promoter and activates NFIA expression.

The present results suggest that RBPjκ itself may inhibit the expression of NFIA by a putative negative feedback loop to ensure stem cell maintenance. Whether NFIA is repressed directly by RBPJκ/Notch or whether NFIA is regulated by RBPJκ/Notch through an indirect mechanism needs to be determined in future experiments. This question could be addressed by investigating the effect of RBPJκ/NICD on *Nfia* promoter as well as by analysis of the impact of NICD overexpression on *Nfia* promoter in luciferase assays. It will also be fascinating to examine whether a NFIA gain-of-function approach will result in *in vivo* inhibition of Notch signalling in the adult

neurogenic niche and will - similar to RBPJk loss of-function - result in precocious differentiation and depletion of neural stem cells. This would be in contrast to a very recent work in which it was shown, that in utero overexpression of *Nfia* leads to massive astro-gliogenesis rather than increased neurogenesis in the developing hippocampus of mouse embryos (Subramanian et al., 2011), which is consistent with the known astro-gliogenic effect of NFIA (das Neves et al., 1999; Deneen et al., 2006). To study the effect of NFIA knockout specifically in adult neural stem cells *in vivo*, conditional knockout NFIA reporter mice (Nfia tm1e, EUCOMM, Helmholtz Center Munich) could be crossed with Glast-CreER^{T2} mice (Mori et al., 2006) and the progeny analyzed. GLAST is an astrocyte-specific glutamate transporter, which allows CRE-driven recombination of *Nfia* specifically in astrocytes and therefore radial-glia like stem cells in the adult brain as well.

It needs to be mentioned that I also found NFIB expression in aNSCs as well as an inhibitory effect of NFIB on Notch signalling, indicating a redundant function of NFI transcription factors (Piper et al., 2010). Intriguingly, *Nfib* mRNA is expressed in neurogenic astrocytes of the SVZ but is absent from non-neurogenic astrocytes of the diencephalon (Beckervordersandforth et al., 2010). Consistent with the expression of *Nfib* mRNA in neurogenic astrocytes, I found NFIA and NFIB to be highly expressed in the SVZ and RMS.

In contrast to the hippocampal neurogenic lineage, I observed that in the SVZ/OB system a sub-population of immature DCX-positive neurons did not express NFIA (see Fig. 22C) and that some mature granular and periglomerular interneurons in the OB continued to express NFIA (see Fig. 22B). Thus, it is possible that NFIA fullfils different functions in the SVZ/RMS compared to the SGZ. To study and compare putative gene targets of NFIA in particular developmental stages of adult neurogenesis, mice could be injected into SVZ, RMS or DG with retroviruses encoding a dominant negative NFIA (CAG-dnNfia-IRES-GFP) or control GFP protein (CAG-GFP-IRES-GFP). The GFP fluorescent cells could be then specifically isolated from tissue by laser-capture microdissection (Simone et al., 1998) and changes in gene expression further investigated by microarrays or Next-generation sequencing in order to obtain insight into the NFIA dependent gene network in adult neurogenesis.

Overall the data of the present study together with previous work suggest a novel regulatory function of NFIA during neural stem cell differentiation and neurogenesis.

It might also be interesting to investigate whether NFIA might regulate reprogramming of somatic cells into neurons by directly up-regulating pro-neuronal genes on the one hand or by regulating demethylation of pro-neuronal genes on the other hand, like it was already shown for the *Gfap* promoter (Namihira et al., 2009). Given such potential key regulatory function in neural fate decisions it will be fascinating to investigate whether the function of NFIA may be useful for regenerative strategies and could be exploited to promote neurogenesis in non-neurogenic regions of the adult brain.

5.6 Cross-talk of the Notch signalling pathway with other signalling pathways

One of the greatest challenges in studying neural stem cells is the understanding of how the rate of neurogenesis is adjusted in response to a multitude of different complex environmental and cognitive stimuli. One mechanism how this may be achieved is through a complex interaction of a core transcriptional network that integrates different signalling pathways which allows the cell to respond in a fine-tuned manner rather than an on/off-fashion (Merz et al., 2011; Ng and Surani 2011; Fuchs et al., 2004). Intensive cross-talk between the Notch pathway and other pathways, such as the PI3K, Wnt, BMP or TGFβ pathways, contributes to signalling diversity (Ables et al., 2010; Andersson et al., 2010; Wang et al., 2007b; Poellinger and Lendahl, 2008). In this work, I described the interaction of Notch/RBPJκ signalling pathway with the PI3K/FOXO pathway and found hints for a possible interplay of Notch with Wnt/β-catenin and TGFβ/Smad3 pathway (β-catenin and SMAD3, data not shown). The TGFβ/SMAD3 pathway inhibits neural stem cell proliferation (Buckwalter et al., 2006; Wachs et al., 2006) and has been reported to interact with Notch signalling in the mediation of *Hes1* (Nyhan et al.; Blokzijl et al., 2003) and *Hey1* expression (Zavadil et al., 2004).

Moreover, I found transcription factor FHL1 to be enriched in the tandem mass spectrometry (MS/MS) analysis of RBPJκ IPs in neurospheres. FHL1 has been shown to interact with SMAD3 to cooperatively down-regulate cell proliferation by activating transcription of *cmyc* and *p21Cip1* expression (Ding et al., 2009). Furthermore, FHL1 was also reported to inhibit Notch signalling through binding to RBPJκ and thereby regulating the recruitment of co-repressors to the RBPJκ transcriptional co-repressor complex (Taniguchi et al., 1998; Qin et al., 2005; Wang

et al., 2007a). Interestingly, preliminary MS/MS results of DNAse/RNAse pre-treated IPs of RBPJκ in ESCs could also show a strong enrichment of FHL1, which might suggest a putative interaction of FHL1 with RBPJκ.

Hence, the potential for manifold interactions of Notch-signalling raise the possibility that crosstalk modulates the genetic program of maintenance and quiescence and thus allows the neural stem cell pool to integrate multiple signals and to respond to acute changes in the strength of external signals (Schwarz et al., 2012 in press).

It will be fascinating to further verify these interactions and to determine whether they are essential for fine regulation of the Notch signalling pathway and whether such protein interactions indeed explain the modulation of stem cell behaviour through multiple pathways. Furthermore, performing proteomic analysis in the context of Notch-signalling pathway activation in aNSCs *in vitro* could reveal how the RBPJk interactome and thus RBPJκ-dependent transcriptional activity are modulated during different states of pathway activation. Combining these experimental paradigms with ChIP-seq and Next-generation sequencing (Margulies et al., 2005; Shendure et al., 2005) might also be used to decipher differences in gene targets and their expression. In this regard, investigating putative gene targets of RBPJκ interactors as well would shed even more light on the complex picture of stem cell regulation.

It will also be interesting to examine differences in the interactome of RBPJκ between aNSCs and a non-stem cell related cell line such as fibroblasts to find stem cell specific interactors. However, since aNSC cultures consist of a quite heterogeneous cell population and RBPJκ is expressed also in precursor and glia cells (Komine et al., 2007), analysing the complex modulation of RBPJκ interactome and effects on transcription might not be stem cell specific. One possible solution to circumvent this problem in future experiments could be the utilization of neural stem cells derived from ESC cultures, which are more homogenous (Bibel et al., 2007).

Summarized, the Notch-signaling pathway with its central function in stem cell maintenance and its multiple putative interactions provides a molecular entry point to test for the existence and identity of a core transcriptional network in the control of adult hippocampal stem cell maintenance and proliferation (Schwarz et al., 2012 in press).

5.7 Is Notch signalling impaired in neurodegenerative disease?

An association between impaired Notch signalling and neurodegenerative diseases has primarily been shown for Alzheimer´s disease (Ethell, 2011) and Prion disorders (Ishikura et al., 2005). Initially, Notch signalling pathway has been linked to Alzheimer´s disease due to the fact that the y-secretase is the main protease processing both the Notch intracellular domain NICD and the amyloid precursor protein APP (Berezovska et al., 1998; McGeer et al., 1998). Intriguingly, multiple proteins, that co-immunoprecipitated with RBPJĸ, could be linked to Alzheimer´s disease (33 genes), Parkinson´s disease (34 genes) and Huntington disease (38 genes) (see Fig. 10). Whether Notch signalling might play a role in neurodegenerative diseases other than Alzheimer´s disease, however, is not understood yet. The identification of a putative role of TDP-43 as a direct regulator of the Notch/RBPJĸ signalling pathway raises the question whether Notch/RBPJĸ signalling pathway is affected in patients with ALS and FTLD-U. Until now, there is no direct link between Notch/RBPJĸ and ALS or FTLD-U.

Several reports have shown that induction of NF-ĸB signalling pathway is associated with ALS onset and progression (Crosio et al.; 2010 Maruyama et al.; 2011 Tolosa et al.; 2011 Migheli et al., 1997; Casciati et al., 2002). NF-ĸB consists of two subunits, p50 and p65 that were described to play a role in many processes during development, maintenance and progression of many chronic diseases (Pahl, 1999). Very recently, work by Swarup and colleagues (2011) indicated an interaction between NF-ĸB and TDP-43 in spinal cord samples of ALS patients in which mRNA levels of both NF-ĸB and TDP-43 were elevated (Swarup et al., 2011). Interestingly, they also show that TDP-43 can act as a coactivator of NF-ĸB in transcription. Moreover, blocking the NF-ĸB pathway in transgenic mice overexpressing TDP-43 ameliorated ALS associated motor impairment. Numerous studies in different cell types already demonstrated interaction between NF-ĸB and Notch/RBPJĸ pathways (Bonini et al. 2011; Espinosa et al. 2010; Wang et al., 2001; Screpanti et al., 2003; Shin et al., 2006; Vilimas et al., 2007). Work by Espinosa and colleagues (2010) showed that HES1 directly represses CYLD, a negative regulator of NF-ĸB, and that shRNA-mediated down-regulation of *Hes1* prevented NF-ĸB activity in Jurkat cells. Intriguingly, interaction of NF-ĸB pathway and Notch signaling has been indicated in the regulation of neuronal plasticity in the brain. Bonini and colleagues (2011)

demonstrated an up-regulation of Notch signalling in the developing cortex of mouse embryos, which are deficient for the NfkB subunit p50. In addition, primary cortical neuron cultures indicated decreased branching of neurites, which could be restored by direct inhibition of Notch signalling through overexpression of siRNAs against Notch (Bonini et al., 2011). Whether Notch/RBPJκ is also up-regulated in ALS and FTLD-U and interacts with/regulate NF-κB pathway is not clear yet and need further examination.

The results of these studies together with my findings, however, might give new insights into disease mechanisms of ALS or FTLD-U to develop new therapeutic approaches in future.

6   Material and Methods

6.1   Material

All chemicals used in this work were, if not stated otherwise, purchased from Sigma-Aldrich (Deisenhofen, Germany), Biomol (Hamburg, Germany), Biorad (Munich, Germany), Fluka (by Sigma-Aldrich, Deisenhofen, Germany), Invitrogen (Karlsruhe, Germany), Kodak (Stuttgart, Germany), Merck (Darmstadt, Germany), Roth (Karlsruhe, Germany), Riedel de Haen (Seelze, Germany), Serva (Heidelberg, Germany). Reagents for molecular biology were purchased from Applied Biosystems (Darmstadt, Germany), New England Biolabs (Frankfurt am Main, Germany), PeproTech (Hamburg, Germany), Promega (Mannheim, Germany), Roche (Mannheim, Germany) and Waters (Germany). MilliQ water was used for the generation of solutions (Millipore, Schwalbach,Germany). All restriction enzymes and their respective buffers were purchased from Fermentas (St. Leon-Rot, Germany), Roche (Mannheim, Germany) and New England Biolabs (NEB) (Frankfurt am Main, Germany). Master-Mixes for PCR were purchased from Eppendorf (Hamburg, Germany).

6.1.1   Histological solutions

Borate buffer	Boric Acid	100	mM
	Dissolve in H_2O and adjust to pH 8.5		
Cryoprotect solution	Glycine	25	% (v/v)
	Ethylenglycol	25	% (v/v)
	Phosphate buffer	0,1	M
DAPI	DAPI	14.3	M
4% PFA	PFA	4	% (w/v)
	NaOH	2-3	pellets
	Dissolve in 0.1 M PO_4-Buffer. Heat up to solve; pH 7.4		
Phosphate buffer 0.2 M	Sodium phosphate monobasic	0,552	% (w/v)
	Sodium phosphate dibasic	2,19	% (w/v)
Sucrose 30%	Sucrose	30	% (w/v)
	Dissolved in 0.1 M Phosphate-buffer.		

TBS (10x)	Tris	250	mM
	NaCl	1.37	M
	KCl	26	mM
	Adjust to pH 7.5		
TBS++	TBS	1	x
	Donkey serum	3	% (v/v)
	Triton-X100	0.25	% (v/v)

6.1.2 Cell culture media and solutions

CaCl$_2$	CaCl$_2$ in H$_2$O	2	M
Dissociation solution	Trypsin (Sigma T4665)	0,13	% (w/v)
	Hyaluronidase (Sigma H3884)	0,07	% (w/v)
	Solve in solution 1, filtrate steril and prewarm at 37°C.		
ESC growth medium	DMEM (Gibco 21969)	500	ml
	MEM-NEAA (Gibco 11140-100x)	1,2	% (v/v)
	PenStrep (Gibco 15140-100x)	1	% (v/v)
	β-Mercaptoethanol (Gibco 31350-50mM)	0,24	% (v/v)
	FBS (Pan Biotech Sera ES 2602-P282905)	15,5	% (v/v)
	L-Glutamine (Gibco 25030-200mM)	1,8	% (v/v)
	HEPES (Gibco 15630-1M)	2,4	% (v/v)
	LIF	1000	U/ml media
HBS (2x)	NaCl	16	% (w/v)
	KCl	0,74	% (w/v)
	Na$_2$HPO$_4$ x 7 H$_2$O	0,402	% (w/v)
	Glucose	2	% (w/v)
	HEPES	10	% (w/v)
	NaOH, adjust to pH 7.05		
HEK293T and N2A cell medium	DMEM (Gibco 41966)	500	ml
	FBS (PAA A15-102)	10	% (v/v)
	Anti-anti (Gibco 15240-062-100x)	1	% (v/v)

Neurosphere medium	DMEM/F12 (GIBCO-31331)	500	ml
	B27 (Gibco 08-0085SA-50x)	2	% (v/v)
	Anti-anti (Gibco 15240-062-100x)	1	% (v/v)
	HEPES (Gibco 15630-1M)	1	% (v/v)
	Add 10ng EGF and FGF per ml medium fresh		
	every second day.		
Solution 1 (NSC preparation)	HBSS (Life Tech 10x)	10	% (v/v)
	D-Glucose (Sigma)	1,8	% (v/v)
	HEPES (Life Tech, 1M)	1,5	% (v/v)
	pH 7.5		
Solution 2 (NSC preparation)	HBSS (Life Tech 10x)	5	% (v/v)
	Sucrose (Sigma)	30,8	% (w/v)
	pH 7.5		
Solution 3 (NSC preparation)	BSA (Sigma A4503)	4	% (w/v)
	HEPES (Life Tech, 1M)	2	% (v/v)
	EBSS (Life Tech 1x)	98	% (v/v)
	pH 7.5		

6.1.3 Molecular biology solutions

DNA-Loading dye (6 x)	Tris/HCl, pH 7.5	10	mM
	Glycerol	50%	(v/v)
	EDTA	100	mM
	Xylencyanol	0,25 % (w/v)	
	Bromphenol blue	0,25 % (w/v)	
EtBr	Ethidiumbromide staining solution	1	µg/ml
LB medium	Bacto-Trypton	10	g/l
	Bacto-yeast extract	5	g/l
	NaCl	10	g/l
	pH 7.0; autoclave (120°C, 20 min)		
LB agar	Bacto-Trypton	10	g/l
	Bacto-yeast extract	5	g/l
	NaCl	10	g/l

| | Bacto-agar | 15 | g/l |
| | pH 7.0; autoclave (120°C, 20 min) | | |

| LB^amp agar plates | LB agar + Ampicillin | 0.1 | % (m/v) |

Loading dye (6x)	Tris-HCl, pH 7.5	10	mM
	EDTA	100	mM
	Glycerol	50	% (v/v)
	Xylencyanol	0.25	% (v/v)
	Bromphenolblue	0.25	% (v/v)

PBS (10x)	NaCl	137	mM
	KCl	2.7	mM
	Na_2HPO_4	8	mM
	KH_2PO_4	1.4	mM
	Adjust to pH 7.4		

TAE-buffer (5x)	Tris, pH 8.3	90	mM
	Acetic acid	90	mM
	EDTA	2.5	mM

6.1.4 Protein isolation solutions

All buffers contained the following substances added before use:

	DTT	1	mM
	PMSF (in 100% isopropanol)	1	mM
	Complete mini Proteinase Inhibitor tablet		
	PhosphoStop Phosphatase Inhibitor tablet		

Buffer A	HEPES	10	mM
	EDTA	1	mM
	EGTA	1	mM
	KCl	10	mM
	$MgCl_2$	1,5	mM

Buffer C	HEPES	20	mM
	EDTA	0,2	mM
	KCl	400	mM
	$MgCl_2$	1,5	mM
Buffer D	HEPES	20	mM
	EDTA	0,2	mM
	$MgCl_2$	1,5	mM
	Glycerol	26,6	% (v/v)
Buffer E	HEPES	20	mM
	EDTA	0,2	mM
	KCl	200	mM
	NP40	0,02	% (v/v)

6.1.5 Western blot analysis solutions

APS solution	Ammonium persulfate	440	mM
Coomassie brilliant blue	Methanol	40	% (v/v)
	Acetic acid	10	% (v/v)
	Coomassie R250	0.4	% (w/v)
	Coomassie G250	0.4	% (w/v)
Developer solution	Sodium carbonate	6	% (w/v)
	STS solution	2,5	% (v/v)
	H_2O	97,5	% (v/v)
	Formaldehyde (37 %)	0,05	% (v/v)
Fixer solution	Methanol	50	% (v/v)
	Acetic acid	12	% (v/v)
	H_2O	38	% (v/v)
	Formaldehyde (37 %)	0,05	% (v/v)
Laemli buffer (5x)	SDS	19,8	mM
	Glycerine	479,6	mM
	Tris/HCl, pH 6,8	300	mM
	β-Mercaptoethanol	0,358	mM

PAGE buffer 10x	Tris	0,25	M
	Glycine	1,92	M
	SDS	1	% (w/v)
	Solve in 1000 ml H_2O		
Preserver solution	Ethanol	20%	(v/v)
	H_2O	78%	(v/v)
	Glycerol	2%	(v/v)
Silver solution	Silver nitrate	0,2	% (w/v)
	Add 7,5 µl formaldehyde (37%) / 10 ml solution		
SDS (10x)	Sodium dodecyl sulfate	10	% (v/v)
	Adjust to pH 7.2 (HCl)		
SDS PAGE transfer buffer	Tris base	25	mM
	Glycine	192	mM
	Methanol	20	% (v/v)
STS solution	Sodium Thiosulfate	1,25	mM
	H_2O		
Stripping solution	Glycine	200	mM
	Adjust to pH 2-3		
TBST	TBS	1	x
	Tween	0.1	% (v/v)
TBST+	TBST	1	x
	Milk powder	5	% (w/v)
TFA solution	Trifluoroacetic acid in HPLC H_2O	0,5	% (v/v)
Tris-HCl	TRIZMA Base	0.1	M

6.1.6 Mass spectrometry analysis solutions

ABC solution	Ammoniumbicarbonate	50	mM
	Dissolve in HPLC H_2O		

| Acetonitril | Acetonitril in HPLC H_2O | 40 | % (v/v) |

| IAA solution | Iodoacetamide | 300 | mM |
| | Dissolve in HPLC H_2O and store in darkness | | |

| RapiGest | RapiGest (Waters) dissolve in 50 µl HPLC H_2O. | | |

6.1.7 Commercial kits

Commercial kit	Manufacturer
AB solution for Western blots	Peqlab Biotechnologie, Erlangen, Ger.
DNA Maxi Prep	Promega, Mannheim, Germany
DNA Mini Prep	Macherey-Nagel, Düren, Germany
Dual luciferase assay	Promega, Mannheim, Germany
ECL solution for Western blots	GE Healthcare, Munich, Germany
ICPL Kit	Serva Electrophoresis, Heidelberg, Ger.
PCR Master Mix	Eppendorf, Hamburg, Germany
RNeasy Kit	Qiagen, Hilden, Germany
cDNA Kit SuperScript III	Invitrogen, Karlsruhe, Germany
Gel extraction	Qiagen, Hilden, Germany

6.1.8 Primary antibodies

Antibody	Species	Dilution	Company
BrdU	rat	1:500	AbD Serotec
β-Actin	mouse	1:10000	Abcam
CTCF (D31H2)	rabbit	1:250	Cell Signaling
DCX (C-18)	goat	1:250	Santa Cruz Biotechnology
FOXO1 (C29H4)	rabbit	1:200	Cell Signalling
FOXO3 (H-144)	rabbit	1:200	Santa Cruz Biotechnology
Fus/TLS	rabbit	1:1000	Bethyl Laboratories, Inc.
GFAP	mouse	1:1000	Zytomed Systems
GFP	chicken	1:1000	Aves Labs
HES1	rabbit	1:1000	Abcam (ab71559)
NFIA	rabbit	1:1000 (WB)	Active Motif
		1:1000 (IHC)	
		1µg (IP)	
NFIB	rabbit	1:200	Active Motif
RBPJκ (6E7)	rat	1 µg	Non-commercial, from Dr. E. Kremmer
			Helmholtz Center Munich, Germany

RBPJκ (7A11)	rat	1 μg	Non-commercial, from Dr. E. Kremmer Helmholtz Center Munich, Germany
Sox2 (Y-17)	goat	1:1000	Santa Cruz Biotechnology
TDP-43 (G400)	rabbit	1:2000 (WB) 1:250 (IHC)	Protein Tech Group
DAPI (fluorescent dye)		1:10000	Sigma

6.1.9 Secondary antibodies

All secondary antibodies were purchased from Jackson ImmunoResearch Laboratories, Inc. Following fluorophore-conjugated antibodies directed against different species, according to primary antibodies, were used in this work: Alexa 488, Alexa 543, Cy3, Cy5, FITC and HRP. Dilutions of secondary antibodies for IHC: 1:500, WB 1:10000 in combination with ECL and 1:100000 when AB reagent (Peqlab) has been used for PVDF membrane developing.

6.1.10 Plasmids

Name	Properties	Reference
pBose-HA-Nfia	Expression vector, Ampr	Namihira et al., (2009)
pBose-NICD	Expression vector, Ampr	Mizushima and Nagata, (1990)
pCAG-hA315T-TARDBP	Expression vector, Ampr	obtained from PD. Dr. Thomas Floss Helmholtz Center Munich
pCAG-hTARDBP	Expression vector, Ampr	obtained from PD. Dr. Thomas Floss Helmholtz Center Munich
pCAG-Nfia-IRES-GFP	Expression vector, Ampr	this work
pCAG-dnNfia-IRES-GFP	Expression vector, Ampr	this work
pCAG-Nfib-IRES-GFP	Expression vector, Ampr	this work
pcDNA3-β-catenin-S33Y	Expression vector, Ampr	Group Prof. Dr. Lie
pCMX-RBP-J/R218H	Expression vector, Ampr	Kato et al., (1997)
pFG-dnNfia	Expression vector, Ampr	Namihira et al., (2009)
pGL3-Hes1	Expression vector, Ampr	Group Prof. Dr. Lie
pGL3-Hes5	Expression vector, Ampr	Group Prof. Dr. Lie
pGL3-Sox2	Luciferase vector, Ampr	Mizushima and Nagata, (1990)
phEF-Renilla	Luciferase vector, Ampr	Nakashima et al., (2005)
pMYs-HA-Nfib	Expression vector, Ampr	Namihira et al., (2009)
pSuper 8x TOPFLASH	Luciferase vector, Ampr	Korinek et al., (1997)

For luciferase assay analyses shown in this work, nuclear factor constructs were subcloned (CAG-NFI-IRES-GFP).

6.1.11 Primers

Primers for mutation in TDP-43 DNA binding site on *Hes1* promoter luciferase reporter in PCR:

Name		Sequence (5' – 3' direction)
TARDBP DBS 1 Mut	For	gggaaagaaagtttgggaagtttcgggcgagccgttcgcgtgc
TARDBP DBS 1 Mut	Rev	gcacgcgaacggctcgcccgaaacttcccaaactttctttccc
TARDBP DBS 2 Mut	For	gccagggcctgcggatcagggaggatctggagc
TARDBP DBS 2 Mut	Rev	gctccagatcctccctgatccgcaggccctggc

PCR program for mutagenesis:

1x	95°C	1 min				
18x	95°C	50 sec	60°C	50 sec	68°C	50 sec
1x	68°C	7 min				

6.1.12 Software

Cytoscape	http://www.cytoscape.org/
FluoView 1.7	Olympus, Hamburg, Germany
Fusion	Vilber Lourmat, Eberhardzell, Germany
Genomatix	Genomatix Software GmbH, Munich, Germany
Leica Application Suite AF	Leica Microsystems, Wetzlar, Germany
Proteome Discoverer 1.2	Thermo Scientific, Munich, Germany
Scaffold 3	Proteome Software Inc. Portland, Oregon, USA
Vector NTI	Invitrogen, Karlsruhe, Germany

6.2 Methods

6.2.1 Immunohistochemical methods

6.2.1.1 Animals

For all experiments, 8 and 12 weeks of age adult mice were used in this work. Mice were group housed in standard cages under a 12 hour light/dark cycle and had ad libitum access to food and water.

C57BL/6 mice were obtained from Charles River (Wilmington, USMA). Glast::CreER^{T2} x RBPJκ$^{loxP/loxP}$ x R26::EYFP (RBPJκ cKO) mice are described by Ehm et al., (2010). Glast::CreER^{T2} x Foxo1/3/4$^{loxP/loxP}$ x Rosa26::βGal mice were obtained from Dr. Amir Khan, Helmholtz Center Munich (unpublished data).

6.2.1.2 Tissue processing

Mice were deeply anaesthetised by CO_2 and then transcardially perfused with PBS (pH 7.4) at a speed of 10 ml per minute for 5 minutes in total, followed by 4% Paraformaldehyde (PFA) for 5 minutes. Animals were decapitated, brains removed and post-fixed in 4 % PFA overnight at 4°C. Next day brains were transferred to a 30 % sucrose solution and stored at 4°C until usage. For immunohistochemistry 40 µm thick coronal or sagittal brain sections were cut/prepared using a sliding microtome (Leica Microsystems, Wetzlar, Germany).

6.2.1.3 Immunohistochemistry

Brain tissue sections were rinsed 3 times in 1xTBS for 15 min each and then blocked with TBS++ for 1 hour at room temperature. Sections were then incubated in primary antibody solutions for 48 hours at 4ºC. Subsequently they were washed 3 times in 1xTBS for 10 min each, blocked with TBS++ for 30 minutes at room temperature and incubated with appropriate secondary antibodies (Donkey IgGs anti protein) in TBS++ for 2 hours in the dark at room temperature. For preventing bleaching of fluorescence further processing of sections was performed in the dark. Sections were rinsed in 1xTBS for 10 min, 1xTBS containing DAPI for 15 min and then washed twice for 10 min each in 1xTBS. Slices were mounted in 1xTBS on superfrost glass slides (Menzel-Gläser, Braunschweig) using Aqua/Polymount (Polysciences Inc., Warrington, USA). Mounted sections were kept overnight at RT to harden and then stored at 4°C. Confocal single plane images and Z-stacks were taken on an Olympus FluoView 1000 (Olympus, Hamburg, Germany) or on a Leica SP5 confocal microscope (Leica Microsystems).

6.2.2 Cell Culture Methods

6.2.2.1 HEK293T

Human embryonic kidney cells 293T (HEK293T cells) were grown in DMEM (high glucose + pyruvate) supplemented with 10 % of bovine serum albumin and 1x penicillin / streptomycin / fungizone (Anti-Anti). Cells were grown on uncoated cell culture plates and passaged by trypsination when cell density reached 70% confluence.

6.2.2.2 Mouse adult neural stem cells (neurospheres)

Neurosphere cultures were grown from neural stem cell isolated from adult mouse brain. For tissue preparation, mice were killed by cervical dislocation and brains immediately transferred to ice-cold DPBS. Hemispheres were separated sagitally and SVZs of lateral ventricles were taken out by cutting very thinly the wall of the SVZ. Tissue was transferred to 5 ml dissociation media and incubated for 15 min at 37°C. After gentle mechanical disruption by using glass pipettes, until medium became grey, incubation was continued for additional 15 min at 37°C. Subsequently enzymatic reaction was stopped by application of 5 ml ice-cold solution 3, cells were passed through a 70 µm strainer (Falcon Cat.: 352350) and then centrifuged at 300 rcf for 10 min. Supernatant was discarded, pellet resuspended in 10 ml ice cold solution 2 and spun down at 300 rcf for 10 min. Supernatant was then removed, cells were resuspended in 2 ml ice cold solution 3 and gently transferred to a new 15 ml tube on top of 12 ml of ice cold solution 3. After centrifugation at 400 rcf for 10 min the pellet was resuspended in neurosphere (NS) medium containing 10 ng/ml EGF (Peprotech) and FGF (Peprotech). Neurospheres were cultivated in NS media at 37°C and 5 % CO_2 and were passaged every 5-7th day when they reached a certain size (100 – 140 µm in diameter). For this, neurospheres were transferred to a 15 ml tube and centrifuged down at 100 rcf for 5 min. Supernatant was filtrated through a 0,40 µm strainer (Falcon Cat.: 352340) and stored. Pellet was washed once in 37°C warm 1 % DPBS, resuspended in 500 µl accutase (Millipore SCR005) and incubated at 37°C for 5 min. Neurospheres were dissociated by gentle trituration (20 times) through a 200 µl pipette tip on top of a 5 ml pipette and then incubate at 37°C for 3 min. Enzymatic reaction was stopped by applying 2 ml pre-warmed neurosphere NS medium. Cells were centrifuged at 400 rcf for 7 min, resuspended in neurosphere medium and counted in a haemocytometer. After first passage cells were taken up in 15 ml NS medium containing 20 % (v/v) of old medium (supernatant from first centrifugation). Cell density after following passages was 200.000 cells / 15 ml (medium flask).

Neurospheres were kept in culture for 8 passages before new stem cells were isolated.

6.2.2.3 Embryonic stem cells

Embryonic stem cells (ESC) were grown on gelatine-coated culture dishes in the presence of leukaemia inhibitory factor (LIF 1000 U per ml medium). One vial ($5x10^6$ ESC) was removed from liquid nitrogen, ESC were quickly thawed in 37°C incubator, resuspended in pre-warmed ESC medium containing LIF and then centrifuged at 120 rcf for 5 min. Cell pellet was resuspended in pre-warmed ESC medium and seeded on coated 6-well plates. Prior to passaging, new dishes were incubated for at least 30 min with 0,1 % gelatine. Culturing procedure was like following: Medium was renewed every day and ESCs were passaged every second day. After thawing ESC were seeded on 6-cm dishes and then on 10-cm dishes. ESCs were passaged as follows: Medium was aspirated and plate washed once with pre-warmed DPBS and once with 0,05 % Trypsin. Cells were then incubated in 0,05 % Trypsin (4 ml / 10-cm dish) for 5 min at 37°C. Detachment of cells was controlled by eye and ESC clumps were broken by gentle trituration with glass Pasteur pipettes to avoid differentiation of the ESCs. ESC suspension was transferred to 10 ml ESC media, mixed to stop trypsination and centrifuged at 120 rcf for 5 min. Supernatant was discarded and cells distributed on new gelatinised/coated 10-cm dishes. ESC WT cells were passaged 1:4 and RBPJκ KO ESCs 1:3 due to slightly reduced proliferation. WT D3 ESCs were obtained from PD. Dr. Ralf Kühn (Helmholtz Center Munich, Institute of Developmental Genetics) and RBPJκ KO D3 ESCs from PD. Dr. Timm Schröder, Helmholtz Center Munich, Institute for Stem cell Research).

6.2.2.4 Calcium chloride mediated transfection

HEK293T were passaged and seeded in appropriate density one day before transfection. DNA was mixed to a final volume of 547,5 µl with water, then 77,5 µl $CaCl_2$ was added. After drop-wise application of 625 µl 2x HBS (pH 7,0) mixture was incubated at RT for 30 min and then added to cells. 14 hours later medium was changed and cells were grown for further 24 h (luciferase assay / RNA isolation) or 72 h (protein isolation).

Application	Well plate	Growth area (cm^2)	Cells per well	Volume medium (ml)	µl/1250µl added to cells
Luciferase	24	2	50000	1	100
RNA isolation	12	3,8	100000	2	200
Protein isolation	6	9,6	250000	4	500

6.2.2.5 Luciferase reporter assay

To study the effect of specific proteins on the activity of gene promoters the luciferase reporter assay was used. The gene promoter was cloned into the pGL3-luciferase backbone, where the firefly luciferase is under the control of the gene promoter. The firefly catalyses the ATP-dependent oxidation of D-luciferin to oxyluciferin, which results in emission of light that can be measured by Centro LB 960 luminometer (Berthold Technologies GmbH & Co). Cells were transfected with 160 ng DNA of the promoter luciferase construct, 16 ng DNA of Renilla firefly (transfection normalization control) and different amounts of sample DNA (see results). Transient transfections were performed in HEK293T.

6.2.3 Molecular Biological Methods

6.2.3.1 Prediction of putative transcription factor binding sites

Prediction of putative transcription factor binding sites on the promoters of *Hes1, Hes5, Sox2* and the synthetic TCF/LEF promoter TOPFlash was performed by sequence analyses with Genomatix El Dorado suite and UCSD genome browser.

6.2.3.2 Statistical analysis

Unpaired Student's t-test was used for analysis of most experiments. Before the t-test, an f-test was performed. In those cases in which the f-test resulted in a difference in the variances, a Mann-Whitney-Wilcoxon rank sum test was applied. Differences were considered statistically significant at $p < 0.05$. If not stated otherwise, all data are presented as mean ± s.e.m.

6.2.3.3 Transformation

For transformation DH5a or TOP10 heat shock competent cells were used. Cells were thawed on ice for 10 min. Then 90 µl cell suspension were transferred to 14 ml round-bottom tubes (Falcon) mixed with DNA and incubated on ice for 30 min. For heat shock, tubes were put into a 42°C warm water bath for 45 sec and then back on ice for 2 min. After addition of 1 ml LB medium cells were incubated for 60 min at 37°C under slight shaking and then plated on agar plates containing Ampicilin (100 µg/ml).

6.2.3.4 Isolation and purification of DNA

DNA was isolated with NucleoSpin Plasmid Kit (Macherey-Nagel) or with Pure Yield Plasmid Midiprep system (Promega). For PCR purification DNA was run on an agarose gel, the proper band cot out and extracted with the Nucleo Spin Extract II (Macherey-Nagel) kit. For DNA precipitation, DNA solution was mixed with 1/10 3 M NaAc (pH 4.6) (v/v) and 2,5x

100 % ethanol (v/v), incubated at -20°C for 1 h and then centrifuged at 13000 rcf at 4°C for 30 min. DNA was dried on air for 10 min and resuspended in 20 µl ddH$_2$O. Concentrations were measured with Nano Drop.

6.2.3.5 Isolation of RNA

Total RNA was isolated from micro-dissected dentate gyrus, from whole hippocampus or from cell culture by using the Trizol method (Invitrogen). 100 mg of tissue was taken up in 1 ml Trizol and homogenized. After incubation at RT for 5 min, 200 µl Chloroform / 1 ml Trizol was added and mixture was vigorously vortexed for 15 sec. Trizol/Chlorophorm mixture was incubated for further 3 min at RT and subsequently centrifuged (14000rcf/4°C/15min). Then the upper phase was transferred to a new tube, 500 µl ice cold isopropanol per 1 ml Trizol was applied and after 10 min incubation at RT solution was centrifuged (14000rcf/4°C/30min). The supernatant was discarded, the pellet washed once with 75 % EtOH and then dried on air for 5 min. RNA was dissolved in RNAse free water at 55°C for 10 min and stored at -80°C.

6.2.3.6 cDNA synthesis and DNA sequencing

For cDNA synthesis Superscript III Kit (Invitrogen) was used. Genomic DNA was digested before by DNAse (Promega) treatment according to manufacturer's protocol.
For sequencing 100 ng plasmid DNA and 2 pmol primer were sent to MWG Operon.

6.2.3.7 Mutagenesis of transcription factor binding sites on DNA

To study the direct or indirect effect of transcription factors (TF) on certain gene promoters, putative TF binding sites were predicted by literature search and mutated by using the QuikChange II site-directed mutagenesis Kit (Stratagene) according the manufacturers protocol. Primer were designed with 3 nucleotide exchanges in the TF binding site of the DNA sequence by using Quick change primer design program (www.genomics.agilent.com).

6.2.3.8 Cloning procedures

For cloning, the DNA of interest was either amplified with specific primers by PCR or subcloned from other constructs. PCR product or cDNA of interest were digested with the appropriate restriction endonucleases and further cloned into KSSP or KSPS (both pBluescript II) shuttle vector. Finally, cDNA was excised in the correct orientation and ligated in the retroviral vector of choice.
Buffers, enzymes and incubation times were as given in the protocol (NEB). To prevent re-ligation of opened vector, vector was dephosphorylated by incubation with 5 U phosphatase

(New England biolabs) at 37°C for 30 min. Afterwards fragments were purified by agarose gel electrophoresis and ligated 3:1 (c[DNA] insert : c[DNA] vector) with 400 U T4-DNA-ligase (NEB) in the appropriate buffer at 16°C for 14 h. As negative control 1 µl of digested vector without insert was used.

6.2.4 Protein Biochemical Methods

6.2.4.1 Protein isolation from free floating neurospheres

Neurospheres were harvested by centrifugation at 160 rcf. Pellet was washed once with DPBS and then resuspended in buffer A (4 times volume per pellet size) and left for 14 min on ice. 10 % NP40 was added to a final concentration of 0.1 % (v/v) to break the cell membrane and cell suspension was vortexed every minute for 10 sec. After 4 min cells were centrifuged (2000rcf/4°C/7min) and nuclei washed once with buffer A. The nuclei pellet was resuspended harshly in buffer C (2x vol of pellet) and then incubated for 30 minutes on a rotor shaker at 4°C.

After centrifugation (14000 rcf/10 min/4°C) nucleic protein extracts were transferred to a new tube. Protein concentrations were determined by using the BCA kit according to manufacturer's instructions (Thermo Scientific Pierce) and subsequent measurement with a Nano Drop (Thermo Scientific). Proteins were frozen in liquid nitrogen and stored at -80°C.

6.2.4.2 Protein isolation from monolayer cell cultures

Plates were washed once with pre-warmed 37°C DPBS, scrapped from the plates, centrifuged at 200 rcf/5 min/RT and cell pellet was resuspended in buffer A. Nuclear protein extraction was as described above.

6.2.4.3 Immunoprecipitation

Immunoprecipitations were used to detect interacting proteins of RBPJκ. All steps were carried out at 4°C. For IPs 1 mg of nuclear protein was used. 50 µg were used for input control and salt concentration was adjusted to 120 mm KCl with buffer D. Extracts were divided in two tubes and pre-cleared once with 30 µl slurry Protein G sepharose (PGS; Millipore) beads each for 1 h on a rotor shaker. Beads were collected at 500 rcf for 1 min and supernatants were transferred to a new reaction tube. For IP 1 µg of antibody or control IgG was added and samples were incubated on a rotating wheel for 2 hours. To avoid bridging effects by DNA or RNA, samples were digested with benzonase (200 U/mg protein; Novagen) during IP. For IPs performed with the 6E7 RBPJκ clone, 10 µl antibody supernatant was used since it was estimated by analyses of the heavy chains, that 10 µl have the same concentration of 1 µg non-immune rat IgGs. Meanwhile 30 µl PGS were

washed once in ice cold PBS and stored on ice. After 2 hours, IPs were shortly centrifuged (500rcf/1min), transferred to the pre-washed beads and incubated for one more hour.

Beads were collected at 500 rcf for 1 min and supernatants were further used for DNA isolation as control for the benzonase treatment. Beads were washed 3 times with 1 ml buffer E and incubated on ice for 10 min each time. For washing control 20 µl of the last washing step were collected, beads resuspeded in 20 µl of 2x Laemmli buffer and boiled at 95°C.

6.2.4.4 SDS-polyacrylamid gel electrophoresis (SDS PAGE)

SDS PAGE was used to separate proteins based on their molecular weight. Depending on the size of the protein the concentration of acrylamid varied from 7,5 -15 % in the separating gel. Gels were prepared in MINI protean system (Bio-Rad Laboratories) or in PerfectBlue Twin-gel wide-format-system (Peqlab Biotechnologie). After covering the separating gel with isopropanol and polymerization, isopropanol was soaked by a Whatman paper (GE Healthcare) and the stacking gel was added. Following volumes were doubled for Twin-gel wide-format-system gels:

Separating Gel	7,5 %	10 %	12 %	15 %
Lower Tris [ml]	1,25	1,25	1,25	1,25
ddH$_2$O [ml]	2,81	2,50	2,25	1,875
40 % Acrylamid [ml]	0,94	1,25	1,50	1,875
TEMED [µl]	5	5	5	5
10 % APS [µl]	20	20	20	20

Stacking gel	5 %
Upper Tris [ml]	0,625
ddH$_2$O [ml]	1,563
40 % Acrylamid [ml]	0,312
TEMED [µl]	3
10 % APS [µl]	15

Proteins samples were denaturized in Laemmli buffer at 95°C for 5 min. For size estimation of proteins Page Ruler Plus pre-stained Protein Ladder (Fermentas-Thermo Scientific) was loaded. Proteins were separated at 120 V in TRIS-running buffer.

For mass spectrometry analysis 4-12 % or 10 % Bis-TRIS pre-cast gels (Invitrogen) were used. Proteins were shortly separated at 80 V in Mops-SDS running buffer (Invitrogen NuPage) until the loading dye entered 1-1,5 cm of the gel.

6.2.4.5 Silver staining of protein gels

For better estimation of the efficiency of the immunoprecipitation of RBPJκ protein complexes, SDS PAGE gels were stained with silver. After separation of the proteins by SDS PAGE the gel was incubated 2x 30 min in Fixer solution. The gel was washed 2x 20 min in 50 % Ethanol and then transferred for 20 sec in STS solution. Subsequently the gel was rinsed two times for few seconds in ddH$_2$O and then stained for 20 min in silver solution. During incubation the gel becomes slightly brown. The gel was then washed twice in ddH$_2$O for few seconds and then transferred to the developer solution. Incubation time was estimated by eye since staining can vary from seconds to minutes due to protein concentrations. The reaction was stopped at the appropriate time by rinsing the gel in fixer for 10 min. For preservation, the gel was washed 2x 10 min in preserver solution and then stored in preserver solution at 4°C.

6.2.4.6 Coomassie staining of protein gels

For visualization of proteins, gels were rinsed once in water to remove excessive SDS from running buffer and then incubated in Coomassie-Blue stain solution (Sigma G1041) for 30-60 min. After detection of proteins, gels were washed in Coomassie-blue destain for 15 min and then processed to western blot analyses.

6.2.4.7 Western blot

To detect and visualize specific proteins the western blot method was used. After separation of proteins by their molecular weight in SDS PAGE, proteins were transferred to a matrix by electric current. Proteins can then be detected by specific primary antibodies. Secondary antibodies coupled to horse radish peroxidase are used to catalyze a chemiluminescent reaction which can be detected by light sensitive films or by a camera detection system (Peqlab Biotechnologie).

The protein gel was covered by a PVDF (Polyvinylidene fluoride, Roche) membrane which was activated by rinsing in methanol for one minute. Both were wrapped in three Whatman paper on each side moistend with transfer buffer. Membrane was placed into a semidry blotting chamber (Bio-Rad) facing the cathode and gel facing the anode, respectively. Transfer settings were dependent on the molecular weight of the protein to be analysed (10 – 40 kDa: 19 V for 30 min; 40-100 kDa: 11 V for 60 min and proteins >100 kDa at 11 V for 60-

90 min). Afterwards the membrane was blocked in 5 % milk in TBST for 1h at RT and then incubated over night with primary antibodies in 5 % BSA in TBST at 4°C. The membrane was washed 3 times for 10 min in TBST and then incubated for 60 min in secondary antibody solution (1:10000 in TBST for ECL/ 1:100000 in TBST for AB) at RT. After 6x5 min washing in TBST the membrane was incubated for 1 min with ECL (Enhanced Chemiluminescence, Amersham GE Healthcare). Signals were detected by ECL-hyperfilm (Amersham GE healthcare) or AB solution (Peqlab Biotechnologie) and subsequent development in a developer machine (Kodak) or by camera detection (Peqlab Biotechnologie).

6.2.4.8 Stripping of antibodies from PVDF membrane

PVDF membrane was covered with 200 mM glycine solution (pH 2,5) and incubated for 10 min under shaking at RT. Subsequently membrane was rinsed 3 times in TBST for 10 min each and then blocked and incubated with primary antibody like described above.

6.2.4.9 DMP Cross-linking of antibodies to Protein G Sepharose

To reduce background of the IgGs in the mass spectrometer, antibodies were cross-linked to Protein G Sepharose. 100 µl of Protein G Sepharose (slurry beads) were transferred to a microfuge tube and washed three times each with 1 ml HEPES lysis buffer by pipetting up and down. Centrifugation steps were always performed at 4°C for 1 min at 500 rcf. Then 50 µg of the antibody [6E7 RBPJκ (0,1 µg/µl) or rat IgGs (Jackson laboratories, Chrom Pure rat IgGs 11 µg/µl, Cat.012-000-003)] and 800 µl of HEPES lysis buffer were added and incubated at 4°C on a rotating wheel for 2 hours. As a control to test for the binding efficiency, 20 µl of the supernatant were used. Beads were washed three times with 1 ml HEPES lysis buffer and two times with 1 ml HEPES cross-linking buffer. Then, beads were incubated with 1 ml cross-linking buffer containing freshly added DMP (Pierce, Cat.21667) on a shaker at RT. After centrifugation 20 µl were used for cross-linking control. Samples were subsequently washed two times with 1 ml HEPES cross-linking wash buffer and quenched by adding 1 ml 100 mM TRIS/HCl on a shaker for 30 min at RT.

Beads were washed two times with 1 ml HEPES lysis buffer. To avoid the presence of non-cross-linked IgGs, beads were incubated twice with 1 ml of 100 mM glycine (pH 2,5) for 2 minutes each. From each glycine step 20 µl were used for control. Then beads were washed twice with DPBS and then resuspended in 200 µl of DPBS-glycerol (v/v) solution and stored at -20°C until usage. To test for cross-linking efficiency controls were proceeded to SDS PAGE. Protocol was adjusted according to Kriegsheim et al., (2008).

6.2.4.10   Tandem Mass spectrometry

To analyse the interactome of RBPJκ and to discover new proteins expressed in adult neural stem cells the tandem mass spectrometry (MS/MS) method was used. By using MS/MS, proteins can be detected by their specific m/c (mass/charge) value and specific peptide sequence. For data analyses the Proteome Discoverer program was used. Neurospheres were harvested or used from frozen stocks stored at -80°C. Nuclear proteins were isolated following the protocol described before in this work. For protein concentration measurements a BCA standard curve was prepared every time a protein measurement was needed to ensure precise concentration values. Nuclear protein samples were mixed together to ensure equal protein distribution for the IP and measured at the Nano Drop. Buffer A was added to a final concentration of 140 mM KCl. All steps were carried out at 4°C. The sample was pre-cleared with Protein G Sepharose beads. For 1 mg protein extracts 20 µl of slurry beads pre-washed in buffer A were added and incubated slightly shaking for 1 hour. Beads were centrifuged at 200 rcf, supernatant was removed and 30 µl of cross-linked antibodies were added to 1 mg of protein. For the interactome screens of RBPJκ 12,5 mg nuclear protein and 100 µl of cross-linked antibodies for IP were used. Samples were incubated on a rolling platform for 3 hours at 4ºC and then recovered by centrifugation at 2000 rcf for 1 min. Supernatant was removed and beads were washed three times for 10 min each in buffer E on ice.

6.2.4.11   In-liquid digestion

After IP, 200 µl glycine (200 mM pH 2,5) were added to the antibody cross-linked beads, transferred to Illustra micro spin columns (GE Healthcare) and incubated on ice for 2 min. The tap of the column was removed and columns were centrifuged at lowest speed for 20 sec in bench centrifuge. Flow through was collected and glycine extraction repeated once more. The two glycine fractions (in total 400 µl) were combined, devided into two 200 µl samples, transferred to 2 ml sample tubes and pH adjusted to 8-9 with 2 M NaOH. 800 µl of methanol were added, mixed and samples centrifuged (7500rcf/20sec/RT). Then, 200 µl of chloroform were added, samples vortexed and centrifugation step repeated. After addition of 600 µl HPLC water, samples were vortexed for 5 sec and centrifuged (9000rcf/1min/RT) and the upper phase was carefully removed and discarded.

The protein solution was gently mixed with 600 µl methanol and centrifuged (7500rcf/2min/RT). Supernatant was carefully removed and pellet left to dry on air for 10 min. After resuspension of one of the two pellets (in 30 µl ammonium bicarbonate, 4 µl RapiGest (Waters) was applied, strongly vortexed and centrifuged (200rcf/30sec/RT). The whole solution was transferred to the residing pellet and incubated at 60°C, 1000 rpm for 5 min on a Thermoblock. After a short centrifugation (200rcf/30sec/RT) and application of 1 µl 100 mM

DTT (prepared freshly) the sample was further incubated at 60°C, 250 rpm for 10 min. The mixture was again centrifuged, 1 µl iodoacetamide (300 mM) was added and then incubated for 30 min at RT in darkness.

After incubation of the mixture with 2U Trypsin (sequencing grade Promega) over night at 37°C, samples recovered by centrifugation (9000rcf/1min/RT) and the enzymatic reaction was stopped by addition of 2 µl conc. HCl (37%). Solution was transferred to a polypropylene insert with bottom spring (200 µl PP insert, SUPELCO 24722) which was placed into a 1,5 ml tube, incubated for 10 min at RT and then centrifuged in a speed vacuum centrifuge at 30°C till the volume was reduced from 40 µl to 10 µl.

Half of the sample was then analysed by LTQ Orbitrap and values were processed in UniRef100 database. For further analyses Proteome Discoverer or Scaffold 3 software was used.

6.2.4.12   In-gel digestion and ICPL labelling

For elution of immunoprecipitated proteins, cross-linked beads were resuspended in 200 µl 200 mM glycine (pH 2,5; 500 mM NaCl), incubated for 15 min on ice and carefully vortexed every 5 minutes. Beads were centrifuged (20s/100rcf/RT), supernatant transferred to microspin columns (GE Healthcare) and centrifuged again (5s/16000rcf/RT). Subsequently, supernatant was transferred to new tube and stored on ice. Beads were resuspeded in further 200 µl of glycine buffer and treated like described before. Solutions were transferred to the corresponding Microspin columns prepared before, centrifuged and then combined with the other SN. For neutralization 30 µl 2 M TRIS pH 9 was added, samples were transferred to a 10 kDa cut-off column and centrifuged (14000 rcf, ~20 min) until ~30 µl were left. Supernatant, which consists of proteins bigger than 10 kDa, was transferred to a new tube, 0,5 µl of reduction buffer (provided by manufacturer of ICPL KIT) was added and solution was incubated for 30 min at 60°C on a shaker (600 rpm). Then samples were cooled down to RT on bench for 5 min and then alkylated with 0,5 µl of iodacedamide buffer for 30 min on RT in the dark. For ICPL, 3 µl of C12 or C13 ICPL was added to RBPJκ IP or control IgG IP, respectively, samples covered with argon gas to stop oxidation process, shortly vortexed and sonicated for 1 min. Samples were quickly centrifuged, incubated for 120 min at RT and afterwards reaction was stopped with 2 µl stop solution (Provided by the manufacturer of ICPL KIT) for 20 min at RT. After this step samples (RBPJκ and non-immun IgG IPs) were combined and processed together. Next, the pH of the combined sample was neutralized with 1 M NaOH and proteins were precipitated by the methanol/chloroform method. Protein solutions were mixed with 400 µl methanol and recovered at 16000 rcf for 20 sec at RT. Then, 100 µl of chloroform were added, mixed samples and spun down again.

Afterwards samples were mixed with 300 µl HPLC water, vortexed for 5 sec and centrifuged with 16000 rcf for 1 min at RT. The upper phase (aqueous phase contains salts), was carefully removed and discarded. The lower organic phase which contains the proteins was gently mixed with 300 µl methanol and centrifuged (16000rcf/2min/RT). The methanol was carefully aspirated and pellet dried on air for 5 min. Afterwards pellet was resuspended in 20 µl 2x Laemmli, harshly vortexed and loaded on a 10 % Bis-TRIS pre-cast SDS PAGE gel (Invitrogen). Electrophoresis was performed at 80 V until samples run about 1-1.5 cm. Gel was fixed on a shaker for 15 min in "Fixation Solution" (40 % MeOH, 10 % acetic acid) and then stained with "Coomassie-Staining solution" (Fixation solution + 0.1 % (w/v) Coomassie brilliant blue R-250) until protein bands were visible. Subsequently the gel was de-stained in fixation solution for 15-30 min, washed with water for 10 min and then cut into 5 stripes with the most prominent Coomassie stained protein bands. Each gel stripe was cut into small pieces (1mm³) and transferred to a well of a 96-well plate. Samples were washed once with 100 µl HPLC water for 5 min and then de-stained three times in 100 µl 40 % (v/v) acetonitrile for 15 min each on shaker. After incubation in 100 µl 100 % (v/v) acetonitrile till the gel pieces became white, 100 µl DTT (5 mM) was added and the pieces incubated at 60°C for 15 min. Samples were cooled down to RT and SN was removed. 100 µl 25 mM iodacetamide was applied and gel pieces were incubated for 45 min in darkness at RT. After 2 times washing for 15 min with 100 µl 40 % (v/v) acetonitrile, once with 100 % (v/v) acetonitrile for 5 min solution was discarded and gel pieces were dried on air for 5 min. For enzymatic protein digestion 30 µl of 50 mM ammonium bicarbonate with trypsin (1:50 dilution from stock solution [0.5 µg/µl] sequencing grade Promega) was added, 96-well plate was sealed with Parafilm and incubated at 37°C over night.

Next day 6 µl 0,5 % (v/v) trifluoroacetic acid (TFA) was applied and samples were strongly shaken for 15 min at RT. SN was transferred to another tube and samples were taken up in 100 µl 40 % (v/v) acetonitril + 0,5 % (v/v) TFA and was agitated for 15 min on a shaker. Supernatants were combined, 100 µl 99 % (v/v) acetonitrile 0,5 % (v/v) TFA was mixed with gel pieces and incubated for 5 min till they became white. The last SN was combined with the ones before, samples were vacuum dried to almost complete dryness (5 µl were left) and 15 µl 0.5 % (v/v) TFA was added. Samples were then subjected to analysis with the LTQ OrbiTrap mass spectrometer.

7 Abbreviations

aa	Amino acid
Akt	Protein kinase B
ALS	Amyotrophic lateral sclerosis
Amp	Ampicillin
APS	Ammonium persulfate
bHLH	Basic helix-loop-helix
bp	Base pair
BrdU	Bromodesoxy uridin
BSA	Bovine serum albumin
°C	Degrees Celsius
$CaCl_2$	Calcium Chloride
cDNA	copy DNA
ChIP	Chromatin immuno precipitation
Cir	Corepressor interacting with RBPJ
cKO	conditional knockout
CNS	Central nervous system
CO_2	Carbon dioxide
CTBP	C-terminal binding protein
CtIP	C-terminal interacting protein
Dab1	Disabled 1
DAPI	4′,6-Diamidino-2-phenylindol
DG	Dentate Gyrus
Dll	Delta-like
DMP	Dimethyl pimelimidate
DNA	Desoyxribonucleic acid
DCX	Doublecortin
Dsh	Disheveled
DTT	Dithiothreitol
E	Embryonic day
E.coli	*Escherichia coli*
EBSS	Earle´s balanced salt solution
EDTA	Ethylendiamintetraacetat
EGF	Epthelial growth factor
EGTA	Ethylene glycol tetraacetic acid
EMSA	Electrophoretic mobility shift assay
ESC	Embryonic stem cell
EtOH	Ethanol
et al.	et alteri
FCS	Fetal calf serum
FGF	Fibrillary growth factor
Fig.	Figure

FITC	Fluorescein
FOXO	Forkhead box O
FTLD-U	Frontotemporal lobar degeneration with Ubiquitin positive inclusions
g	Gram(s), gravitation
GABA	γ-Aminobutyric acid
GCL	Granular cell layer of DG
GFAP	Glial fibrillary acidic protein
(E)GFP	(enhanced) green fluorescent protein
Glast	Glutamate aspartate transporter
h	Hours
HAT	Histone acetyle transferase
HBSS	Hank´s balanced salt solution
HD	Heterodimerization domain
HDAC	Histone deacetylases
HEK	Human embryonic kidney cell
HEPES	4-(2-hydroxyethyl)-1-iperazineethanesulfonic acid
Hes	Hairy and enhancer of Split
HMG box	High monility group box
HPLC	High performance liquid chromatography
ICPL	Isotope-coded protein label
IHC	Immunohistochemistry
IRES	Internal ribosomal entry side
IP	Immunoprecipitation
Jag	Jagged
kDa	Kilo Dalton
l	Liter
LB	Lysogeni Broth
LEF	Lymphoid enhancer factor
Lif	Leukemia inhibitory factor
LV	Lateral ventricle
M	Molar, mol
m	Milli (10-3)
µ	Micro (10-6)
Mash1	Achaete-scute complex-like 1
MES	2-(N-morpholino)ethanesulfonic acid
min.	Minute(s)
mNSC	Neural stem cells from mouse
MS/MS	Tandem mass spectrometry
Mut	Mutant
NICD	Notch intracellular domain
NFI	Nuclear factor 1
NRR	Negative regulatory region

n	Sample size
nt	Nucleotides
N2A	Neuroblastoma cell line
NP40	Nonidet P-40
OB	Olfactory bulb
Oct 4	Octamer binding protein 4
OD	Optical density
P	Post natal day
p	p-value for statistical analysis
PAA	Polyacrylamide
PAGE	Polyacrylamide gel electrophoresis
PARP	Poly [ADP-ribose] polymerase
PBS	Phosphate buffered saline
Pcaf	P300/CBP-associated factor
PCR	Polymerase chain reaction
Pest domain	Proline (P), glutamic acid (E), serine (S) and threonine (T) rich domain
PFA	Paraformaldehyd
pH	Potentium hydrogenii
PMSF	polymethylsulfonylfluorid
PSM	Peptide spectrum match
Ram domain	RBPJκ-associated module
RBPJκ	Recombination signal binding protein
Rcf	Centrifugal force (g force)
RMS	Rostral migratory stream
RNA	Ribonucleic acid
RT	Room temperature
SDS	Sodium dodecyl sulfate
s.e.m.	Standard error of the mean
SGZ	Subgranular zone
SHARP	Smart/hdac1 associated repressor protein
Shh	Sonic hedgehog
SILAC	Stable isotope labeling by amino acid in cell culture
Sirt1	Sirtuin 1
SMAD	Mothers against decapentaplegic homolog 4
SMRT	Silencing Mediator for Retinoic acid and Thyroid hormone receptor
SN	supernatant
SOX	Sry-box containing gene 2
Stat3	Signal transducer and activator of transcription
SVZ	Subventricular zone
Tab	Table

TAD	Trans-activation domain
TAE	Tris acetate with EDTA
TBS	Tris buffered saline
TBST	Tris buffered saline with Tween
TCF	T-cell factor
TDP-43	TAR DNA binding protein 43 kDa
TE	Tris EDTA
TEMED	N,N,N´,N´-Tetramethylethylendiamin
TF	Transcription factors
TFA	Trifluoroacetic acid
TGF	Transforming growth factor
TLX	Tailless
Tris	Tris-(hydroxymethyl-) aminomethan
TBS	Tris buffered saline
TSS	Transcription start site
Tween-20	Polyoxyethlensorbitanmonolaurat
U	Units
V	Volt
(v/v)	Volume / volume
(w/v)	Weight / volume
Wnt	Wingless
WT	Wildtype
x	Symbol for crosses between mouse lines
YFP	Yellow fluorescent protein

8 References

Ables JL, Decarolis NA, Johnson MA, Rivera PD, Gao Z, Cooper DC, Radtke F, Hsieh J, Eisch AJ (2010) Notch1 is required for maintenance of the reservoir of adult hippocampal stem cells. J Neurosci 30:10484-10492.

Acharya KK, Govind CK, Shore AN, Stoler MH, Reddi PP (2006) cis-requirement for the maintenance of round spermatid-specific transcription. Dev Biol 295:781-790.

Ahn S, Joyner AL (2005) In vivo analysis of quiescent adult neural stem cells responding to Sonic hedgehog. Nature 437:894-897.

Aimone JB, Deng W, Gage FH (2011) Resolving new memories: a critical look at the dentate gyrus, adult neurogenesis, and pattern separation. Neuron 70:589-596.

Aizawa K, Ageyama N, Yokoyama C, Hisatsune T (2009) Age-dependent alteration in hippocampal neurogenesis correlates with learning performance of macaque monkeys. Exp Anim 58:403-407.

Almeida M, Han L, Martin-Millan M, O'Brien CA, Manolagas SC (2007) Oxidative stress antagonizes Wnt signaling in osteoblast precursors by diverting beta-catenin from T cell factor- to forkhead box O-mediated transcription. J Biol Chem 282:27298-27305.

Alvarez-Buylla A, Garcia-Verdugo JM (2002) Neurogenesis in adult subventricular zone. J Neurosci 22:629-634.

Amador-Ortiz C, Lin WL, Ahmed Z, Personett D, Davies P, Duara R, Graff-Radford NR, Hutton ML, Dickson DW (2007) TDP-43 immunoreactivity in hippocampal sclerosis and Alzheimer's disease. Ann Neurol 61:435-445.

Ambrosetti DC, Basilico C, Dailey L (1997) Synergistic activation of the fibroblast growth factor 4 enhancer by Sox2 and Oct-3 depends on protein-protein interactions facilitated by a specific spatial arrangement of factor binding sites. Mol Cell Biol 17:6321-6329.

Ambrosetti DC, Scholer HR, Dailey L, Basilico C (2000) Modulation of the activity of multiple transcriptional activation domains by the DNA binding domains mediates the synergistic action of Sox2 and Oct-3 on the fibroblast growth factor-4 enhancer. J Biol Chem 275:23387-23397.

Andersson ER, Sandberg R, Lendahl U (2011) Notch signaling: simplicity in design, versatility in function. Development 138:3593-3612.

Arden KC, Biggs WH, 3rd (2002) Regulation of the FoxO family of transcription factors by phosphatidylinositol-3 kinase-activated signaling. Arch Biochem Biophys 403:292-298.

Ayala YM, Zago P, D'Ambrogio A, Xu YF, Petrucelli L, Buratti E, Baralle FE (2008) Structural determinants of the cellular localization and shuttling of TDP-43. J Cell Sci 121:3778-3785.

Bakker WJ, Blazquez-Domingo M, Kolbus A, Besooyen J, Steinlein P, Beug H, Coffer PJ, Lowenberg B, von Lindern M, van Dijk TB (2004) FoxO3a regulates erythroid differentiation and induces BTG1, an activator of protein arginine methyl transferase 1. J Cell Biol 164:175-184.

Beatus P, Lundkvist J, Oberg C, Lendahl U (1999) The notch 3 intracellular domain represses notch 1-mediated activation through Hairy/Enhancer of split (HES) promoters. Development 126:3925-3935.

Beckervordersandforth R, Tripathi P, Ninkovic J, Bayam E, Lepier A, Stempfhuber B, Kirchhoff F, Hirrlinger J, Haslinger A, Lie DC, Beckers J, Yoder B, Irmler M, Gotz M (2010) In vivo fate mapping and expression analysis reveals molecular hallmarks of prospectively isolated adult neural stem cells. Cell Stem Cell 7:744-758.

Benayoun BA, Caburet S, Veitia RA (2011) Forkhead transcription factors: key players in health and disease. Trends Genet 27:224-232.

Berezovska O, Xia MQ, Hyman BT (1998) Notch is expressed in adult brain, is coexpressed with presenilin-1, and is altered in Alzheimer disease. J Neuropathol Exp Neurol 57:738-745.

Bergami M, Berninger B, Canossa M (2009) Conditional deletion of TrkB alters adult hippocampal neurogenesis and anxiety-related behavior. Commun Integr Biol 2:14-16.

Bergami M, Rimondini R, Santi S, Blum R, Gotz M, Canossa M (2008) Deletion of TrkB in adult progenitors alters newborn neuron integration into hippocampal circuits and increases anxiety-like behavior. Proc Natl Acad Sci U S A 105:15570-15575.

Bibel M, Richter J, Lacroix E, Barde YA (2007) Generation of a defined and uniform population of CNS progenitors and neurons from mouse embryonic stem cells. Nat Protoc 2:1034-1043.

Biggs WH, 3rd, Cavenee WK, Arden KC (2001) Identification and characterization of members of the FKHR (FOX O) subclass of winged-helix transcription factors in the mouse. Mamm Genome 12:416-425.

Bisgrove DA, Monckton EA, Packer M, Godbout R (2000) Regulation of brain fatty acid-binding protein expression by differential phosphorylation of nuclear factor I in malignant glioma cell lines. J Biol Chem 275:30668-30676.

Blokzijl A, Dahlqvist C, Reissmann E, Falk A, Moliner A, Lendahl U, Ibanez CF (2003) Cross-talk between the Notch and TGF-beta signaling pathways mediated by interaction of the Notch intracellular domain with Smad3. J Cell Biol 163:723-728.

Boiani M, Scholer HR (2005) Regulatory networks in embryo-derived pluripotent stem cells. Nat Rev Mol Cell Biol 6:872-884.

Bonaguidi MA, Wheeler MA, Shapiro JS, Stadel RP, Sun GJ, Ming GL, Song H (2011) In vivo clonal analysis reveals self-renewing and multipotent adult neural stem cell characteristics. Cell 145:1142-1155.

Bonini SA, Ferrari-Toninelli G, Uberti D, Montinaro M, Buizza L, Lanni C, Grilli M, Memo M (2011) Nuclear factor kappaB-dependent neurite remodeling is mediated by Notch pathway. J Neurosci 31:11697-11705.

Borggrefe T, Oswald F (2009) The Notch signaling pathway: transcriptional regulation at Notch target genes. Cell Mol Life Sci 66:1631-1646.

Bose JK, Wang IF, Hung L, Tarn WY, Shen CK (2008) TDP-43 overexpression enhances exon 7 inclusion during the survival of motor neuron pre-mRNA splicing. J Biol Chem 283:28852-28859.

Boyer LA, Lee TI, Cole MF, Johnstone SE, Levine SS, Zucker JP, Guenther MG, Kumar RM, Murray HL, Jenner RG, Gifford DK, Melton DA, Jaenisch R, Young RA (2005) Core transcriptional regulatory circuitry in human embryonic stem cells. Cell 122:947-956.

Breunig JJ, Silbereis J, Vaccarino FM, Sestan N, Rakic P (2007) Notch regulates cell fate and dendrite morphology of newborn neurons in the postnatal dentate gyrus. Proc Natl Acad Sci U S A 104:20558-20563.

Bruel-Jungerman E, Veyrac A, Dufour F, Horwood J, Laroche S, Davis S (2009) Inhibition of PI3K-Akt signaling blocks exercise-mediated enhancement of adult neurogenesis and synaptic plasticity in the dentate gyrus. PLoS One 4:e7901.

Brunet A, Bonni A, Zigmond MJ, Lin MZ, Juo P, Hu LS, Anderson MJ, Arden KC, Blenis J, Greenberg ME (1999) Akt promotes cell survival by phosphorylating and inhibiting a Forkhead transcription factor. Cell 96:857-868.

Brunet A, Sweeney LB, Sturgill JF, Chua KF, Greer PL, Lin Y, Tran H, Ross SE, Mostoslavsky R, Cohen HY, Hu LS, Cheng HL, Jedrychowski MP, Gygi SP, Sinclair DA, Alt FW, Greenberg ME (2004) Stress-dependent regulation of FOXO transcription factors by the SIRT1 deacetylase. Science 303:2011-2015.

Brunner A, Keidel EM, Dosch D, Kellermann J, Lottspeich F ICPLQuant (2010) - A software for non-isobaric isotopic labeling proteomics. Proteomics 10:315-326.

Buckwalter MS, Yamane M, Coleman BS, Ormerod BK, Chin JT, Palmer T, Wyss-Coray T (2006) Chronically increased transforming growth factor-beta1 strongly inhibits hippocampal neurogenesis in aged mice. Am J Pathol 169:154-164.

Buratti E, Baralle FE (2011) The multiple roles of TDP-43 in pre-mRNA processing and gene expression regulation. RNA Biol 7:420-429.

Buratti E, Baralle FE (2001) Characterization and functional implications of the RNA binding properties of nuclear factor TDP-43, a novel splicing regulator of CFTR exon 9. J Biol Chem 276:36337-36343.

Buratti E, Dork T, Zuccato E, Pagani F, Romano M, Baralle FE (2001) Nuclear factor TDP-43 and SR proteins promote in vitro and in vivo CFTR exon 9 skipping. EMBO J 20:1774-1784.

Buratti E, Brindisi A, Giombi M, Tisminetzky S, Ayala YM, Baralle FE (2005) TDP-43 binds heterogeneous nuclear ribonucleoprotein A/B through its C-terminal tail: an important region for the inhibition of cystic fibrosis transmembrane conductance regulator exon 9 splicing. J Biol Chem 280:37572-37584.

Campbell CE, Piper M, Plachez C, Yeh YT, Baizer JS, Osinski JM, Litwack ED, Richards LJ, Gronostajski RM (2008) The transcription factor Nfix is essential for normal brain development. BMC Dev Biol 8:52.

Casciati A, Ferri A, Cozzolino M, Celsi F, Nencini M, Rotilio G, Carri MT (2002) Oxidative modulation of nuclear factor-kappaB in human cells expressing mutant fALS-typical superoxide dismutases. J Neurochem 83:1019-1029.

Cebolla B, Vallejo M (2006) Nuclear factor-I regulates glial fibrillary acidic protein gene expression in astrocytes differentiated from cortical precursor cells. J Neurochem 97:1057-1070.

Chambers I, Silva J, Colby D, Nichols J, Nijmeijer B, Robertson M, Vrana J, Jones K, Grotewold L, Smith A (2007) Nanog safeguards pluripotency and mediates germline development. Nature 450:1230-1234.

Chaudhry AZ, Vitullo AD, Gronostajski RM (1999) Nuclear factor I-mediated repression of the mouse mammary tumor virus promoter is abrogated by the coactivators p300/CBP and SRC-1. J Biol Chem 274:7072-7081.

Chen H, Thiagalingam A, Chopra H, Borges MW, Feder JN, Nelkin BD, Baylin SB, Ball DW (1997) Conservation of the Drosophila lateral inhibition pathway in human lung cancer: a hairy-related protein (HES-1) directly represses achaete-scute homolog-1 expression. Proc Natl Acad Sci U S A 94:5355-5360.

Chen X, Xu H, Yuan P, Fang F, Huss M, Vega VB, Wong E, Orlov YL, Zhang W, Jiang J, Loh YH, Yeo HC, Yeo ZX, Narang V, Govindarajan KR, Leong B, Shahab A, Ruan Y, Bourque G, Sung WK, Clarke ND, Wei CL, Ng HH (2008) Integration of external signaling pathways with the core transcriptional network in embryonic stem cells. Cell 133:1106-1117.

Chew JL, Loh YH, Zhang W, Chen X, Tam WL, Yeap LS, Li P, Ang YS, Lim B, Robson P, Ng HH (2005) Reciprocal transcriptional regulation of Pou5f1 and Sox2 via the Oct4/Sox2 complex in embryonic stem cells. Mol Cell Biol 25:6031-6046.

Cirillo LA, Zaret KS (2007) Specific interactions of the wing domains of FOXA1 transcription factor with DNA. J Mol Biol 366:720-724.

Clelland CD, Choi M, Romberg C, Clemenson GD, Jr., Fragniere A, Tyers P, Jessberger S, Saksida LM, Barker RA, Gage FH, Bussey TJ (2009) A functional role for adult hippocampal neurogenesis in spatial pattern separation. Science 325:210-213.

Conlon RA, Reaume AG, Rossant J (1995) Notch1 is required for the coordinate segmentation of somites. Development 121:1533-1545.

Crosio C, Valle C, Casciati A, Iaccarino C, Carri MT (2011) Astroglial inhibition of NF-kappaB does not ameliorate disease onset and progression in a mouse model for amyotrophic lateral sclerosis (ALS). PLoS One 6:e17187.

das Neves L, Duchala CS, Tolentino-Silva F, Haxhiu MA, Colmenares C, Macklin WB, Campbell CE, Butz KG, Gronostajski RM (1999) Disruption of the murine nuclear factor I-A gene (Nfia) results in perinatal lethality, hydrocephalus, and agenesis of the corpus callosum. Proc Natl Acad Sci U S A 96:11946-11951.

Dawson SR, Turner DL, Weintraub H, Parkhurst SM (1995) Specificity for the hairy/enhancer of split basic helix-loop-helix (bHLH) proteins maps outside the bHLH domain and suggests two separable modes of transcriptional repression. Mol Cell Biol 15:6923-6931.

de Celis JF, Bray S (1997) Feed-back mechanisms affecting Notch activation at the dorsoventral boundary in the Drosophila wing. Development 124:3241-3251.

de la Pompa JL, Wakeham A, Correia KM, Samper E, Brown S, Aguilera RJ, Nakano T, Honjo T, Mak TW, Rossant J, Conlon RA (1997) Conservation of the Notch signalling pathway in mammalian neurogenesis. Development 124:1139-1148.

de la Torre-Ubieta L, Gaudilliere B, Yang Y, Ikeuchi Y, Yamada T, DiBacco S, Stegmuller J, Schuller U, Salih DA, Rowitch D, Brunet A, Bonni A (2010) A FOXO-Pak1 transcriptional pathway controls neuronal polarity. Genes Dev 24:799-813.

Deneen B, Ho R, Lukaszewicz A, Hochstim CJ, Gronostajski RM, Anderson DJ (2006) The transcription factor NFIA controls the onset of gliogenesis in the developing spinal cord. Neuron 52:953-968.

Deng W, Saxe MD, Gallina IS, Gage FH (2009) Adult-born hippocampal dentate granule cells undergoing maturation modulate learning and memory in the brain. J Neurosci 29:13532-13542.

Drapeau E, Mayo W, Aurousseau C, Le Moal M, Piazza PV, Abrous DN (2003) Spatial memory performances of aged rats in the water maze predict levels of hippocampal neurogenesis. Proc Natl Acad Sci U S A 100:14385-14390.

Dreumont N, Hardy S, Behm-Ansmant I, Kister L, Branlant C, Stevenin J, Bourgeois CF (2010) Antagonistic factors control the unproductive splicing of SC35 terminal intron. Nucleic Acids Res 38:1353-1366.

Driller K, Pagenstecher A, Uhl M, Omran H, Berlis A, Grunder A, Sippel AE (2007) Nuclear factor I X deficiency causes brain malformation and severe skeletal defects. Mol Cell Biol 27:3855-3867.

Duncan AW, Rattis FM, DiMascio LN, Congdon KL, Pazianos G, Zhao C, Yoon K, Cook JM, Willert K, Gaiano N, Reya T (2005) Integration of Notch and Wnt signaling in hematopoietic stem cell maintenance. Nat Immunol 6:314-322.

Dupret D, Revest JM, Koehl M, Ichas F, De Giorgi F, Costet P, Abrous DN, Piazza PV (2008) Spatial relational memory requires hippocampal adult neurogenesis. PLoS One 3:e1959.

Ehm O, Goritz C, Covic M, Schaffner I, Schwarz TJ, Karaca E, Kempkes B, Kremmer E, Pfrieger FW, Espinosa L, Bigas A, Giachino C, Taylor V, Frisen J, Lie DC (2010) RBPJkappa-dependent signaling is essential for long-term maintenance of neural stem cells in the adult hippocampus. J Neurosci 30:13794-13807.

Enard W, Przeworski M, Fisher SE, Lai CS, Wiebe V, Kitano T, Monaco AP, Paabo S (2002) Molecular evolution of FOXP2, a gene involved in speech and language. Nature 418:869-872.

Encinas JM, Vaahtokari A, Enikolopov G (2006) Fluoxetine targets early progenitor cells in the adult brain. Proc Natl Acad Sci U S A 103:8233-8238.

Espinosa L, Cathelin S, D'Altri T, Trimarchi T, Statnikov A, Guiu J, Rodilla V, Ingles-Esteve J, Nomdedeu J, Bellosillo B, Besses C, Abdel-Wahab O, Kucine N, Sun SC, Song G, Mullighan CC, Levine RL, Rajewsky K, Aifantis I, Bigas A (2010) The Notch/Hes1 pathway sustains NF-kappaB activation through CYLD repression in T cell leukemia. Cancer Cell 18:268-281.

Esposito MS, Piatti VC, Laplagne DA, Morgenstern NA, Ferrari CC, Pitossi FJ, Schinder AF (2005) Neuronal differentiation in the adult hippocampus recapitulates embryonic development. J Neurosci 25:10074-10086.

Essers MA, de Vries-Smits LM, Barker N, Polderman PE, Burgering BM, Korswagen HC (2005) Functional interaction between beta-catenin and FOXO in oxidative stress signaling. Science 308:1181-1184.

Ethell DW (2010) An amyloid-notch hypothesis for Alzheimer's disease. Neuroscientist 16:614-617.

Favaro R, Valotta M, Ferri AL, Latorre E, Mariani J, Giachino C, Lancini C, Tosetti V, Ottolenghi S, Taylor V, Nicolis SK (2009) Hippocampal development and

neural stem cell maintenance require Sox2-dependent regulation of Shh. Nat Neurosci 12:1248-1256.

Fehon RG, Kooh PJ, Rebay I, Regan CL, Xu T, Muskavitch MA, Artavanis-Tsakonas S (1990) Molecular interactions between the protein products of the neurogenic loci Notch and Delta, two EGF-homologous genes in Drosophila. Cell 61:523-534.

Fiesel FC, Kahle PJ (2011) TDP-43 and FUS/TLS: cellular functions and implications for neurodegeneration. FEBS J 278:3550-3568.

Filippov V, Kronenberg G, Pivneva T, Reuter K, Steiner B, Wang LP, Yamaguchi M, Kettenmann H, Kempermann G (2003) Subpopulation of nestin-expressing progenitor cells in the adult murine hippocampus shows electrophysiological and morphological characteristics of astrocytes. Molecular and cellular neurosciences 23:373-382.

Fisher SE, Scharff C (2009) FOXP2 as a molecular window into speech and language. Trends Genet 25:166-177.

Fletcher CF, Jenkins NA, Copeland NG, Chaudhry AZ, Gronostajski RM (1999) Exon structure of the nuclear factor I DNA-binding domain from C. elegans to mammals. Mamm Genome 10:390-396.

Fryer CJ, White JB, Jones KA (2004) Mastermind recruits CycC:CDK8 to phosphorylate the Notch ICD and coordinate activation with turnover. Mol Cell 16:509-520.

Fuchs E, Tumbar T, Guasch G (2004) Socializing with the neighbors: stem cells and their niche. Cell 116:769-778.

Fuentealba RA, Udan M, Bell S, Wegorzewska I, Shao J, Diamond MI, Weihl CC, Baloh RH (2010) Interaction with polyglutamine aggregates reveals a Q/N-rich domain in TDP-43. J Biol Chem 285:26304-26314.

Furuyama T, Nakazawa T, Nakano I, Mori N (2000) Identification of the differential distribution patterns of mRNAs and consensus binding sequences for mouse DAF-16 homologues. Biochem J 349:629-634.

Garthe A, Behr J, Kempermann G (2009) Adult-generated hippocampal neurons allow the flexible use of spatially precise learning strategies. PLoS One 4:e5464.

Ge S, Goh EL, Sailor KA, Kitabatake Y, Ming GL, Song H (2006) GABA regulates synaptic integration of newly generated neurons in the adult brain. Nature 439:589-593.

Gloeckner CJ, Boldt K, Schumacher A, Ueffing M (2009) Tandem affinity purification of protein complexes from mammalian cells by the Strep/FLAG (SF)-TAP tag. Methods Mol Biol 564:359-372.

Godena VK, Romano G, Romano M, Appocher C, Klima R, Buratti E, Baralle FE, Feiguin F (2011) TDP-43 regulates Drosophila neuromuscular junctions growth by modulating Futsch/MAP1B levels and synaptic microtubules organization. PLoS One 6:e17808.

Goertz MJ, Wu Z, Gallardo TD, Hamra FK, Castrillon DH (2011) Foxo1 is required in mouse spermatogonial stem cells for their maintenance and the initiation of spermatogenesis. J Clin Invest 121:3456-3466.

Gonzales KA, Ng HH (2011) FoxO: a new addition to the ESC cartel. Cell Stem Cell 9:181-183.

Gould E, Reeves AJ, Fallah M, Tanapat P, Gross CG, Fuchs E (1999) Hippocampal neurogenesis in adult Old World primates. Proc Natl Acad Sci U S A 96:5263-5267.

Grbavec D, Stifani S (1996) Molecular interaction between TLE1 and the carboxyl-terminal domain of HES-1 containing the WRPW motif. Biochem Biophys Res Commun 223:701-705.

Gronostajski RM (2000) Roles of the NFI/CTF gene family in transcription and development. Gene 249:31-45.

Hannenhalli S, Kaestner KH (2009) The evolution of Fox genes and their role in development and disease. Nat Rev Genet 10:233-240.

Hatakeyama J, Bessho Y, Katoh K, Ookawara S, Fujioka M, Guillemot F, Kageyama R (2004) Hes genes regulate size, shape and histogenesis of the nervous system by control of the timing of neural stem cell differentiation. Development 131:5539-5550.

Hoekman MF, Jacobs FM, Smidt MP, Burbach JP (2006) Spatial and temporal expression of FoxO transcription factors in the developing and adult murine brain. Gene Expr Patterns 6:134-140.

Hsieh JJ, Hayward SD (1995) Masking of the CBF1/RBPJ kappa transcriptional repression domain by Epstein-Barr virus EBNA2. Science 268:560-563.

Hsieh JJ, Zhou S, Chen L, Young DB, Hayward SD (1999) CIR, a corepressor linking the DNA binding factor CBF1 to the histone deacetylase complex. Proc Natl Acad Sci U S A 96:23-28.

Imayoshi I, Shimogori T, Ohtsuka T, Kageyama R (2008a) Hes genes and neurogenin regulate non-neural versus neural fate specification in the dorsal telencephalic midline. Development 135:2531-2541.

Imayoshi I, Sakamoto M, Yamaguchi M, Mori K, Kageyama R (2010) Essential roles of Notch signaling in maintenance of neural stem cells in developing and adult brains. J Neurosci 30:3489-3498.

Imayoshi I, Sakamoto M, Ohtsuka T, Takao K, Miyakawa T, Yamaguchi M, Mori K, Ikeda T, Itohara S, Kageyama R (2008b) Roles of continuous neurogenesis in the structural and functional integrity of the adult forebrain. Nat Neurosci 11:1153-1161.

Ishibashi M, Ang SL, Shiota K, Nakanishi S, Kageyama R, Guillemot F (1995) Targeted disruption of mammalian hairy and Enhancer of split homolog-1 (HES-1) leads to up-regulation of neural helix-loop-helix factors, premature neurogenesis, and severe neural tube defects. Genes Dev 9:3136-3148.

Ishikura N, Clever JL, Bouzamondo-Bernstein E, Samayoa E, Prusiner SB, Huang EJ, DeArmond SJ (2005) Notch-1 activation and dendritic atrophy in prion disease. Proc Natl Acad Sci U S A 102:886-891.

Iso T, Chung G, Hamamori Y, Kedes L (2002) HERP1 is a cell type-specific primary target of Notch. J Biol Chem 277:6598-6607.

Iso T, Sartorelli V, Poizat C, Iezzi S, Wu HY, Chung G, Kedes L, Hamamori Y (2001) HERP, a novel heterodimer partner of HES/E(spl) in Notch signaling. Mol Cell Biol 21:6080-6089.

Ivanova N, Dobrin R, Lu R, Kotenko I, Levorse J, DeCoste C, Schafer X, Lun Y, Lemischka IR (2006) Dissecting self-renewal in stem cells with RNA interference. Nature 442:533-538.

Jacobs FM, van der Heide LP, Wijchers PJ, Burbach JP, Hoekman MF, Smidt MP (2003) FoxO6, a novel member of the FoxO class of transcription factors with distinct shuttling dynamics. J Biol Chem 278:35959-35967.

Johnson JE, Birren SJ, Saito T, Anderson DJ (1992) DNA binding and transcriptional regulatory activity of mammalian achaete-scute homologous (MASH) proteins

revealed by interaction with a muscle-specific enhancer. Proc Natl Acad Sci U S A 89:3596-3600.

Kageyama R, Ohtsuka T, Kobayashi T (2007) The Hes gene family: repressors and oscillators that orchestrate embryogenesis. Development 134:1243-1251.

Kandasamy M, Couillard-Despres S, Raber KA, Stephan M, Lehner B, Winner B, Kohl Z, Rivera FJ, Nguyen HP, Riess O, Bogdahn U, Winkler J, von Horsten S, Aigner L (2010) Stem cell quiescence in the hippocampal neurogenic niche is associated with elevated transforming growth factor-beta signaling in an animal model of Huntington disease. J Neuropathol Exp Neurol 69:717-728.

Kao HY, Ordentlich P, Koyano-Nakagawa N, Tang Z, Downes M, Kintner CR, Evans RM, Kadesch T (1998) A histone deacetylase corepressor complex regulates the Notch signal transduction pathway. Genes Dev 12:2269-2277.

Katsube K, Sakamoto K (2005) Notch in vertebrates--molecular aspects of the signal. Int J Dev Biol 49:369-374.

Kempermann G, Kuhn HG, Gage FH (1997) More hippocampal neurons in adult mice living in an enriched environment. Nature 386:493-495.

Kempermann G, Kuhn HG, Gage FH (1998) Experience-induced neurogenesis in the senescent dentate gyrus. J Neurosci 18:3206-3212.

Kitagawa M, Oyama T, Kawashima T, Yedvobnick B, Kumar A, Matsuno K, Harigaya K (2001) A human protein with sequence similarity to Drosophila mastermind coordinates the nuclear form of notch and a CSL protein to build a transcriptional activator complex on target promoters. Mol Cell Biol 21:4337-4346.

Kitamura T, Ido Kitamura Y (2007) Role of FoxO Proteins in Pancreatic beta Cells. Endocr J 54:507-515.

Kitamura T, Kitamura YI, Funahashi Y, Shawber CJ, Castrillon DH, Kollipara R, DePinho RA, Kitajewski J, Accili D (2007) A Foxo/Notch pathway controls myogenic differentiation and fiber type specification. J Clin Invest 117:2477-2485.

Kitamura T, Saitoh Y, Takashima N, Murayama A, Niibori Y, Ageta H, Sekiguchi M, Sugiyama H, Inokuchi K (2009) Adult neurogenesis modulates the hippocampus-dependent period of associative fear memory. Cell 139:814-827.

Klein T, Brennan K, Arias AM (1997) An intrinsic dominant negative activity of serrate that is modulated during wing development in Drosophila. Dev Biol 189:123-134.

Koch U, Radtke F (2011) Notch in T-ALL: new players in a complex disease. Trends Immunol 32:434-442.

Komine O, Nagaoka M, Watase K, Gutmann DH, Tanigaki K, Honjo T, Radtke F, Saito T, Chiba S, Tanaka K (2007) The monolayer formation of Bergmann glial cells is regulated by Notch/RBP-J signaling. Dev Biol 311:238-250.

Korinek V, Barker N, Morin PJ, van Wichen D, de Weger R, Kinzler KW, Vogelstein B, Clevers H (1997) Constitutive transcriptional activation by a beta-catenin-Tcf complex in APC-/- colon carcinoma. Science 275:1784-1787.

Kopp JL, Ormsbee BD, Desler M, Rizzino A (2008) Small increases in the level of Sox2 trigger the differentiation of mouse embryonic stem cells. Stem Cells 26:903-911.

Kovall RA (2008) More complicated than it looks: assembly of Notch pathway transcription complexes. Oncogene 27:5099-5109.

Kovall RA, Blacklow SC (2010) Mechanistic insights into Notch receptor signaling from structural and biochemical studies. Curr Top Dev Biol 92:31-71.

Kovall RA, Hendrickson WA (2004) Crystal structure of the nuclear effector of Notch signaling, CSL, bound to DNA. EMBO J 23:3441-3451.

Krejci A, Bray S (2007) Notch activation stimulates transient and selective binding of Su(H)/CSL to target enhancers. Genes Dev 21:1322-1327.

Kriegstein A, Alvarez-Buylla A (2009) The glial nature of embryonic and adult neural stem cells. Annu Rev Neurosci 32:149-184.

Kronenberg G, Bick-Sander A, Bunk E, Wolf C, Ehninger D, Kempermann G (2006) Physical exercise prevents age-related decline in precursor cell activity in the mouse dentate gyrus. Neurobiol Aging 27:1505-1513.

Kronenberg G, Reuter K, Steiner B, Brandt MD, Jessberger S, Yamaguchi M, Kempermann G (2003) Subpopulations of proliferating cells of the adult hippocampus respond differently to physiologic neurogenic stimuli. The Journal of comparative neurology 467:455-463.

Kuhn HG, Dickinson-Anson H, Gage FH (1996) Neurogenesis in the dentate gyrus of the adult rat: age-related decrease of neuronal progenitor proliferation. J Neurosci 16:2027-2033.

Kurooka H, Honjo T (2000) Functional interaction between the mouse notch1 intracellular region and histone acetyltransferases PCAF and GCN5. J Biol Chem 275:17211-17220.

Kuwabara T, Hsieh J, Muotri A, Yeo G, Warashina M, Lie DC, Moore L, Nakashima K, Asashima M, Gage FH (2009) Wnt-mediated activation of NeuroD1 and retro-elements during adult neurogenesis. Nat Neurosci 12:1097-1105.

Lagier-Tourenne C, Cleveland DW (2009) Rethinking ALS: the FUS about TDP-43. Cell 136:1001-1004.

Lai K, Kaspar BK, Gage FH, Schaffer DV (2003) Sonic hedgehog regulates adult neural progenitor proliferation in vitro and in vivo. Nat Neurosci 6:21-27.

Lalmansingh AS, Urekar CJ, Reddi PP (2011) TDP-43 is a transcriptional repressor: the testis-specific mouse acrv1 gene is a TDP-43 target in vivo. J Biol Chem 286:10970-10982.

Liang J, Wan M, Zhang Y, Gu P, Xin H, Jung SY, Qin J, Wong J, Cooney AJ, Liu D, Songyang Z (2008) Nanog and Oct4 associate with unique transcriptional repression complexes in embryonic stem cells. Nat Cell Biol 10:731-739.

Lie DC, Dziewczapolski G, Willhoite AR, Kaspar BK, Shults CW, Gage FH (2002) The adult substantia nigra contains progenitor cells with neurogenic potential. J Neurosci 22:6639-6649.

Lie DC, Colamarino SA, Song HJ, Desire L, Mira H, Consiglio A, Lein ES, Jessberger S, Lansford H, Dearie AR, Gage FH (2005) Wnt signalling regulates adult hippocampal neurogenesis. Nature 437:1370-1375.

Ling SC, Albuquerque CP, Han JS, Lagier-Tourenne C, Tokunaga S, Zhou H, Cleveland DW (2010) ALS-associated mutations in TDP-43 increase its stability and promote TDP-43 complexes with FUS/TLS. Proc Natl Acad Sci U S A 107:13318-13323.

Loh YH, Wu Q, Chew JL, Vega VB, Zhang W, Chen X, Bourque G, George J, Leong B, Liu J, Wong KY, Sung KW, Lee CW, Zhao XD, Chiu KP, Lipovich L, Kuznetsov VA, Robson P, Stanton LW, Wei CL, Ruan Y, Lim B, Ng HH. (2006) The Oct4 and Nanog transcription network regulates pluripotency in mouse embryonic stem cells. Nat Genet 38:431-440.

Lugert S, Basak O, Knuckles P, Haussler U, Fabel K, Gotz M, Haas CA, Kempermann G, Taylor V, Giachino C (2010) Quiescent and active

hippocampal neural stem cells with distinct morphologies respond selectively to physiological and pathological stimuli and aging. Cell Stem Cell 6:445-456.

Machold R, Hayashi S, Rutlin M, Muzumdar MD, Nery S, Corbin JG, Gritli-Linde A, Dellovade T, Porter JA, Rubin LL, Dudek H, McMahon AP, Fishell G (2003) Sonic hedgehog is required for progenitor cell maintenance in telencephalic stem cell niches. Neuron 39:937-950.

Manganas LN, Zhang X, Li Y, Hazel RD, Smith SD, Wagshul ME, Henn F, Benveniste H, Djuric PM, Enikolopov G, Maletic-Savatic M (2007) Magnetic resonance spectroscopy identifies neural progenitor cells in the live human brain. Science 318:980-985.

Margulies M et al. (2005) Genome sequencing in microfabricated high-density picolitre reactors. Nature 437:376-380.

Marin-Burgin A, Mongiat LA, Pardi MB, Schinder AF (2012) Unique Processing During a Period of High Excitation/Inhibition Balance in Adult-Born Neurons. Science in press.

Maris C, Dominguez C, Allain FH (2005) The RNA recognition motif, a plastic RNA-binding platform to regulate post-transcriptional gene expression. FEBS J 272:2118-2131.

Maruyama H, Morino H, Ito H, Izumi Y, Kato H, Watanabe Y, Kinoshita Y, Kamada M, Nodera H, Suzuki H, Komure O, Matsuura S, Kobatake K, Morimoto N, Abe K, Suzuki N, Aoki M, Kawata A, Hirai T, Kato T, Ogasawara K, Hirano A, Takumi T, Kusaka H, Hagiwara K, Kaji R, Kawakami H (2010) Mutations of optineurin in amyotrophic lateral sclerosis. Nature 465:223-226.

Mason S, Piper M, Gronostajski RM, Richards LJ (2009) Nuclear factor one transcription factors in CNS development. Mol Neurobiol 39:10-23.

Masui S, Shimosato D, Toyooka Y, Yagi R, Takahashi K, Niwa H (2005) An efficient system to establish multiple embryonic stem cell lines carrying an inducible expression unit. Nucleic Acids Res 33:e43.

Masui S, Nakatake Y, Toyooka Y, Shimosato D, Yagi R, Takahashi K, Okochi H, Okuda A, Matoba R, Sharov AA, Ko MS, Niwa H (2007) Pluripotency governed by Sox2 via regulation of Oct3/4 expression in mouse embryonic stem cells. Nat Cell Biol 9:625-635.

McGeer PL, Kawamata T, McGeer EG (1998) Localization and possible functions of presenilins in brain. Rev Neurosci 9:1-15.

Medina-Martinez O, Jamrich M (2007) Foxe view of lens development and disease. Development 134:1455-1463.

Meisterernst M, Gander I, Rogge L, Winnacker EL (1988) A quantitative analysis of nuclear factor I/DNA interactions. Nucleic Acids Res 16:4419-4435.

Mercado PA, Ayala YM, Romano M, Buratti E, Baralle FE (2005) Depletion of TDP 43 overrides the need for exonic and intronic splicing enhancers in the human apoA-II gene. Nucleic Acids Res 33:6000-6010.

Mermod N, O'Neill EA, Kelly TJ, Tjian R (1989) The proline-rich transcriptional activator of CTF/NF-I is distinct from the replication and DNA binding domain. Cell 58:741-753.

Merz K, Herold S, Lie DC (2011) CREB in adult neurogenesis--master and partner in the development of adult-born neurons? Eur J Neurosci 33:1078-1086.

Micchelli CA, Rulifson EJ, Blair SS (1997) The function and regulation of cut expression on the wing margin of Drosophila: Notch, Wingless and a dominant negative role for Delta and Serrate. Development 124:1485-1495.

Migheli A, Piva R, Atzori C, Troost D, Schiffer D (1997) c-Jun, JNK/SAPK kinases and transcription factor NF-kappa B are selectively activated in astrocytes, but not motor neurons, in amyotrophic lateral sclerosis. J Neuropathol Exp Neurol 56:1314-1322.

Ming GL, Song H (2011) Adult neurogenesis in the mammalian brain: significant answers and significant questions. Neuron 70:687-702.

Miyamoto K, Araki KY, Naka K, Arai F, Takubo K, Yamazaki S, Matsuoka S, Miyamoto T, Ito K, Ohmura M, Chen C, Hosokawa K, Nakauchi H, Nakayama K, Nakayama KI, Harada M, Motoyama N, Suda T, Hirao A (2007) Foxo3a is essential for maintenance of the hematopoietic stem cell pool. Cell Stem Cell 1:101-112.

Mizutani K, Yoon K, Dang L, Tokunaga A, Gaiano N (2007) Differential Notch signalling distinguishes neural stem cells from intermediate progenitors. Nature 449:351-355.

Motta MC, Divecha N, Lemieux M, Kamel C, Chen D, Gu W, Bultsma Y, McBurney M, Guarente L (2004) Mammalian SIRT1 represses forkhead transcription factors. Cell 116:551-563.

Nagata K, Guggenheimer RA, Hurwitz J (1983) Specific binding of a cellular DNA replication protein to the origin of replication of adenovirus DNA. Proc Natl Acad Sci U S A 80:6177-6181.

Nagata K, Guggenheimer RA, Enomoto T, Lichy JH, Hurwitz J (1982) Adenovirus DNA replication in vitro: identification of a host factor that stimulates synthesis of the preterminal protein-dCMP complex. Proc Natl Acad Sci U S A 79:6438-6442.

Nakae J, Park BC, Accili D (1999) Insulin stimulates phosphorylation of the forkhead transcription factor FKHR on serine 253 through a Wortmannin-sensitive pathway. J Biol Chem 274:15982-15985.

Nakae J, Kitamura T, Silver DL, Accili D (2001) The forkhead transcription factor Foxo1 (Fkhr) confers insulin sensitivity onto glucose-6-phosphatase expression. J Clin Invest 108:1359-1367.

Nakashima-Yasuda H et al. (2007) Co-morbidity of TDP-43 proteinopathy in Lewy body related diseases. Acta Neuropathol 114:221-229.

Namihira M, Kohyama J, Semi K, Sanosaka T, Deneen B, Taga T, Nakashima K (2009) Committed neuronal precursors confer astrocytic potential on residual neural precursor cells. Dev Cell 16:245-255.

Neumann M, Sampathu DM, Kwong LK, Truax AC, Micsenyi MC, Chou TT, Bruce J, Schuck T, Grossman M, Clark CM, McCluskey LF, Miller BL, Masliah E, Mackenzie IR, Feldman H, Feiden W, Kretzschmar HA, Trojanowski JQ, Lee VM (2006) Ubiquitinated TDP-43 in frontotemporal lobar degeneration and amyotrophic lateral sclerosis. Science 314:130-133.

Ng HH, Surani MA (2011) The transcriptional and signalling networks of pluripotency. Nat Cell Biol 13:490-496.

Nichols J, Zevnik B, Anastassiadis K, Niwa H, Klewe-Nebenius D, Chambers I, Scholer H, Smith A (1998) Formation of pluripotent stem cells in the mammalian embryo depends on the POU transcription factor Oct4. Cell 95:379-391.

Niu W, Zou Y, Shen C, Zhang CL (2011) Activation of postnatal neural stem cells requires nuclear receptor TLX. J Neurosci 31:13816-13828.

Niwa H, Miyazaki J, Smith AG (2000) Quantitative expression of Oct-3/4 defines differentiation, dedifferentiation or self-renewal of ES cells. Nat Genet 24:372-376.

Nyhan KC, Faherty N, Murray G, Cooey LB, Godson C, Crean JK, Brazil DP (2010) Jagged/Notch signalling is required for a subset of TGFbeta1 responses in human kidney epithelial cells. Biochim Biophys Acta 1803:1386-1395.

Obsil T, Obsilova V (2008) Structure/function relationships underlying regulation of FOXO transcription factors. Oncogene 27:2263-2275.

Ogg S, Paradis S, Gottlieb S, Patterson GI, Lee L, Tissenbaum HA, Ruvkun G (1997) The Fork head transcription factor DAF-16 transduces insulin-like metabolic and longevity signals in C. elegans. Nature 389:994-999.

Ohtsuka T, Sakamoto M, Guillemot F, Kageyama R (2001) Roles of the basic helix-loop-helix genes Hes1 and Hes5 in expansion of neural stem cells of the developing brain. J Biol Chem 276:30467-30474.

Ohtsuka T, Asahi M, Matsuura N, Kikuchi H, Hojo M, Kageyama R, Ohkubo H, Hoshimaru M (1998) Regulated expression of neurogenic basic helix-loop-helix transcription factors during differentiation of the immortalized neuronal progenitor cell line HC2S2 into neurons. Cell Tissue Res 293:23-29.

Oka C, Nakano T, Wakeham A, de la Pompa JL, Mori C, Sakai T, Okazaki S, Kawaichi M, Shiota K, Mak TW, Honjo T (1995) Disruption of the mouse RBP-J kappa gene results in early embryonic death. Development 121:3291-3301.

Ong SE, Foster LJ, Mann M (2003) Mass spectrometric-based approaches in quantitative proteomics. Methods 29:124-130.

Ong SE, Blagoev B, Kratchmarova I, Kristensen DB, Steen H, Pandey A, Mann M (2002) Stable isotope labeling by amino acids in cell culture, SILAC, as a simple and accurate approach to expression proteomics. Mol Cell Proteomics 1:376-386.

Oswald F, Winkler M, Cao Y, Astrahantseff K, Bourteele S, Knochel W, Borggrefe T (2005) RBP-Jkappa/SHARP recruits CtIP/CtBP corepressors to silence Notch target genes. Mol Cell Biol 25:10379-10390.

Ou SH, Wu F, Harrich D, Garcia-Martinez LF, Gaynor RB (1995) Cloning and characterization of a novel cellular protein, TDP-43, that binds to human immunodeficiency virus type 1 TAR DNA sequence motifs. J Virol 69:3584-3596.

Pahl HL (1999) Activators and target genes of Rel/NF-kappaB transcription factors. Oncogene 18:6853-6866.

Paik JH, Ding Z, Narurkar R, Ramkissoon S, Muller F, Kamoun WS, Chae SS, Zheng H, Ying H, Mahoney J, Hiller D, Jiang S, Protopopov A, Wong WH, Chin L, Ligon KL, DePinho RA (2009) FoxOs cooperatively regulate diverse pathways governing neural stem cell homeostasis. Cell Stem Cell 5:540-553.

Pan G, Li J, Zhou Y, Zheng H, Pei D (2006) A negative feedback loop of transcription factors that controls stem cell pluripotency and self-renewal. FASEB J 20:1730-1732.

Paradis S, Ruvkun G (1998) Caenorhabditis elegans Akt/PKB transduces insulin receptor-like signals from AGE-1 PI3 kinase to the DAF-16 transcription factor. Genes Dev 12:2488-2498.

Pardo M, Lang B, Yu L, Prosser H, Bradley A, Babu MM, Choudhary J (2010) An expanded Oct4 interaction network: implications for stem cell biology, development, and disease. Cell Stem Cell 6:382-395.

Parent JM, Yu TW, Leibowitz RT, Geschwind DH, Sloviter RS, Lowenstein DH (1997) Dentate granule cell neurogenesis is increased by seizures and contributes to aberrant network reorganization in the adult rat hippocampus. J Neurosci 17:3727-3738.

Paroush Z, Finley RL, Jr., Kidd T, Wainwright SM, Ingham PW, Brent R, Ish-Horowicz D (1994) Groucho is required for Drosophila neurogenesis, segmentation, and sex determination and interacts directly with hairy-related bHLH proteins. Cell 79:805-815.

Passoni M, De Conti L, Baralle M, Buratti E UG (2011) Repeats/TDP-43 Interactions near 5' Splice Sites Exert Unpredictable Effects on Splicing Modulation. J Mol Biol 415:46-60.

Pesiridis GS, Lee VM, Trojanowski JQ (2009) Mutations in TDP-43 link glycine-rich domain functions to amyotrophic lateral sclerosis. Hum Mol Genet 18:R156-162.

Petcherski AG, Kimble J (2000) Mastermind is a putative activator for Notch. Curr Biol 10:R471-473.

Pevny LH, Nicolis SK (2010) Sox2 roles in neural stem cells. Int J Biochem Cell Biol 42:421-424.

Piatti VC, Davies-Sala MG, Esposito MS, Mongiat LA, Trinchero MF, Schinder AF (2011) The timing for neuronal maturation in the adult hippocampus is modulated by local network activity. J Neurosci 31:7715-7728.

Piper M, Barry G, Hawkins J, Mason S, Lindwall C, Little E, Sarkar A, Smith AG, Moldrich RX, Boyle GM, Tole S, Gronostajski RM, Bailey TL, Richards LJ (2010) NFIA controls telencephalic progenitor cell differentiation through repression of the Notch effector Hes1. J Neurosci 30:9127-9139.

Plachez C, Lindwall C, Sunn N, Piper M, Moldrich RX, Campbell CE, Osinski JM, Gronostajski RM, Richards LJ (2008) Nuclear factor I gene expression in the developing forebrain. J Comp Neurol 508:385-401.

Poellinger L, Lendahl U (2008) Modulating Notch signaling by pathway-intrinsic and pathway-extrinsic mechanisms. Curr Opin Genet Dev 18:449-454.

Polymenidou M, Lagier-Tourenne C, Hutt KR, Huelga SC, Moran J, Liang TY, Ling SC, Sun E, Wancewicz E, Mazur C, Kordasiewicz H, Sedaghat Y, Donohue JP, Shiue L, Bennett CF, Yeo GW, Cleveland DW (2011) Long pre-mRNA depletion and RNA missplicing contribute to neuronal vulnerability from loss of TDP-43. Nat Neurosci 14:459-468.

Qin H, Du D, Zhu Y, Li J, Feng L, Liang Y, Han H (2005) The PcG protein HPC2 inhibits RBP-J-mediated transcription by interacting with LIM protein KyoT2. FEBS Lett 579:1220-1226.

Rao MS, Hattiangady B, Shetty AK (2006) The window and mechanisms of major age-related decline in the production of new neurons within the dentate gyrus of the hippocampus. Aging Cell 5:545-558.

Rebay I, Fleming RJ, Fehon RG, Cherbas L, Cherbas P, Artavanis-Tsakonas S (1991) Specific EGF repeats of Notch mediate interactions with Delta and Serrate: implications for Notch as a multifunctional receptor. Cell 67:687-699.

Redmond L, Oh SR, Hicks C, Weinmaster G, Ghosh A (2000) Nuclear Notch1 signaling and the regulation of dendritic development. Nat Neurosci 3:30-40.

Renault VM, Rafalski VA, Morgan AA, Salih DA, Brett JO, Webb AE, Villeda SA, Thekkat PU, Guillerey C, Denko NC, Palmer TD, Butte AJ, Brunet A (2009) FoxO3 regulates neural stem cell homeostasis. Cell Stem Cell 5:527-539.

Revest JM, Dupret D, Koehl M, Funk-Reiter C, Grosjean N, Piazza PV, Abrous DN (2009) Adult hippocampal neurogenesis is involved in anxiety-related behaviors. Mol Psychiatry 14:959-967.

Rodda DJ, Chew JL, Lim LH, Loh YH, Wang B, Ng HH, Robson P (2005) Transcriptional regulation of nanog by OCT4 and SOX2. J Biol Chem 280:24731-24737.

Sahay A, Wilson DA, Hen R (2011) Pattern separation: a common function for new neurons in hippocampus and olfactory bulb. Neuron 70:582-588.

Sahay A, Scobie KN, Hill AS, O'Carroll CM, Kheirbek MA, Burghardt NS, Fenton AA, Dranovsky A, Hen R (2011) Increasing adult hippocampal neurogenesis is sufficient to improve pattern separation. Nature 472:466-470.

Sanchez-Irizarry C, Carpenter AC, Weng AP, Pear WS, Aster JC, Blacklow SC (2004) Notch subunit heterodimerization and prevention of ligand-independent proteolytic activation depend, respectively, on a novel domain and the LNR repeats. Mol Cell Biol 24:9265-9273.

Sasai Y, Kageyama R, Tagawa Y, Shigemoto R, Nakanishi S (1992) Two mammalian helix-loop-helix factors structurally related to Drosophila hairy and Enhancer of split. Genes Dev 6:2620-2634.

Saxe MD, Battaglia F, Wang JW, Malleret G, David DJ, Monckton JE, Garcia AD, Sofroniew MV, Kandel ER, Santarelli L, Hen R, Drew MR (2006) Ablation of hippocampal neurogenesis impairs contextual fear conditioning and synaptic plasticity in the dentate gyrus. Proc Natl Acad Sci U S A 103:17501-17506.

Schmidt-Hieber C, Jonas P, Bischofberger J (2004) Enhanced synaptic plasticity in newly generated granule cells of the adult hippocampus. Nature 429:184-187.

Schmidt A, Kellermann J, Lottspeich F (2005) A novel strategy for quantitative proteomics using isotope-coded protein labels. Proteomics 5:4-15.

Screpanti I, Bellavia D, Campese AF, Frati L, Gulino A (2003) Notch, a unifying target in T-cell acute lymphoblastic leukemia? Trends Mol Med 9:30-35.

Seoane J, Le HV, Shen L, Anderson SA, Massague J (2004) Integration of Smad and forkhead pathways in the control of neuroepithelial and glioblastoma cell proliferation. Cell 117:211-223.

Sestan N, Artavanis-Tsakonas S, Rakic P (1999) Contact-dependent inhibition of cortical neurite growth mediated by notch signaling. Science 286:741-746.

Shendure J, Porreca GJ, Reppas NB, Lin X, McCutcheon JP, Rosenbaum AM, Wang MD, Zhang K, Mitra RD, Church GM (2005) Accurate multiplex polony sequencing of an evolved bacterial genome. Science 309:1728-1732.

Shi Y, Chichung Lie D, Taupin P, Nakashima K, Ray J, Yu RT, Gage FH, Evans RM (2004) Expression and function of orphan nuclear receptor TLX in adult neural stem cells. Nature 427:78-83.

Shihabuddin LS, Horner PJ, Ray J, Gage FH (2000) Adult spinal cord stem cells generate neurons after transplantation in the adult dentate gyrus. J Neurosci 20:8727-8735.

Shin HM, Minter LM, Cho OH, Gottipati S, Fauq AH, Golde TE, Sonenshein GE, Osborne BA (2006) Notch1 augments NF-kappaB activity by facilitating its nuclear retention. EMBO J 25:129-138.

Shors TJ, Miesegaes G, Beylin A, Zhao M, Rydel T, Gould E (2001) Neurogenesis in the adult is involved in the formation of trace memories. Nature 410:372-376.

Shu T, Butz KG, Plachez C, Gronostajski RM, Richards LJ (2003) Abnormal development of forebrain midline glia and commissural projections in Nfia knock-out mice. J Neurosci 23:203-212.

Simone NL, Bonner RF, Gillespie JW, Emmert-Buck MR, Liotta LA (1998) Laser-capture microdissection: opening the microscopic frontier to molecular analysis. Trends Genet 14:272-276.

Snyder JS, Soumier A, Brewer M, Pickel J, Cameron HA (2011) Adult hippocampal neurogenesis buffers stress responses and depressive behaviour. Nature 476:458-461.

Steele-Perkins G, Plachez C, Butz KG, Yang G, Bachurski CJ, Kinsman SL, Litwack ED, Richards LJ, Gronostajski RM (2005) The transcription factor gene Nfib is essential for both lung maturation and brain development. Mol Cell Biol 25:685-698.

Steiner B, Klempin F, Wang L, Kott M, Kettenmann H, Kempermann G (2006) Type-2 cells as link between glial and neuronal lineage in adult hippocampal neurogenesis. Glia 54:805-814.

Strong MJ, Volkening K, Hammond R, Yang W, Strong W, Leystra-Lantz C, Shoesmith C (2007) TDP43 is a human low molecular weight neurofilament (hNFL) mRNA-binding protein. Mol Cell Neurosci 35:320-327.

Suarez I, Bodega G, Fernandez B (2002) Glutamine synthetase in brain: effect of ammonia. Neurochem Int 41:123-142.

Subramanian L, Sarkar A, Shetty AS, Muralidharan B, Padmanabhan H, Piper M, Monuki ES, Bach I, Gronostajski RM, Richards LJ, Tole S (2011) Transcription factor Lhx2 is necessary and sufficient to suppress astrogliogenesis and promote neurogenesis in the developing hippocampus. Proc Natl Acad Sci U S A 108:E265-274.

Suh H, Consiglio A, Ray J, Sawai T, D'Amour KA, Gage FH (2007) In Vivo Fate Analysis Reveals the Multipotent and Self-Renewal Capacities of Sox2(+) Neural Stem Cells in the Adult Hippocampus. Cell Stem Cell 1:515-528.

Suhonen JO, Peterson DA, Ray J, Gage FH (1996) Differentiation of adult hippocampus-derived progenitors into olfactory neurons in vivo. Nature 383:624-627.

Swarup V, Phaneuf D, Bareil C, Robertson J, Rouleau GA, Kriz J, Julien JP (2011) Pathological hallmarks of amyotrophic lateral sclerosis/frontotemporal lobar degeneration in transgenic mice produced with TDP-43 genomic fragments. Brain 134:2610-2626.

Swarup V, Phaneuf D, Dupre N, Petri S, Strong M, Kriz J, Julien JP (2011) Deregulation of TDP-43 in amyotrophic lateral sclerosis triggers nuclear factor kappaB-mediated pathogenic pathways. J Exp Med 208:2429-2447.

Swiatek PJ, Lindsell CE, del Amo FF, Weinmaster G, Gridley T (1994) Notch1 is essential for postimplantation development in mice. Genes Dev 8:707-719.

Tamura K, Taniguchi Y, Minoguchi S, Sakai T, Tun T, Furukawa T, Honjo T (1995) Physical interaction between a novel domain of the receptor Notch and the transcription factor RBP-J kappa/Su(H). Curr Biol 5:1416-1423.

Tanigaki K, Honjo T (2010) Two opposing roles of RBP-J in Notch signaling. Curr Top Dev Biol 92:231-252.

Taniguchi Y, Furukawa T, Tun T, Han H, Honjo T (1998) LIM protein KyoT2 negatively regulates transcription by association with the RBP-J DNA-binding protein. Mol Cell Biol 18:644-654.

Tissenbaum HA, Ruvkun G (1998) An insulin-like signaling pathway affects both longevity and reproduction in Caenorhabditis elegans. Genetics 148:703-717.

Tollervey JR, Curk T, Rogelj B, Briese M, Cereda M, Kayikci M, Konig J, Hortobagyi T, Nishimura AL, Zupunski V, Patani R, Chandran S, Rot G, Zupan B, Shaw CE, Ule J (2011) Characterizing the RNA targets and position-dependent splicing regulation by TDP-43. Nat Neurosci 14:452-458.

Tolosa L, Caraballo-Miralles V, Olmos G, Llado J (2011) TNF-alpha potentiates glutamate-induced spinal cord motoneuron death via NF-kappaB. Mol Cell Neurosci 46:176-186.

Tothova Z, Kollipara R, Huntly BJ, Lee BH, Castrillon DH, Cullen DE, McDowell EP, Lazo-Kallanian S, Williams IR, Sears C, Armstrong SA, Passegue E, DePinho

RA, Gilliland DG (2007) FoxOs are critical mediators of hematopoietic stem cell resistance to physiologic oxidative stress. Cell 128:325-339.

Tun T, Hamaguchi Y, Matsunami N, Furukawa T, Honjo T, Kawaichi M (1994) Recognition sequence of a highly conserved DNA binding protein RBP-J kappa. Nucleic Acids Res 22:965-971.

Udan M, Baloh RH (2011) Implications of the prion-related Q/N domains in TDP-43 and FUS. Prion 5:1-5.

van den Berg DL, Snoek T, Mullin NP, Yates A, Bezstarosti K, Demmers J, Chambers I, Poot RA (2010) An Oct4-centered protein interaction network in embryonic stem cells. Cell Stem Cell 6:369-381.

van der Heide LP, Smidt MP (2005) Regulation of FoxO activity by CBP/p300-mediated acetylation. Trends Biochem Sci 30:81-86.

van Der Heide LP, Hoekman MF, Smidt MP (2004) The ins and outs of FoxO shuttling: mechanisms of FoxO translocation and transcriptional regulation. Biochem J 380:297-309.

van der Horst A, Burgering BM (2007) Stressing the role of FoxO proteins in lifespan and disease. Nat Rev Mol Cell Biol 8:440-450.

van der Horst A, Tertoolen LG, de Vries-Smits LM, Frye RA, Medema RH, Burgering BM (2004) FOXO4 is acetylated upon peroxide stress and deacetylated by the longevity protein hSir2(SIRT1). J Biol Chem 279:28873-28879.

van Praag H, Kempermann G, Gage FH (1999) Running increases cell proliferation and neurogenesis in the adult mouse dentate gyrus. Nat Neurosci 2:266-270.

van Praag H, Shubert T, Zhao C, Gage FH (2005) Exercise enhances learning and hippocampal neurogenesis in aged mice. J Neurosci 25:8680-8685.

Vilimas T, Mascarenhas J, Palomero T, Mandal M, Buonamici S, Meng F, Thompson B, Spaulding C, Macaroun S, Alegre ML, Kee BL, Ferrando A, Miele L, Aifantis I (2007) Targeting the NF-kappaB signaling pathway in Notch1-induced T-cell leukemia. Nat Med 13:70-77.

Villeda SA, Luo J, Mosher KI, Zou B, Britschgi M, Bieri G, Stan TM, Fainberg N, Ding Z, Eggel A, Lucin KM, Czirr E, Park JS, Couillard-Després S, Aigner L, Li G, Peskind ER, Kaye JA, Quinn JF, Galasko DR, Xie XS, Rando TA, Wyss-Coray T (2011) The ageing systemic milieu negatively regulates neurogenesis and cognitive function. Nature 477:90-94.

Wachs FP, Winner B, Couillard-Despres S, Schiller T, Aigner R, Winkler J, Bogdahn U, Aigner L (2006) Transforming growth factor-beta1 is a negative modulator of adult neurogenesis. J Neuropathol Exp Neurol 65:358-370.

Walker TL, White A, Black DM, Wallace RH, Sah P, Bartlett PF (2008) Latent stem and progenitor cells in the hippocampus are activated by neural excitation. J Neurosci 28:5240-5247.

Wallberg AE, Pedersen K, Lendahl U, Roeder RG (2002) p300 and PCAF act cooperatively to mediate transcriptional activation from chromatin templates by notch intracellular domains in vitro. Mol Cell Biol 22:7812-7819.

Waltzer L, Bourillot PY, Sergeant A, Manet E (1995) RBP-J kappa repression activity is mediated by a co-repressor and antagonized by the Epstein-Barr virus transcription factor EBNA2. Nucleic Acids Res 23:4939-4945.

Wang J, Shelly L, Miele L, Boykins R, Norcross MA, Guan E (2001) Human Notch-1 inhibits NF-kappa B activity in the nucleus through a direct interaction involving a novel domain. J Immunol 167:289-295.

Wang J, Rao S, Chu J, Shen X, Levasseur DN, Theunissen TW, Orkin SH (2006) A protein interaction network for pluripotency of embryonic stem cells. Nature 444:364-368.

Wang J, Qin H, Liang J, Zhu Y, Liang L, Zheng M, Han H (2007a) The transcriptional repression activity of KyoT2 on the Notch/RBP-J pathway is regulated by PIAS1-catalyzed SUMOylation. J Mol Biol 370:27-38.

Wang T, Holt CM, Xu C, Ridley C, R POJ, Baron M, Trump D (2007b) Notch3 activation modulates cell growth behaviour and cross-talk to Wnt/TCF signalling pathway. Cell Signal 19:2458-2467.

Wang W, Stock RE, Gronostajski RM, Wong YW, Schachner M, Kilpatrick DL (2004) A role for nuclear factor I in the intrinsic control of cerebellar granule neuron gene expression. J Biol Chem 279:53491-53497.

Weigel D, Jurgens G, Kuttner F, Seifert E, Jackle H (1989) The homeotic gene fork head encodes a nuclear protein and is expressed in the terminal regions of the Drosophila embryo. Cell 57:645-658.

Wharton KA, Yedvobnick B, Finnerty VG, Artavanis-Tsakonas S (1985) opa: a novel family of transcribed repeats shared by the Notch locus and other developmentally regulated loci in D. melanogaster. Cell 40:55-62.

Wickner RB, Edskes HK, Roberts BT, Baxa U, Pierce MM, Ross ED, Brachmann A (2004) Prions: proteins as genes and infectious entities. Genes Dev 18:470-485.

Wu L, Aster JC, Blacklow SC, Lake R, Artavanis-Tsakonas S, Griffin JD (2000) MAML1, a human homologue of Drosophila mastermind, is a transcriptional co-activator for NOTCH receptors. Nat Genet 26:484-489.

Xuan Z, Zhang MQ (2005) From worm to human: bioinformatics approaches to identify FOXO target genes. Mech Ageing Dev 126:209-215.

Yamamura Y, Lee WL, Inoue K, Ida H, Ito Y (2006) RUNX3 cooperates with FoxO3a to induce apoptosis in gastric cancer cells. J Biol Chem 281:5267-5276.

Zappone MV, Galli R, Catena R, Meani N, De Biasi S, Mattei E, Tiveron C, Vescovi AL, Lovell-Badge R, Ottolenghi S, Nicolis SK (2000) Sox2 regulatory sequences direct expression of a (beta)-geo transgene to telencephalic neural stem cells and precursors of the mouse embryo, revealing regionalization of gene expression in CNS stem cells. Development 127:2367-2382.

Zavadil J, Cermak L, Soto-Nieves N, Bottinger EP (2004) Integration of TGF-beta/Smad and Jagged1/Notch signalling in epithelial-to-mesenchymal transition. EMBO J 23:1155-1165.

Zhang CL, Zou Y, He W, Gage FH, Evans RM (2008) A role for adult TLX-positive neural stem cells in learning and behaviour. Nature 451:1004-1007.

Zhang X, Yalcin S, Lee DF, Yeh TY, Lee SM, Su J, Mungamuri SK, Rimmele P, Kennedy M, Sellers R, Landthaler M, Tuschl T, Chi NW, Lemischka I, Keller G, Ghaffari S (2011) FOXO1 is an essential regulator of pluripotency in human embryonic stem cells. Nat Cell Biol 13:1092-1099.

Zhao C, Deng W, Gage FH (2008) Mechanisms and functional implications of adult neurogenesis. Cell 132:645-660.

Zheng S, Eacker SM, Hong SJ, Gronostajski RM, Dawson TM, Dawson VL (2010) NMDA-induced neuronal survival is mediated through nuclear factor I-A in mice. J Clin Invest 120:2446-2456.

Zhou Q, Chipperfield H, Melton DA, Wong WH (2007) A gene regulatory network in mouse embryonic stem cells. Proc Natl Acad Sci U S A 104:16438-16443.

9 Appendix

Acknowledgements

Erklärung

Ich erkläre an Eides statt, dass ich die der Fakultät Wissenschaftszentrum Weihenstephan für Ernährung, Landnutzung und Umwelt der Technischen Universität München zur Promotionsprüfung vorgelegte Arbeit mit dem Titel:

Examining new interactors of Notch/RBPJκ signalling in adult neural stem cells

Am Lehrstuhl für Genetik unter der Anleitung und Betreuung durch

Univ.-Prof. Dr. W. Wurst

ohne sonstige Hilfe erstellt und bei der Abfassung nur die gemäß § 6 Abs. 5 angegebenen Hilfsmittel benutzt habe.

- Ich habe die Dissertation in dieser oder ähnlicher Form in keinem anderen Prüfungsverfahren als Prüfungsleistung vorgelegt.

- Ich habe den angestrebten Doktorgrad **noch nicht** erworben und bin **nicht** in einem früheren Promotionsverfahren für den angestrebten Doktorgrad endgültig gescheitert.

- Die Promotionsordnung der Technischen Universität München ist mir bekannt.

München den,…………… ……………………………

Curriculum vitae

Persönliche Daten

Name	Tobias Johannes Schwarz
Anschrift	Barthstrasse 17
	80339 München
Telefon:	+49 (89) 38900702
E-Mail	tobi0702@web.de
Geburtsdatum	07.02.1980
Geburtsort	München
Nationalität	deutsch
Familienstand	ledig

Doktorarbeit

02/2008 - 02/2012   Promotion am Helmholtz Zentrum München
Institut für Entwicklungsgenetik
Prof. Wolfgang Wurst
Arbeitsgruppe „Adulte Neurale Stammzellen und Neurogenese"

Thema der Dissertation: Examining new interactors of Notch/RBPJκ signalling in adult neural stem cells

Studium

09/2003 – 12/2007   Studium der Biologie an der
Ludwig-Maximillians-Universität, München

Diplomarbeit über: Regulation der adulten hippokampalen Neurogenese durch Engrailed exprimierende Neurotransmittersysteme (Prof. Wolfgang Wurst)

Abschluß mit Diplom im Dezember 2007

11/2005 – 04/2006   Forschungspraktikum Dr.Alejandro Schinder, Instituto Leloir, Buenos Aires, Argentinien

10/2001 – 07/2003   Studium der Chemie und Biochemie an der LMU München

Zivildienst

09/2000 – 07/2001   Krankenhaus Neuperlach

Schule

09/1998 – 06/2000   Heinrich-Heine-Gymnasium München
09/1990 – 07/1998   Werner-von-Siemens-Gymnasium München
09/1986 – 07/1990   Kafka-Grundschule München

Publications

Schwarz TJ, Ebert B and Lie DC (2012) Stem cell maintenance in the adult mammalian hippocampus: a matter of signal integration? Dev Neurobiol 72 (7); 1006-15

Ehm O, Goritz C, Covic M, Schaffner I, **Schwarz TJ**, Karaca E, Kempkes B, Kremmer E, Pfrieger FW, Espinosa L, Bigas A, Giachino C, Taylor V, Frisen J, Lie DC (2010) RBPJkappa-dependent signaling is essential for long-term maintenance of neural stem cells in the adult hippocampus. J Neurosci 30:13794-13807.

Haslinger A, **Schwarz TJ**, Covic M, Lie DC (2009) Expression of Sox11 in adult neurogenic niches suggests a stage-specific role in adult neurogenesis. Eur J Neurosci 29:2103-2114.

Manuscripts in /preparation

Schwarz TJ, Vogt A, Cernilogar F, Ebert B, Stribl C, Floss T, Michaelidis TM, Gloeckner CJ and Lie DC (2012) TDP-43 regulates adult neural stem cell maintenance via modulation of Notch signalling (*in preparation*)

Schwarz TJ, Doberauer K, Darsinou M, Nakashima K, Michaelidis TM and Lie DC (2012) NFIA overexpression *in vivo* increases adult hippocampal neurogenesis via repression of Notch signalling (*in preparation*)

Khan MA, Schaffner I, **Schwarz TJ**, Pinho R and Lie DC (2012) Conditional knockout of FOXO1/3/4 in adult hippocampal stem cells lead to the progressive loss of adult neural stem cell activity (*in preparation*)